Towards a Holographic Description of Pulsar Glitch Mechanism

Anuj Misra

THESIS SUBMITTED IN PART FULFILMENT FOR THE DEGREE
OF
MSC IN ASTROPHYSICS AND SPACE SCIENCE

National Astrophysics and Space Science Programme (NASSP)
Department of Mathematics and Applied Mathematics
University of Cape Town

November 2014

Declaration

This stands to declare that I know the meaning of Plagiarism and all of the work in this document, save for that which is properly acknowledged, is my own. This dissertation is being submitted for the degree of MSc in Astrophysics and Space Science with the Department of Mathematics and Applied Mathematics, University of Cape Town and has not been submitted before for any degree or examination in any other university.

Signature of Author . . . . . .

Cape Town
November 2014

Abstract

This work aims to review the progress in understanding the underlining physics of pulsar glitches: beginning from the pedagogical development of the subject to eventually motivating the use of AdS/CFT techniques in studying a certain class of condensed matter systems.

The foundation of this work is built upon the Gross Pitaevskii (GP) model of superfluidity applied to the interior matter of neutron stars, where the condensate wave function acts as the order parameter of the macroscopic coherence theory. The excitation modes of the field equations are found to be solitonic vortices, which then go on to present a theoretical basis to the plausible theories of pulsar glitches involving vortex dynamics.

The second major thrust of this thesis is in reviewing the application of AdS/CFT in study of strongly-coupled condensed matter systems, with special attention to the models of holographic superfluidity that admit vortex-like solutions. The basic identification of the characteristic free energy configuration of global vortices in the AdS/CFT prescription enables to motivate its use in studying the pulsar glitch mechanism.

The last part of this work traces the conclusions of this review and attempts to present the current state-of-progress of the field with its extensive domain of purview and open lines of inquiry.

Acknowledgements

To begin with, I would like to thank my supervisor Jeff Murugan for his patience and guidance through this project. It would not have been possible for me to complete this work without his supervision and his *unique* ability of making his students engage in elenctic examination of their own ideas to further their critical thinking ability. Over the course of my study, it has been the continual questions Jeff made me ask that made me develop, sustain and extend an ongoing interest in this topic. His enthusiasm and passion for teaching physics invariably inspires and motivates even the most disillusioned students in his class! With his constant support, Jeff has helped me mature my own critical thought and for that I will always be grateful. His approach to physics continues to remain pegged on two things: his thirst for knowledge and the constant smile on his face! Thanks Jeff, I'm in your debt!

I'd like to thank my programme director, Prof. Peter Dunsby for his guidance, support and assistance that has allowed for me to study at the National Astrophysics and Space Science Programme (NASSP) here at University of Cape Town. It is indeed an honour to have been given an opportunity to study at NASSP. Prof. Dunsby has faith in all his students and is always willing to help us with any problems/issues we encounter. His impartial advice and motivation throughout my time at UCT has helped me tremendously and for that I thank him!

A big shout to my office mates Dino Giovannoni, Dawie De Klerk, Terrence Goldberg and James Newling for being an amazing bunch of people to work with. Our discussions and chats have been thoroughly enjoyable and will be deeply missed, especially our random banter and incessant conversational critique.

To all my friends in Cape Town, I'd like to acknowledge their patience with me as they bore the brunt of my irritability. Many a weekday afternoons were spent with me oppressing their ever-so-willing ears with my rants on the incomprehensibility of theoretical physics. Their care and support has definitely been the wind in my sails through my time at UCT. In particular, one Mr Gordon Angus has even helped me draw out some of the figures used in this thesis and just for that I'd have to mention: "Gordon, you were right all along! It is the $\mathfrak{M}^2$ matrix-representation of vector $\mathcal{V}_9$ parabolic forces!". My friends are an amazing bunch of eccentric people and I'm truly lucky to have them in my life. Thank you guys!

At this point, I'd like to thank my family who have been very supportive and encouraging to all my interests in life, no matter how outrageous it seemingly sounded! Everything I am today is due to their unconditional love and unflinching support through my years of life. I thank them for making me a better human being and hope to make them proud of me!

In going, I'd like to especially mention one Mr. Edward O'Reilly, who has been a brother to me and one of my closest friends. It is his kindness and love that opened his heart, his home and his family to me from the first day I set foot in South Africa. His *silent* support and *unselfish* generosity make him one of the nicest people I have known in my life. I owe him more than I can mention here, but I would like to take this space to say how lucky I consider myself to have found a friend and a brother in Ed! Thank you captain! As I have always said, "You're ace!"

Anuj Misra

“

Illud in his quoque te rebus cognoscere avemus, corpora cum deorsum rectum per inane feruntur ponderibus propriis, incerto tempore ferme incertisque locis spatio depellere paulum, tantum quod momen mutatum dicere possis. quod nisi declinare solerent, omnia deorsum imbris uti guttae caderent per inane profundum nec foret offensus natus nec plaga creata principiis; ita nihil umquam natura creasset.

”

In these affairs We wish thee also well aware of this:
The atoms, as their own weight bears them down
Plumb through the void, at scarce determined times,
In scarce determined places, from their course
Decline a little-call it, so to speak,
Mere changed trend. For were it not their wont
Thuswise to swerve, down would they fall, each one,
Like drops of rain, through the unbottomed void;
And then collisions ne'er could be nor blows
Among the primal elements; and thus
Nature would never have created aught.

Titus Lucretius Carus in De Rervm Natvra, 50 BCE.

Translated by William Ellery Leonard, *On the Nature of Things*, 1916

Table of Contents

List of Figures

Outline and Overview

One of the fascinating frontiers to emerge from modern physics is the connection between certain condensed matter theoretical systems and their equivalent astrophysical extreme-environment representations. Neutron stars being ultra-dense gravitationally collapsed remnants of stellar evolution, their incredible densities constitute a perfect experimental set-up to study and model finite-temperature, strongly-coupled condensed matter systems. This connection helps look at the observational occurrences of *glitches*: a sudden increase in the average rotational spin-down speeds of pulsars, as a window into the world of superdense matter under ultra strong magnetic fields.

The complex superfluid matter interpenetrating the nuclear-lattice bound crustal structure of neutron stars admit solitonic excitation states that have a conserved topological charge. These vortex-like solutions have been proposed as a potential explanation to many phenomenological theories for pulsar glitch formation and their subsequent relaxation routines. Modern technological advancement and increased engineering sensitivity has resulted in a growing volume of high-precision observational data, discrediting many older models in favour of more comprehensive ones. Within the classical framework, the search for pulsar glitch models remains an actively pursued field of research with a strong significance on phenomenological-modelling corroborating observations. However, despite over four decades of research into the study of pulsar glitchings and many probable alternative theories, there exists no conclusive and definitive model to describe the exact mechanism by which the process occurs.

Separately though, the advancements in theoretical physics over the last decade has introduced a vast mathematical machinery to study complex strongly-coupled quantum fluid systems from ultra cold Fermi gas to finite temperature dense hadron superfluid matter, all the way through to quark gluon plasmas (QGP). A remarkable emergence from this theoretical exercise has been the extension of the holographic principle of quantum gravity/string theory to study strongly correlated field theories via the famous AdS/CFT correspondence.

In utilizing the holographic duality, the bulk black hole with scalar hairs at low temperatures (in the weak coupling limit) maps to the strongly coupled boundary gauge theory with global/background-local spontaneous symmetry-breaking condensate states under the standard prescriptive dictionary identification. This formulation turns out to be incredibly potent in probing the hitherto inaccessible dense neutron star matter with its dilute bound-neutron superfluid/superconductor behaviour at finite (low) temperatures and non-zero chemical potential. Where standard techniques of QCD are limited in their application — at least in this phase regime — AdS/CFT applied to this kind of anisotropic dense hadronic matter yields remarkable results with respect to the vacuum expectation values of the condensate and current in the dual CFT. The realization of holographic vortex solutions to the bulk field equations; with its characteristic logarithmic-divergent free energy, raises the unique possibility of treating the entire scenario of pulsar glitches from a holographic perspective.

The motive and intent of the present work is to review the development of the subject from the classical perspective leading on to the holographic approach. Despite being overshadowed (in a manner of speaking) by the excitement in application of holographic techniques to neutron stars, a lot of concrete physics pertaining to neutron star modelling and its constituent structure, lays encoded in the understanding of stellar superfluidity and hydrodynamics. At the very outset, the complex arrangement of the crust-core composition of neutron stars (along with its exotic matter content); as understood by nuclear astrophysics, plays a vital role in any subsequent effect emanating from these regions like e.g., pulsar glitches. An alternative explanation to the problem then clearly requires a good choice of basis in the true representation space. This is found by looking at the quantum

theory of vortices in superfluids: a major factor underlying most modern theories of glitches.

The uniqueness of studying the astrophysics of a system is in its direct experimental verification by observational astronomical data and keeping this perspective in mind, the various pulsar glitch (and subsequent recovery) theories reviewed here form a unique semi-chronological developmental history of our understanding. Spanning around half a century, a host of different theories have been progressively proposed, modified, amended, retracted or simply discarded in our struggle to understand this illusive pulsar glitch mechanism. The very open-ended nature to this question has made room for introducing the concept of AdS/CFT to this pool of theories. With the increased support for AdS/condensed matter theories, the formal inclusion of the holographic regime to understand pulsar mechanics may hold the key to unlock the hidden physics of pulsar glitches.

The general outline of this work begins with Chapter (1) presenting a fairly detailed review of the basic theory of superfluidity, including discussions on the condensate order parameter, spontaneous symmetry breaking and the Gross Pitaevskii (GP) model that encodes much of the dynamics of the neutron superfluid interior. Chapter (2) builds upon the theory of superfluids by explaining the presence of quantized solitonic excitations of the superfluid spectrum, i.e., vortices. These topologically conserved quantities are studied as an isolated vortex line to explore their characteristic free energy configuration. With this material at hand, Chapter (3) begins to explain the problem of pulsar glitches from a phenomenological perspective and then moves on to the various glitch models that have historically been extended as possible explanations. The chapter also looks at some important post-glitch, recovery-physics mechanisms e.g., vortex creep, and through its counter arguments, maintains the open-ended, unresolved nature of the glitch problem. Chapter (4) brings in the main player of AdS/CFT into the picture, with a generic introduction to the conjecture and motivation towards its application to study neutron superfluids. A major bulk of the chapter reviews the construction of the holographic superfluid model with inhomogeneous vortex solutions and free energy profile of vortices. Its major focus is in eliciting a comparison with the standard GP theory to indicate a first hand validity to the approach. The work ends with Chapter (5) presenting a heuristic synopsis of the material reviewed through the

main body of the text, with special emphasis on the current progress and extension to the holographic study of superfluid phenomenon and pulsar physics.

As is in the nature of any good review, a comprehensive list of references and further reading material has been appended alongside the main body of the text. The content of this work is simply to bring forth a systematic development of the subject – with its subtleties and nuances duly accorded – and motivate towards further detailed study. Most calculations and numerics mentioned through this review have been earnestly redone to appreciate the working of theories in full; they are not meant to be original or unique in any form, but rather an analytical extension along the way. The rigour in this attempt has been to get a firm handle on the relevant content matter, which is spread across a huge domain of applied mathematics, astrophysics and theoretical condensed matter physics. The brevity of space has meant confining detailed mathematical calculations into a more concise form, however, all attempts have been made to clearly elicit the physics behind the formulae.

How on earth can the voltage be exactly zero along a mile of dirty lead wire?

H B G Casmir, 1955

1

Introduction to Stellar Superfluidity

1.1 Neutron star and Pulsars: An overview

Neutron stars are a type of stellar remnants caused due to the gravitational collapse of massive stars and comprise predominantly of neutrons. The enormous gravitational pull compresses matter to the central densities that are of one order higher than what is found in stable atomic nuclei (the nuclear saturation density $\rho_{ns} = 2.8 \times 10^{14}$ g cm^{-3}). This renders neutron stars as unique astrophysical probes of cold (the thermal energies of neutron stars are lower than typical excitation energies) and stable superdense matter that is supported against a complete gravitational cascade into a singularity by quantum degeneracy pressure.

1.1.1 Structure of Neutron stars

A typical neutron star has a mass ranging between 1.35 - 2.0 $M_\odot$ [Kiziltan et al. 2010] with a corresponding radius of about 12 km from the Akmal-Pandharipande-Ravenhall equation of state (APR EOS) that is standardly used [Haensel et al. 2007] (about $60000^{-1} M_\odot$). Also, they are thought to have overall densities — as predicted by the APR EOS — ranging between 3.7×10^{17} - 5.9×10^{17} kg/m^3 (about 2.6×10^{14} - 4.1×10^{14} $\rho_\odot$)

The existence of these cosmic relics rely on the key concept of Fermion degeneracy pressure: a direct manifestation of the residual minimal energy of a thermally cooled system of Fermion gas, where a degeneracy in electron's energy-occupation states due to the Pauli exclusion principle causes a certain minimal energy to remain behind. Up to the Chandrasekhar limit ($\sim 1.44 M_\odot$), the electron-degeneracy pressure in a cold and super-dense gas, acts as a counter to the density driven gravitational collapse. However; in case of a neutron star, the mass range exceeds the Chandrasekhar limit and the further gravitational cascade is contained by a different Fermion degeneracy pressure. At this juncture, the system of cold non-accreting matter of neutron stars is regarded as being in its ground energy state of complete thermal equilibrium with respect to all zero-temperature interactions [Harrison et al. 1965].

The ground state structure of the neutron star (ignoring a predominantly magnetically driven, 1 cm thick atmospheric cover) consists of a solid crust of body-centred cubic lattice of ^{56}Fe nucleus, *cf.* FIG. 1.1.1. The binding energy per nucleon of $^{56}Fe_{26}$ nuclei being the largest [Beskin 1999] and the position of ^{56}Fe being the last remnant of nuclear fusion in stellar evolution collectively attest to the candidature of ^{56}Fe as the material of the outer crust of neutron stars.

Along the interior of the neutron star, the structure changes dramatically with an increase in matter density and pressure leading to full ionisation of the atoms. The increasing matter density extends the electron degeneracy further and with a decreasing spatial radius Δx, Heisenberg uncertainty principle dictates the momentum $\Delta p \gtrsim \hbar / \Delta x$ to dramatically increase. Another way of looking at this is to state that the *Fermi energy* (absolute zero-temperature energy of highest occupied

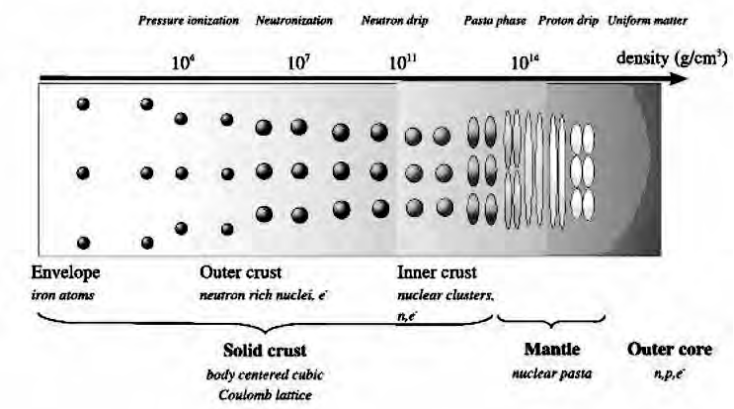

Figure 1.1.1: The ground state structure of neutron stars along the density axis. [1]

state) associated with the free relativistic electrons in the plasma soup increases at $\rho \sim 10^4$ g cm^{-3}. At densities above 10^7 g cm^{-3}, these higher energy relativistic electron combines with a proton in the nucleus to make a neutron and an electron-neutrino by the process of inverse-β decay, $p + e^- \longrightarrow n + \nu_e$. The resultant composition is then, a nuclear matter consisting of predominantly a degenerate neutron gas, sometimes called neutronium, mixed with a small admixture of degenerate proton and electron gases. At this stage, the neutron-rich nuclear matter is tremendously dense and hence is subjected to an incredible gravitational force. The inward collapse of the neutron star is countered by the neutron degeneracy pressure, preventing an all out cascade into a singularity.

In the deeper regions of the neutron star, the neutron number density n_n increases and the associative neutron Fermi momentum, which is given by $p_{\mathcal{F}_n} = \hbar(3\pi^2 n_n)^{\frac{1}{3}}$, subsequently increases. Correspondingly, the Fermi energy $\epsilon_{\mathcal{F}_n}$ defined (with relativistic correction) as $\epsilon_{\mathcal{F}_n} = \sqrt{(p_{\mathcal{F}_n})^2 + m_n^2 c^4}$ also increases, implying that the energy of the highest occupied quantum states for free Fermions (here neutrons) is raised. Here, the newly created neutrons occupying lower-than-top energy levels *drip* out of the nucleus. Typically, the **neutron drip density** ρ_{ND} has a value of 4×10^{11} g cm^{-3}. In this region, there is believed to be the presence of a strongly degenerate neutron gas inter penetrating the crystal lattice structure of heavier, neutron rich nuclei like ^{78}Ni, ^{76}Fe or even ^{118}Kr [Pethick et al. 1995].

[1] Picture sourced from [Chamel and Haensel 2008]

Going radially inwards into the star, the inner crust; extending from ρ_{ND} to $\rho_{ns}/3 \simeq 10^{14}$ g cm^{-3}, is marked by the presence of free neutrons that possibly condense into a superfluid phase in some interior layers. At this place, the crust lattice begins to dissolve, leaving a neutron-degenerate superfluid matter mainly consisting of neutrons and a mixture of protons and electrons, both being 5% by number respectively.

In the densest regions of the inner crust, various exotic configurations of non-spherical nuclear-clusters (nuclei) into cylindrical, slab-like, tube-like and bubbles are proposed [Hashimoto et al. 1984; Watanabe and Maruyama 2012]: this sequencing of nuclear shapes is referred to as *nuclear pasta*. This pasta phases covers a small range of densities near the crust-core interface with $\rho \sim 10^{14}$ g cm^{-3}.

Lastly, the superfluid region, from the nuclear density to central density ($\sim 10^{15}$ g cm^{-3}) is called the core and its underlying physics is not currently understood in completeness. There are many hypotheses regarding the matter present in the inner core — some of which include exotic forms of matter — including degenerate strange matter (containing strange quarks in addition to up and down quarks), matter containing high-energy pions and kaons in addition to neutrons [Haensel et al. 2007] or ultra-dense quark-degenerate matter.

A clear schematic representation of the neutron star, stratified into its different surfaces and interior layers is represented in FIG. 1.1.2.

1.1.2 Rotating Neutron stars - Pulsars

Following the discovery of periodic signals emanating from certain sources in a galactic survey conducted by Jocelyn Bell and Antony Hewish in 1967 [Hewish et al. 1968], a whole series of theoretical predictions were made to establish the nature of the *pulsations* of these objects called **pulsars**. After dismissing a whole range of possible candidates including binary stellar system and white dwarfs, a rotating neutron star was finally proclaimed as the only possible candidate — a result first proposed by Thomas Gold in 1968 [Gold 1968]. To date there are over

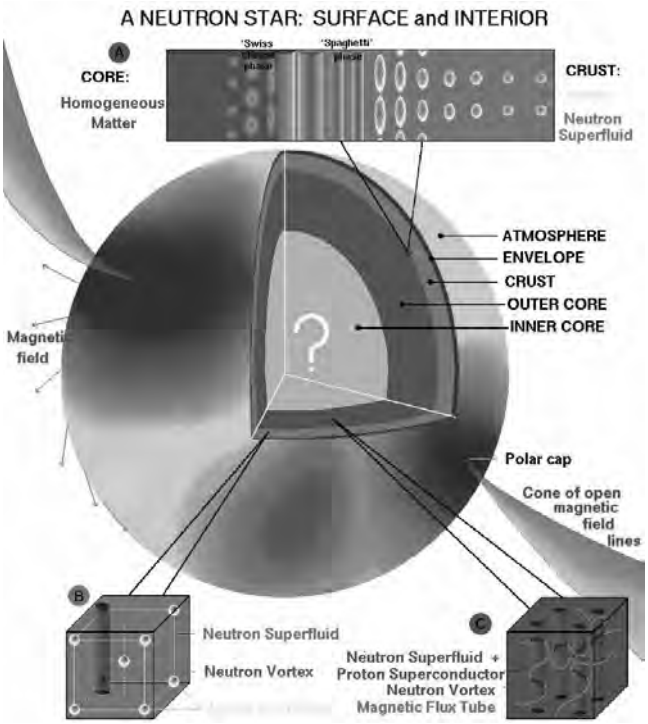

Figure 1.1.2: Diagram of schematic representation of the interior of Neutron star. [2]

2500 neutron stars detected as radio-regime pulsars, with this number constantly increasing.

The central idea in support, lies in looking at the conservation of angular momentum during the evolutionary history of the neutron star from its progenitor star, i.e., $L_{pg} \sim L_{ns}$ where indices pg and ns refer to the progenitor star and neutron star observable respectively. The neutron star has a tiny fraction of its progenitor's radius, i.e., $r_{ns} \ll r_{pg}$, implying that the moment of inertia of the neutron star is sharply reduced, viz.. $I \propto r^2 \Rightarrow I_{ns} \ll I_{pg}$. This leads to the fact that, $L_{pg} = I_{pg}\Omega_{pg} \equiv L_{ns} = I_{ns}\Omega_{ns} \Rightarrow \Omega_{ns} \gg \Omega_{pg}$, i.e., the rotational velocity, Ω_{ns} of the neutron star is very high. This rotational energy of the neutron star creates an induced electromagnetic effect, propelling the charged protons and electrons on the star's surface along an axially-channelled electromagnetic radiation beam, distinctly at the magnetic poles of the pulsar. In general, the misalignment between the rotational and magnetic axes of the pulsar — with the magnetic axis precessing

[2] Picture sourced from `http://www.astroscu.unam.mx/neutrones/NS-Picture/NStar`

around the rotational axis — causes the beam to be seen only once through every rotation of pulsar: the characteristic *pulsed* effect.

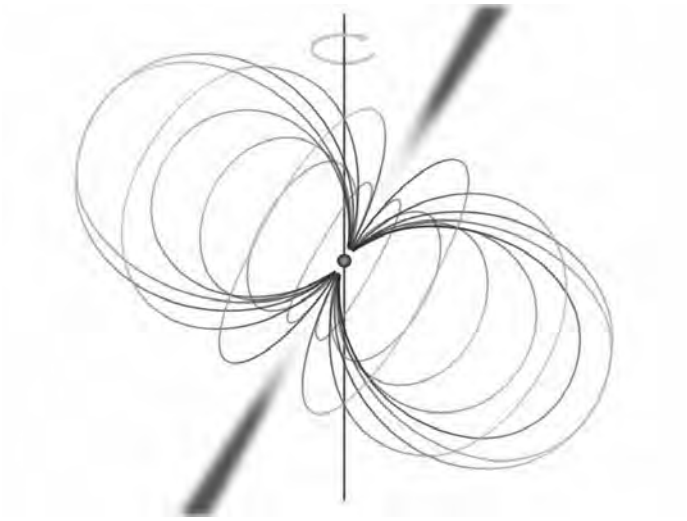

Figure 1.1.3: Diagram of schematic representation of the Pulsar. [3]

1.2 Superfluidity

As is conventionally understood, the behaviour of a neutron star is strongly dependent on the *superfluid* dynamics of its interior. A superfluid is a state of matter in which matter behaves like a fluid with zero viscosity and zero entropy, along with having infinite thermal conductivity. This remarkable property that is shared by systems as different as superconductors where the flowing particles are electrons and by superfluids ^{4}He where the particles are atoms, is due to the macroscopic occupation of a quantum state. The concept of superfluidity discussed here relies quite extensively on this idea of concrete manifestation of the phenomenon of macroscopic quantum coherence.

[3]Picture created by as part of Wikimedia Commons

1.2.1 Origin of the condensate

Intuitively, the macroscopic occupation of a quantum state in Bosonic particles is more readily apprehensible as Bosons are not subjected to the Pauli exclusion principle. When the particle density, $n = N/V$ of N *indistinguishable* Bosonic particles with spin $S = \mathfrak{n}|_{\mathfrak{n}\in\mathbb{Z}^+}$ and mass m, enclosed in volume V, exceeds some *quantum concentration density* n_q, the quantum effects become apparent. Also, the quantum concentration can be understood as the measure for which the inter-particle distance $\langle r\rangle \sim (1/n)^{1/3}$ is of the order of the thermal de Broglie wavelength, $\lambda = h/\sqrt{2\pi m k_B T}$, where T is the temperature of the Bosonic particles with k_B and h being the Boltzmann's constant and Planck's constant respectively. The temperature dependence of quantum concentration maintains that, both the Fermi–Dirac statistics (governing low temperature Fermion systems) and Bose Einstein statistics (governing low temperature Boson systems) become Maxwell-Boltzmann statistics at high temperatures or at low concentrations.

According to the low temperature regime of Boson systems, the *average particle density* of Bosonic particle in the ground state of the system is given as[1] –

$$n_o = \begin{cases} 0 & T_D > T_c \\ n\left[1 - \left(\frac{T_D}{T_c}\right)^{3/2}\right] & T_D \leq T_c \end{cases} \qquad [1.2.1]$$

A schematic representation of the variations in the fractional condensate number density n_0/n with respect to the normalised temperature T_D/T_c (T_c being the critical temperature) is shown in FIG. 1.2.1. This idea has an interesting and important consequence: as $T_D < T_c$, a *macroscopic fraction* of the Bosonic particles occupy the lowest energy level available, with $\vec{k} = 0$ momentum. Moreover as $T \longrightarrow 0$, more and more of these Bosonic particles occupy this level till eventually at $T \sim 0$ all the Bosons are in this lowest energy configuration, i.e., $n_0 \approx n$. This is indeed the expected ground-state for a system of non-interacting Bosonic particles. The phenomenon of having a macroscopic percentage of the Bosonic particles *condense* into the lowest energy level is called **Bose Einstein Condensation**.

[1] A fuller discussion and derivation of Bose Einstein statistics is given in the box on pp. 8–9 in line with [Annett 2004]

Bose Einstein Statistics

For a system of N indistinguishable particles of spin S and corresponding spin projection m, it is impossible to mention which single-particle energy eigenstate $|\vec{k}, S\rangle$ with energy eigenvalue $\epsilon_{\vec{k}}$ each particle finds itself in. Instead, one has to refer to the **occupation number** $n_{\vec{k},m}$ which is the expectation value of finding particles that are in each single-particle energy eigenstate with the the total number of particles in the system as $N_{\{n_{\vec{k},m}\}} = \sum_{\vec{k},m} n_{\vec{k},m}$. In terms of ensemble averages for a Bose Einstein (BE) distribution, the **average occupation number** $\left\langle n_{\vec{k},m} \right\rangle$ of a single-particle energy eigenstate with wave vector $\vec{k}$ and spin degeneracy $m \equiv g_S = 2S+1$ is then given as $\left\langle n_{\vec{k},m} \right\rangle = \left[\frac{1}{e^{\beta(\epsilon_{\vec{k}}-\mu)}-1}\right] \equiv f(\epsilon_{\vec{k}})_{BE}$, where $\beta = 1/k_BT$ and μ is the chemical potential and correspondingly, $\langle N \rangle = \sum_{\vec{k},m} \left\langle n_{\vec{k},m} \right\rangle$. It can be seen here, for a BE-distribution, $e^{\beta(\epsilon_{\vec{k}}-\mu)} \geq 1 \Rightarrow \mu \leq \epsilon_{\vec{k}}\ \forall \vec{k} \Rightarrow \mu \leq 0$, i.e., a **negative chemical potential**.

The grand potential Φ_G for a such a system of homogeneous, non-interacting Boson gas is then given by $\Phi_G \equiv \frac{1}{\beta}\frac{V(2S+1)}{4\pi^2}\left(\frac{2m}{\hbar^2}\right)^{3/2}\int_0^\infty \ln\left(1-e^{-\beta(\epsilon-\mu)}\right)\sqrt{\epsilon}\,\mathrm{d}\epsilon$. Using the grand potential, we can define the **average number of particles** in the system as –

$$\begin{aligned}\langle N \rangle &= \left(\frac{\partial \Phi_G}{\partial \mu}\right)\Big|_{\beta,V \text{ constant}} = \frac{V(2S+1)}{4\pi^2}\left(\frac{2m}{\hbar^2}\right)^{3/2}\int_0^\infty \frac{\sqrt{\epsilon}\,\mathrm{d}\epsilon}{e^{\beta(\epsilon-\mu)}-1} \\ &= \frac{V(2S+1)}{4\pi^2}\left(\frac{2mk_BT}{\hbar^3}\right)^{3/2}\Gamma\left(\frac{3}{2}\right)g_{\frac{3}{2}}(e^{\beta\mu})\end{aligned}$$

where $g_{\frac{3}{2}}(e^{\beta\mu}) = \sum_{p=1}^{\infty}\frac{(e^{\beta\mu})^p}{p^{\frac{3}{2}}}$ is the Riemann-Dirichlet function. This function $g_{\frac{3}{2}}(e^{\beta\mu}) = \frac{\langle N\rangle}{V}\frac{1}{(2S+1)}\left(\frac{2\pi\hbar^2}{mk_BT}\right)^{3/2}$ starts to diverge for $(e^{\beta\mu}) > 1$, with the maximum convergent value being $g_{\frac{3}{2}}(e^{\beta\mu}=1)$. In the high temperature regime, despite $\beta \longrightarrow 0$, the chemical potential μ becomes highly negative making $e^{\beta\mu} \longrightarrow 0$. This then implies that $g_{\frac{3}{2}}(e^{\beta\mu}) = e^{\beta\mu} + \mathcal{O}(e^{2\beta\mu}) + \ldots \sim e^{\beta\mu}$ giving an expression for the chemical potential as $\mu \approx -\frac{3}{2}k_BT\ln\left[\left(\frac{V(2S+1)}{\langle N\rangle}\right)^{2/3}\left(\frac{2\pi mk_BT}{h^2}\right)\right]$. On lowering the temperature as β gets larger but the chemical potential compensates by getting less negative till effectively becoming zero: this provides for the maximally convergent case of $e^{\beta\mu} = 1$. Holding a fixed $\langle N\rangle$, the temperature where $\mu = 0$ is called **critical temperature** $T_c \approx \frac{h^2}{2\pi mk_B}\left\{\frac{\langle N\rangle}{V(2S+1)\zeta\left(\frac{3}{2}\right)}\right\}^{2/3}$

This critical temperature provides for a transitional separation scale when looking at the temperature-dependent behaviour of the Bosonic system —

1. $T \gg T_D$ where T_D is the **low quantum degeneracy temperature**: In this regime the high-temperature behaviour of the system makes the chemical potential strongly negative as seen above.

2. $T_D \geq T_c$: In this regime, the chemical potential starts to get less negative with $\frac{\langle N \rangle}{V} \frac{1}{(2S+1)} \left(\frac{2\pi\hbar^2}{mk_BT_D} \right)^{3/2} \sim g_{\frac{3}{2}}(e^{\beta\mu} < 1) \sim e^{\beta\mu} + \frac{e^{2\beta\mu}}{2^{3/2}} + ...$ When $T_D = T_c$, we find $\mu = 0$ where the factor $e^{\beta\mu} = 1$ reaches maximum convergence; any further reduction in the temperature, i.e., $T \in [0, T_c]$ maintains $\mu \sim 0$.

3. $T_D \leq T_c$: This is where the idea of the macroscopic occupation of the ground state ($\epsilon_{\vec{k}} = 0$) comes into the picture. In a BE-distribution, we can separate the average number of particles in a system as being given by —

$$\begin{aligned} \langle N \rangle &= (2S+1) \left\langle n_{\vec{k}=0} \right\rangle + \sum_{\vec{k} \neq 0, m} \left\langle n_{\vec{k},m} \right\rangle \\ &= (2s+1) \frac{1}{e^{-\beta\mu} - 1} + \frac{V(2S+1)}{(2\pi)^3} \int \frac{\mathrm{d}\vec{k}}{e^{\beta(\epsilon_{\vec{k}} - \mu)} - 1} \\ &\approx \frac{(2S+1)}{e^{-\beta\mu} - 1} + V(2S+1) \left(\frac{mk_BT_D}{2\pi\hbar^2} \right)^{3/2} g_{\frac{3}{2}}(z < 1) \end{aligned}$$

The first term in the above expression contribute to $\langle N \rangle$ in this regime because in the thermodynamic limit ($V \longrightarrow \infty$), $e^{-\beta\mu} \longrightarrow 1$ or effectively, $(2S+1) \left\langle n_{\vec{k}=0} \right\rangle \longrightarrow \infty$. It is here that the **average particle number density** $n_{\vec{k}=0} \triangleq \frac{(2S+1)}{V(e^{-\beta\mu} - 1)}$ remains finite as $V \longrightarrow \infty$ with $\mu \sim 0$, making the **average particle density** of the Bosonic system in its ground state as –

$$\begin{aligned} n &= n_0 + (2S+1) \Big(\frac{2m\pi k_BT_D}{h^2} \Big)^{3/2} g_{\frac{3}{2}}(z \to 1) \\ &= n_0 + n \left(\frac{T_D}{T_c} \right)^{3/2} \frac{g_{\frac{3}{2}}(z \to 1)}{\epsilon\Big(\frac{3}{2}\Big)} \\ \Rightarrow n_0 &\approx n \left[1 - \left(\frac{T_D}{T_c} \right)^{3/2} \right] \because \forall\, T_D < T_C \Rightarrow g_{\frac{3}{2}}(z \to 1) \sim \epsilon\Big(\frac{3}{2}\Big) \end{aligned}$$

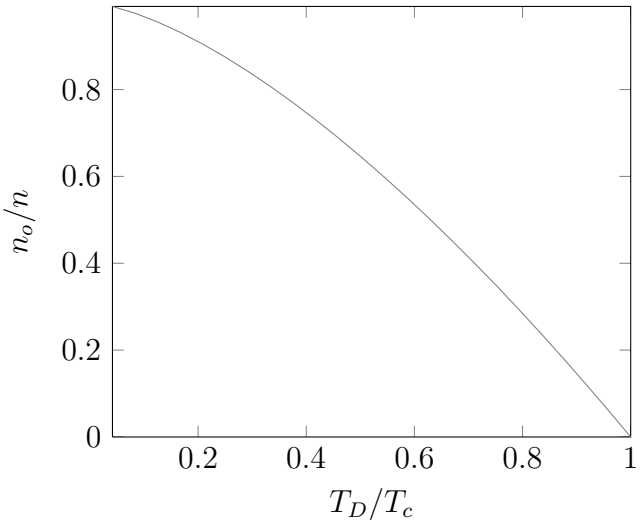

Figure 1.2.1: The Bose condensate number density (fraction) n_0/n as a function of normalised temperature T_D/T_c. The condensate fractional number density reduces from total ground state occupation at $T = 0$ to zero at $T_D \sim T_c$.

Historically, the Indian physicist S. N. Bose wrote to Einstein in 1924 describing his work on the statistical mechanics of photons. Einstein appreciated the significance of this work and used Bose's approach to predict what is now called Bose–Einstein condensation. In the late 1930's, it was discovered that liquid ^{4}He becomes a superfluid when cooled below ~ 2.2 K. Superfluidity is a quantum mechanical state of matter with very unusual properties, such as the ability to flow through very small capillaries with no measurable viscosity. In what followed famously through history, speculations arose as to whether this state of matter was connected with the Bose Einstein condensation phenomenon: an insight that would have tremendous theoretical and experimental impact in the world of condensed matter physics.

1.2.2 Superfluidity of ^{4}He

The comparison of the thermal de Broglie wavelength to the other typical length scales in the fluid, e.g., the inter-atomic distance $\langle r \rangle \sim d$, plays a vital role in determining the quantum nature of the fluid. In case of helium, the thermal de Broglie wavelength $\lambda_{^4\mathrm{He}} \approx 0.4$ nm happens to be *greater* than the typical inter-atomic distance $d \approx 0.27$ nm: this makes the quantum mechanical effects predominant in

liquid ^{4}He. For lighter isotopes like ^{3}He, the thermal de Broglie wavelength is even larger and thus the quantum effects become even more pronounced in its liquid state.

In case of ^{4}He there exists two distinct liquid phases, He I and II as shown in FIG. 1.2.2. He I is a **normal liquid** phase, characterised by fairly standard liquid state properties, but He II is a **superfluid**, characterised by fluid flow with special properties as first discovered and studied in 1938 by Pyotr Kapitsa [Kapitza 1938], John F. Allen and Don Misener [Allen and Misener 1938].

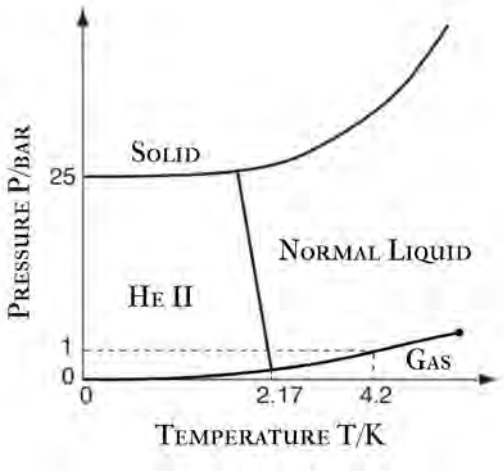

Figure 1.2.2: Schematic phase diagram of ^{4}He showing the two different liquid phases: the normal liquid, He I and the superfluid phases, He II. Note the absence of a triple point. The λ-point is at 2.17 K and the boiling point at 4.2 K. The solid phase only exists at pressures above 25 bar while gas-liquid phase line terminates at the critical point. [4]

In line with László Tisza's original proposal of 1938, a two-fluid model of helium consists of a small percentage of superfluid He II in the Bose Einstein condensed state for temperature $T \in (0\,\mathrm{K}\,, T_c \sim 2.17\,\mathrm{K}]$ [Tisza 1938]. Beyond this critical temperature, the superfluidity disappears and the fluid exists as thermal excitations comprising of the normal fluid He I.

For helium experiencing temperatures $0 \leq T \sim T_D \leq T_c$, there exists a sort of dual phenomenological flow: normal fluid flow subject to viscosity constraints, and the superfluid flow that is a frictionless enterprise. This is analogous to the

[4] Picture simulated with `Adobe Illustrator CS5`

idea of the system having a condensate particle density n_0 in the lowest energy state with momentum $\vec{k} = 0$ (superfluid state) and an average particle density n in the remaining occupied excited states with momentum $\vec{k} \neq 0$. In effect, the thermal properties of the system can be described as a sum of the ground-state condensate fraction $\langle N_0 \rangle$ that are ordered and makes zero entropy contribution, together with the normal fluid fraction $\langle N \rangle$ consisting of the particles in excited states that have a conventional entropy. Ignoring entrainment effects, these two thermodynamic regimes are assumed to have particle-motions that occur internally within them without any transfer of momentum from one to the other. It should however be held that this two-flow description of helium is adopted for the purpose of convenience in its description; an accurate description of helium would have to include the regions of admixture of the two parts of the fluid. Incidentally, at the boundary between He I and II phases, a characteristic singularity in the specific heat of ^{4}He is observed, this is called the λ-point due to the characteristic shape of the curve as seen in FIG. 1.2.3.

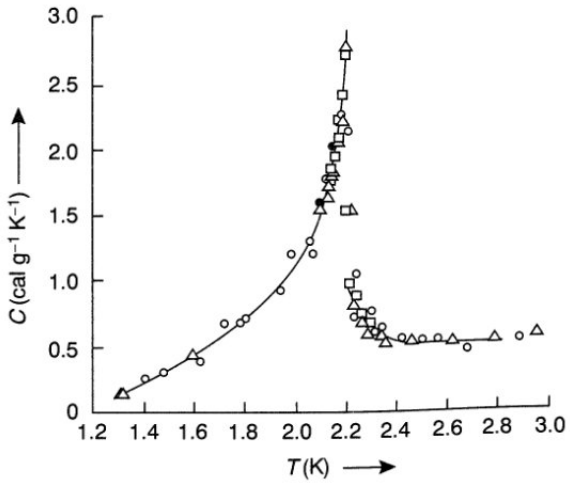

Figure 1.2.3: Specific heat of liquid helium at saturated vapour pressure as a function of temperature showing the λ transition of ^{4}He. [5]

At the very outset, one understands the theory of thermodynamic phase-transitional systems — the ones based on the hypotheses of scaling and the critical exponents — to be calculated using methods of renormalizable group analysis. That is to say,

[5] Picture based on Keemson et. al (1958), sourced from [Pathria 1996]

the scaling of the specific heat $C_V(T)\Big|_{T\longrightarrow T_c}$ in superfluid helium obeys a power law behaviour. At temperatures $T_D \ll T_c$, specific heat is $C_V \sim T_D^3$ in He II. This universality can then be extended to imply the concept of *gauge invariance* as presented by the field theoretical formulation applied to the superfluidity of helium (*cf.* §. 1.3).

1.2.3 Superfluid crustal interiors of Neutron stars

The application of Bardeen–Cooper–Schrieffer (BCS) theory of electron superconductivity [Bardeen et al. 1957] to nuclei commenced with the likes of Aage Bohr, Ben Mottelson *&* David Pines [Bohr et al. 1958] and Spartak Belyaev [Beliaev 1959]. In fact, while looking at the moment of inertia of nuclei, Arkady Migdal [Midgal 1959] indicated to the possibility of superfluidity occurring in the neutron-core of stars. Formally however, it was Vitaly Ginzburg and David Kirzhnits [Ginzburg and Kirzhnits 1964] who theoretically studied the superfluidity inside neutron stars in 1964 and soon after, Richard Wolf [Wolf 1966] calculated that the free neutrons in the crust were in fact a superfluid. Remarkably though, all this work preceded the actual discovery of pulsars by Jocelyn Bell and Anthony Hewish in 1967!

The central idea of BCS theory of superconductivity relies on the coupling of the electrons with the lattice vibrations. This leads to an effective attraction between electrons (generalised to fluid Fermions) despite the repulsive Coulomb force between them: the resultant structure being the **Cooper pairs** of opposite-spin electrons with zero angular momentum effectively behaving like a Boson. The system can then undergo a thermodynamically motivated phase transition and condense into a macroscopically coherent ground energy state giving rise to superfluidity (as in the case of liquid ^{4}He). For charged Fermionic particles, the condensate turns out to be in a superconducting state. In general though, for highly degenerate Fermi systems the pairing occurs mainly between states near the Fermi surface. Thus in heavy nuclei, or in neutron stars, where the ratio of $n_{\text{neutrons}}/n_{\text{protons}}$ is high, one can only consider p-p and n-n pairing because the states with opposite momentum are at different Fermi surfaces for neutrons and protons.

According to our current understanding [Lombardo and Schulze 2000], the interior of neutron stars are permeated by two different kinds of neutron superfluids. Additionally, a proton superconductor — similar to conventional electron superconductors — is also thought to be present in the neutron star interior. Typically though, in the crust and the outer core of the neutron star, the neutron pairs are expected to form an isotropic Bosonic superfluid like ^{4}He, where as in the denser layers, they are believed to form a more exotic kind of (anisotropic) superfluid with constituent member having parallel spin (as in the case of superfluid ^{3}He). Strictly speaking, neutron-proton pairs could also exists, however, the asymmetric nuclear matter of neutron stars do not seem to favour their formation.

According to the calculations of David Pines et al. (1980) [Pines et al. 1980], at least three distinct hadron superfluids are believed to exist inside a neutron star -

1. In the inner crust (4.3×10^{11} g cm^{-3} $< \rho <$ 2×10^{14} g cm^{-3}), the free neutrons may pair in a singlet $^1S_0$ state to form a superfluid amidst the neutron-rich nuclear cluster arranged into a Coulomb bcc lattice.

2. In the quantum liquid regime ($\rho > 2 \times 10^{14}$g cm^{-3}), where the nuclear cluster lattice have dissolved into a degenerate fluid of neutrons and protons, the neutron fluid is likely to be a paired in a triplet $^3P_2$ state, where as the protons in the quantum liquid are expected to be superconducting in a singlet $^1S_0$ state.

According to the Cooper theorem [Cooper 1956], the formation of Cooper pairs and the resulting condensate is expected to occur, given low enough temperature, in any degenerate system of fermions in which there is an attractive interaction between particles whose momenta lie close to the Fermi surface. The *binding energy of the pair* (effectively, the strength of the interaction pair measured as the *gap function*) helps determine the critical temperature T_c at which this pairing phase-transition occurs. This is to say that in neutron star matter, the strong interaction between neutrons, between protons, and probably between hyperons, immediately provide attractive channels for pairing and the pairing gap Δ (that acts as an order parameter) is temperature dependent i.e., $\Delta \equiv \Delta(T)$. The isotropic pairing gap at zero temperature (and Fermi momentum, $p_{\mathcal{F}}$) is related to the critical temperature of superfluid phase transition, T_c by a general expression of the

form: $\Delta_{\mathcal{F}}(T=0) = \pi e^{-\gamma} k_{\mathrm{B}} T_c \simeq 1.76 k_{\mathrm{B}} T_c$ with γ as the Euler-Mascheroni constant (~ 0.58). This expression, shows that $\Delta_{\mathcal{F}}(T=0) \sim 1$ MeV correspond to $T_c \sim 10^{10}$ K: considerably larger than any typical median age neutron stars. For $T > T_c$ the pairing gap vanishes along with any superfluid phase, whereas it rapidly grows when $T < T_c$. This provides the theoretical justification for neutron superfluidity in the inner crust of neutron stars [Bardeen et al. 1957].

The **coherence length or healing length**, which broadly speaking, represents the size of a neutron pair, is important when compared with the characteristic size of the inhomogeneities (taken here to mean, the lattice-arranged nuclei in nuclear clusters). This comparison helps understand the effects of these inhomogeneities on the neutron superfluid. In line with Anderson's theorem [Gennes 1966], the effect of these inhomogeneities on the neutron superfluid is negligible when the coherence length is *larger* than the characteristic size of the inhomogeneities. A rough estimate of coherence length (assuming weak coupling) is provided by the Pippard coherence length expression, given as $\xi = \hbar^2 p_{\mathcal{F}} \Big/ \pi \Delta_G m_{np}$, where Δ_G is the neutron paring gap at the Fermi momentum $p_{\mathcal{F}}$ and m_{np} being the mass of the neutron pair.

The denser regions of the inner crust, where the coherence length is much smaller than the inter-nuclear spacing, the neutron superfluid is a BEC of strongly-bound neutron pairs (like ^{4}He atoms). However, in the shallower layers of the inner crust, the neutron superfluid is in a BCS regime of overlapping loosely-bound Fermion quantum pairs (like in liquid ^{3}He). A detailed discussion of the BCS-BEC cross over, with regards to density profile and strong coupling in neutron star interior can be found in [Sedrakian and Clark 2006]. This then presents a picture of neutron superfluid in the inner crust of the neutron star being an inhomogeneous superfluid rather than a superfluid flowing past clusters like obstacles. The concept of hadron superfluidity within the neutron star matter is pivotal to the explanation of many observational effects — including the sudden changes in the pulsar periods known as glitches [Alpar et al. 1982; Pines et al. 1992] that is of interest here.

1.3 Superfluid condensate wave function

The idea of a coherent macroscopic occupation of ground state being described by a wave function was proposed initially by Fritz London [London 1938] in 1938 who related the formation of the superfluid to a Bose Einstein condensate (BEC). In the description of a superfluid and more specifically BEC, it is useful to discuss its behaviour by using a quantum field theoretic approach to many-body systems (otherwise studied with tools of second quantization). This equivalent approach was formalised by S. T. Beliaev [Beliaev 1958] in 1958 and developed by Nikolay Bogoliubov [Bogoliubov 1970], J. Gavoret and Phillipe Nozières [Gavoret and Nozieres 1964], Peter Martin and Pierre Hohenberg [Hohenberg and Martin 1965] and others in the 1960's [Griffin 1993].

1.3.1 Order parameter and Spontaneous symmetry breaking

According to the rules of second quantization, a quantum operator could be expressed as $\hat{\psi}(\mathbf{r})$ (annihilate an atom at $\mathbf{r}$) or $\hat{\psi}^\dagger(\mathbf{r})$ (creates an atom at $\mathbf{r}$) with the standard Bose commutation relation, $[\hat{\psi}(\mathbf{r}), \hat{\psi}^\dagger(\mathbf{r}')] \equiv \delta(\mathbf{r}-\mathbf{r}')$. All observable can then be written in terms of these quantum field operators, as will be seen in §. 1.3.2

The operator, $\hat{\psi}(\mathbf{r})$ can be decomposed — as original proposed by Nikolay Bogoliubov (1947) and later generalised by S. T. Beliaev — into the condensate term (lowest energy ground state) and the non-condensate components (excited states) in all cases of lowest-energy single particle states having macroscopic occupation as follows –

$$\hat{\psi}(\mathbf{r}) = \left\langle \hat{\psi}(\mathbf{r}) \right\rangle + \delta\hat{\psi}(\mathbf{r}) \qquad [1.3.1]$$

where $\left\langle \hat{\psi}(\mathbf{r}) \right\rangle \equiv \psi_0(\mathbf{r})$ is the Bosonic macroscopic wavefunction. This notion is based on the understanding that while calculating the ensemble-averages in nonlinear dynamics, the macroscopic ground-state occupation (of the condensate with $n_0 \gg 1$) was considered separate to the various other excited states (as seen in §. 1.2.1). This implies a closed form equation of the classical field $\psi_0(\mathbf{r})$ and the small perturbative fluctuations $\delta\hat{\psi}(\mathbf{r})$ around the average value.

The classical field $\psi_0(\mathbf{r})$ is called the **condensate wave function** and plays the role of an **order parameter** for the superfluid transition, i.e.,

$$\psi_0(\mathbf{r}) \begin{cases} = 0 & T_D > T_c \\ \neq 0 & T_D < T_c \end{cases} \qquad [1.3.2]$$

The order parameter $\psi_0(\mathbf{r})$ is characterised by a modulus and a phase: $\psi_0(\mathbf{r}) = |\psi_0(\mathbf{r})|e^{iS(\mathbf{r})}$. The modulus $|\psi_0(\mathbf{r})|$ determines the particle density, $n_0(\mathbf{r}) = |\psi_0(\mathbf{r})|^2$ of the condensate (or effectively, the total condensate particle number $N_0(\mathbf{r})$ as seen from $\int |\psi_0(\mathbf{r})|^2 \, \mathrm{d}\mathbf{r} = \langle N_0 \rangle$) and the arbitrary phase $S(\mathbf{r})$ presents a residual degree of freedom, e.g., multiplication by a phase factor $\gamma \equiv e^{i\alpha}$ without any change to the underlying physics of the system. In order words, the phase of the condensate wavefunction is a global phase $S(\mathbf{r}) \equiv \alpha \in [0, 2k\pi)\Big|_{k\in\mathbb{Z}^+}$ This phenomenon is a direct manifestation of the inherent **gauge symmetry** of the problem. Physically, the lack of phase stabilisation force can be thought of as responsible for the random phase of the condensate.

However, in the superfluid phase following BEC phase transition, the system always *spontaneously* chooses *one fixed value* of α when minimizing the energy, i.e., in the ground state of the system, the phase factor $\gamma_{0_{GS}}$ is fixed. This phase transition then destroys the symmetry of the energy (inherent in the original lagrangian for the system) and this phenomenon is referred to as **spontaneous symmetry breaking**. Making an explicit choice for the phase $\gamma_{0_{GS}}$ in spite of the lack of a preferred phase value, localizes and *clamps* the condensate wave function, which in turn implies that the particle number density n_0 of the condensate is arbitrary: this justifies the claim of a coherent quantum state of occupation.

1.3.2 Dynamics of the order parameter: Gross Pitaevskii Equation

According to the rules of second quantization, the many-body Hamiltonian describing n_0 interacting particles of mass m for the external potential $V_{\text{ext}}(\mathbf{r})$ and particle-particle interaction potential $V_{\text{int}}(\mathbf{r}, \mathbf{r}')$ is expressed in terms of the Bosonic field operators $\hat{\psi}(\mathbf{r})$ $\left[\hat{\psi}^\dagger(\mathbf{r})\right]$ that annihilate [create] Bosons at coordinates $\{\mathbf{r}\}$ and

satisfy the Bosonic commutation algebra as –

$$\hat{\mathcal{H}} = \int \mathrm{d}^3\mathbf{r}\hat{\psi}^\dagger(\mathbf{r})\underbrace{\left\{\left(-\frac{\hbar^2}{2m}\right)\nabla^2 + V_{\text{ext}}(\mathbf{r})\right\}}_{\text{single particle hamiltonian}}\hat{\psi}(\mathbf{r}) \qquad [1.3.3]$$
$$+\frac{1}{2}\int \mathrm{d}^3\mathbf{r}\int \mathrm{d}^3\mathbf{r}'\hat{\psi}^\dagger(\mathbf{r})\hat{\psi}^\dagger(\mathbf{r}')V_{\text{int}}(\mathbf{r},\mathbf{r}')\hat{\psi}(\mathbf{r})\hat{\psi}(\mathbf{r}')$$

For sufficiently dilute Bose gas, the pseudo potential is $V_{\text{int}}(\mathbf{r},\mathbf{r}') \equiv g\delta(\mathbf{r}'-\mathbf{r})$ where $g = 4\pi\hbar^2 a/m$ and a being the s-wave scattering length using the Born approximation [Pitaevskii and Stringari 2003]. Moreover, using the Bosonic commutation relation $[\hat{\psi}(\mathbf{r}'),\hat{\psi}^\dagger(\mathbf{r})] = 0$, the Heisenberg time evolution equation can be expressed as –

$$i\hbar\frac{\partial\hat{\psi}(\mathbf{r}',t)}{\partial t} = [\hat{\psi}(\vec{r'},t),\hat{\mathcal{H}}] = \left\{\left(-\frac{\hbar^2}{2m}\right)\nabla^2 + V_{\text{ext}}(\mathbf{r}) + g\hat{\psi}^\dagger(\mathbf{r}',t)\hat{\psi}(\mathbf{r}',t)\right\}\hat{\psi}(\mathbf{r}',t)$$

Decomposing the Bosonic field operator in terms of the macroscopically populated mean field term (condensate) $\psi_0(\mathbf{r}',t) \equiv \left\langle\hat{\psi}(\mathbf{r})\right\rangle$ and a fluctuation/perturbation term $\delta\hat{\psi}(\mathbf{r}',t)$ as $\hat{\psi}(\mathbf{r}',t) = \psi_0(\mathbf{r}',t) + \delta\hat{\psi}(\mathbf{r}',t)$ and with the idea of symmetry breaking average, we obtain –

$$\begin{aligned}\left\langle\hat{\psi}^\dagger(\mathbf{r}',t)\hat{\psi}(\mathbf{r}',t)\hat{\psi}(\mathbf{r}',t)\right\rangle &= n_0(\mathbf{r}',t)\psi_0(\mathbf{r}',t) + \\ &\quad \tilde{m}\psi_0^*(\mathbf{r}',t) + \tilde{n}\psi_0(\mathbf{r}',t) + \\ &\quad \left\langle\delta\hat{\psi}^\dagger(\mathbf{r}',t)\delta\hat{\psi}(\mathbf{r}',t)\delta\hat{\psi}(\mathbf{r}',t)\right\rangle\end{aligned}$$

where we have

$n_0(\mathbf{r}',t)$	$\lvert\psi_0(\mathbf{r}',t)\rvert^2$	condensate density
$\tilde{m}(\mathbf{r}',t)$	$\left\langle\delta\hat{\psi}(\mathbf{r}',t)\delta\hat{\psi}(\mathbf{r}',t)\right\rangle$	off-diagonal anomalous density
$\tilde{n}(\mathbf{r}',t)$	$\left\langle\delta\hat{\psi}^\dagger(\mathbf{r}',t)\delta\hat{\psi}(\mathbf{r}',t)\right\rangle$	non-condensate density

In general, the Heisenberg time evolution equation for $\hat{\psi}(\mathbf{r}',t)$ is not closed, i.e., it is coupled to the dynamics of the non-condensate. However, for temperatures $T \ll T_{\text{BEC}}$, we can ignore the non-condensate fractions and only consider the

leading order term in $\psi_0(\mathbf{r}', t)$ as (replacing r' by r) –

$$i\hbar\frac{\partial\psi_0(\mathbf{r},t)}{\partial t} = \left\{-\left(\frac{\hbar^2}{2m}\right)\nabla^2 + V_{\text{ext}}(\mathbf{r}) + g|\psi_0(\mathbf{r},t)|^2\right\}\psi_0(\mathbf{r},t) \qquad [1.3.4]$$

This is the *time dependent* expression of the nonlinear Schrödinger equation or **Gross Pitaevskii equation**.

Neglecting the lower order cross terms involving the fluctuation operator $\delta\hat{\psi}(\mathbf{r}', t)$ amounts to neglecting thermal and quantum depletion of the condensate. This is a valid approximation when the temperature is much less than the transition temperature for the onset of condensation and when the condensate is sufficiently weakly interacting — a valid consideration for the scattering length $a \ll \lambda_{\text{dB}}$ where λ_{dB} is the thermal de Broglie wavelength of the particles.

The energy functional $E_{n_0}(\psi_0)$ of the condensate in a coherent state can be shown to be given as –

$$E_{n_0}(\psi_0) = \frac{\langle\phi|\hat{\mathcal{H}}|\phi\rangle}{\langle\phi|\phi\rangle} = \int \mathrm{d}^3\mathbf{r}\left\{\left(\frac{\hbar^2}{2m}\right)|\nabla\psi_0(\mathbf{r})|^2 + V_{\text{ext}}(\mathbf{r})|\psi_0(\mathbf{r})|^2 + \frac{g}{2}|\psi_0(\mathbf{r})|^4\right\} \qquad [1.3.5]$$

We note that with $V_{\text{ext}}(\mathbf{r}) = 0$ and $\nabla^2\psi_0(\mathbf{r}) = 0$ we have –

$$\begin{aligned} E_{n_0}^{\text{cond}} &= \int \mathrm{d}\mathbf{r}\frac{g}{2}|\psi_0(\mathbf{r})|^4 = \frac{gn_0^2}{2}\mathcal{V} \text{ where} \\ n_0 &= \int|\psi_0(\mathbf{r})|^2\,\mathrm{d}\mathbf{r} \text{ and } \int\varphi_0^*(\vec{r})\varphi_0(\vec{r})\,\mathrm{d}\vec{r} \equiv \mathcal{V}\Big|_{\text{volume}} \\ \text{and } \hbar\mu &= gn_0 \end{aligned} \qquad [1.3.6]$$

Also, since the total number of particles in the system $\langle N_0\rangle \equiv n_0$ can be estimated as $n_0 = \int|\psi_0(\mathbf{r})|^2\,\mathrm{d}\mathbf{r}$ and the chemical potential μ is defined as $\mu \equiv \dfrac{\delta E_{n_0}}{\delta n_o}$, we have (treating $\psi_0 \equiv \psi_0(\mathbf{r})$): $f(\psi_0, \psi_0^*) \equiv \delta E_{n_0} - \mu\delta n_0 = \delta(E_{n_0} - \mu n_0)$, leading to the *time independent* expression for the Gross Pitaevskii equation –

$$\mu\psi_0(\mathbf{r}) = \left[-\frac{\hbar^2}{2m}\nabla^2 + V_{\text{ext}}(\mathbf{r}) + g|\psi_0(\mathbf{r})|^2\right]\psi_0(\mathbf{r}) \qquad [1.3.7]$$

This equation is used to determine the order parameter $\psi_0(\mathbf{r})$ of the condensate.

The time dependence of the order parameter is expressed in terms of the chemical potential μ as $\psi_0(\mathbf{r}) \equiv \exp(i\mu t/\hbar)\psi_0(\mathbf{r})$.

Based on the principles of *spontaneous symmetry breaking* (a detailed discussion is found in [Rubakov 2002]), if the chemical potential μ is positive, the potential energy is minimised along a continuous degeneracy and the global U(1) symmetry is then *spontaneously broken.* A physical system undergoes a phase transition at a critical temperature T_c, if a chemical potential satisfies the conditions –

$$\mu \leq 0\,;\; T_D \geq T_c \text{ and } \psi_{GS} = 0 \text{ OR } \mu > 0\,;\; T_D < T_c \text{ and } \psi_{GS} = \sqrt{2\mu/g}$$

A schematic temperature dependence of the potential $V[\psi_0]$ is represented in FIG. 1.3.1. For $T_D > T_c$, the potential has only one minimum at $[\psi_0]_{GS} = 0$ and the curvature at $[\psi_0]_{GS} = 0$ is positive. When $T_D = T_c$, the curvature at the minimum is zero, $\dfrac{\partial^2 V[\psi_0]}{\partial\psi_0\partial\psi_0^*}\Big|_{\psi_{GS}=0} = 0$. For $T_D < T_c$, the curvature at $[\psi_0]_{GS} = 0$ is negative and the scalar field rolls down to the minimum, i.e., $|[\psi_0]_{GS}| = \sqrt{\dfrac{\mu}{g}}$. Thus, there is no barrier of potential between the minimum at $[\psi_0]_{GS} = 0$ and $|[\psi_0]_{GS}| = \sqrt{\dfrac{\mu}{g}}$, indicating a **second-order phase transition**.

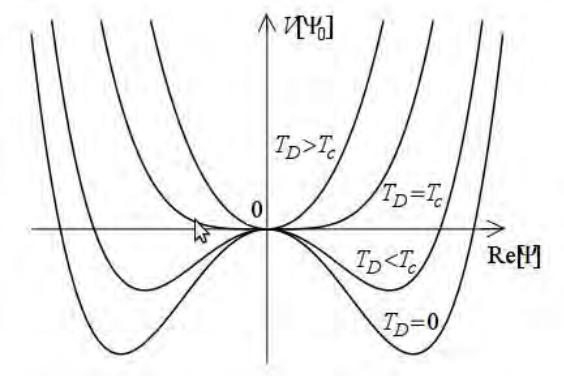

Figure 1.3.1: The schematic temperature dependence of the potential $V[\psi_0]$ for a second-order phase transition. [6]

[6]Figure sourced from [Harada 2009]

1.3.3 Superfluid hydrodynamic formulation

The condensate wave function (order field) $\psi_0(\mathbf{r},t)$ is related to the condensate particle number density $n_0(\mathbf{r},t)$ (which is also identified with the superfluid density $\rho_s(\mathbf{r},t)$ through the mass $m_{np} \equiv m$ of the neutron pairs that forms the superfluid constituent) by the relation –

$$\sqrt{\frac{\rho_s(\mathbf{r},t)}{m}} \equiv \sqrt{n_0(\mathbf{r},t)} = |\psi_0(\mathbf{r},t)| \Rightarrow \langle N_0 \rangle \equiv \int n_0(\mathbf{r},t)\,\mathrm{d}r = \int |\psi_0(\mathbf{r},t)|^2\,\mathrm{d}r \qquad [1.3.8]$$

Also, when the order parameter $\psi_0(\mathbf{r},t)$ is expressed in terms of its amplitude and phase using Madelung's transformation, we have –

$$\psi_0(\mathbf{r},t) \equiv |\psi_0(\mathbf{r},t)|e^{i\alpha} \equiv \sqrt{n_0(\mathbf{r},t)}e^{i\gamma_0(\mathbf{r},t)} \equiv \sqrt{\frac{\rho_s(\mathbf{r},t)}{m}}e^{i\gamma_0(\mathbf{r},t)} \qquad [1.3.9]$$

The wave function is defined up to a global phase factor. The key distinguishing feature of a superfluid is the *symmetry breaking* of this gauge invariance by imposing the phase $\gamma_0(\mathbf{r},t)$ to be *local*, i.e., in effect clamping the phase.

Particle Continuity and Phase Equations

The Euler continuity equation for superfluidity can be calculated as $\frac{\partial}{\partial t}n_0(\mathbf{r},t) + \mathrm{div}[j(\mathbf{r},t)] = 0$, where the particle current density is given as $j(\mathbf{r},t) = -\frac{i\hbar}{2m}(\psi_0^*(\mathbf{r},t)\nabla\psi_0(\mathbf{r},t) - \psi_0(\mathbf{r},t)\nabla\psi_0^*(\mathbf{r},t))$. This Euler continuity equation helps conclude that the Gross Pitaevskii equation guarantees the conservation of the total particle number given by $\langle N_0 \rangle = \int n_0(\mathbf{r},t)\,\mathrm{d}\mathbf{r}$.

Using the definition of the condensate wave function as seen in EQN. [1.3.9], we find that –

$$\begin{aligned}
\nabla\psi_0(\mathbf{r},t) &= e^{\gamma_0(\mathbf{r},t)}\nabla\left(\sqrt{n_0(\mathbf{r},t)}\right) + i\sqrt{n_0(\mathbf{r},t)}e^{i\gamma_0(\mathbf{r},t)}\nabla\gamma_0(\mathbf{r},t) \\
\nabla\psi_0^*(\mathbf{r},t) &= e^{-\gamma_0(\mathbf{r},t)}\nabla\left(\sqrt{n_0(\mathbf{r},t)}\right) - i\sqrt{n_0(\mathbf{r},t)}e^{-i\gamma_0(\mathbf{r},t)}\nabla\gamma_0(\mathbf{r},t)
\end{aligned}$$

The particle current density equation can then be expressed as –

$$j(\mathbf{r},t) = n_0(\mathbf{r},t)\frac{\hbar}{m}\nabla\gamma_0(\mathbf{r},t) \qquad [1.3.10]$$

However, since the condensate density is $n_0(\mathbf{r},t)$ and the net current of particles equals a density times velocity, we can interpret the above result as showing the condensate flowing with particle velocity $\vec{v}_s(\mathbf{r},t)$ given as –

$$\vec{v}_s(\mathbf{r},t) = \frac{\hbar}{m}\nabla\gamma_0(\mathbf{r},t) \qquad [1.3.11]$$

The phase of the order parameter plays the role of a velocity potential and $\vec{v}_s(\mathbf{r},t)$ is referred to as a velocity field. The EQN. [1.3.11] is called the **Landau criterion for superfluidity**.

To relate the Euler continuity equation to its hydrodynamic equivalent, it is useful to make the identification $\rho_s(\mathbf{r},t) = mn_0(\mathbf{r},t)$ and using EQN. [1.3.10] and EQN. [1.3.11], the Euler continuity equation can be expressed in its standard form as seen by –

$$\frac{\partial}{\partial t}\rho_s(\mathbf{r},t) + \nabla.\left[\rho_s(\mathbf{r},t)\,\vec{v}_s(\mathbf{r},t)\right] = 0 \qquad [1.3.12]$$

Further, inserting EQN. [1.3.9] into EQN. [1.3.4], an explicit equation for the phase $\gamma_0(\mathbf{r},t)$ can be derived as –

$$\begin{aligned} -\hbar\frac{\partial}{\partial t}\gamma_0(\mathbf{r},t) \;=\; & \Big\{\frac{1}{2}mv_s^2(\mathbf{r},t) + V_{\text{ext}}(\mathbf{r},t) + gn_0(\mathbf{r},t) - \\ & \underbrace{\frac{\hbar^2}{2m\sqrt{n_0(\mathbf{r},t)}}\nabla^2\sqrt{n_0(\mathbf{r},t)}}_{\text{quantum pressure}}\Big\} \end{aligned} \qquad [1.3.13]$$

The Euler continuity EQN. [1.3.12] along with EQN. [1.3.13] form a closed set of coupled equation that are fully equivalent to the Gross Pitaevskii equation in EQN. [1.3.4].

Back in 1967, G. J. Troup had demonstrated the uncertainty in the particle number, $\langle N\rangle$ and the phase, $\gamma_0(\mathbf{r},t)$ as $\delta\langle N\rangle\,\delta\gamma_0(\mathbf{r},t) \approx 1$ [Troup 1967]. This remarks to

fact of $\langle N \rangle$ and $\hbar\gamma_0(\mathbf{r}, t)$ being treated as conjugate variables in line with standard quantum mechanics techniques.

Using the principles of Hamiltonian mechanics, an **alternative form of Landau criterion for superfluidity** can be derived as –

$$\nabla \times \vec{v}_s(\mathbf{r}, t) = 0 \quad \text{if} \quad v_s(\mathbf{r}, t) \neq 0 \tag{1.3.14}$$

The time independent form of the Gross Pitaevskii equation can be calculated from this approach and is found to be identical to the one seen in EQN. [1.3.7]. The nontrivial, stable and real solution of the equation with the lowest energy defines the order parameter of the ground state. This solution has the form identical to what was seen before corresponding to the minimization of the potential, i.e., $[\psi_0]_{GS} \equiv \frac{\psi_{GS}}{\sqrt{2}} e^{i\gamma_{0GS}} \equiv \sqrt{\frac{\mu}{g}} e^{i\gamma_{0GS}}$. The ground state of the system is the pure superfluid state and all the excited states are then complex perturbative functions upon the ground state — the quantized vortex state being the most famous example of such an excited state.

Big whirls have little whirls
That feed on their velocity,
And little whirls have lesser whirls
And so on to viscosity.

Lewis Fry Richardson, 1922

2

Vortices: Theory and Dynamics

2.1 Flux quantization and Vortices

The Landau criterion for superfluidity bears an important impact on superfluid rotation and this can be seen by defining the **circulation** of the superfluid as –

$$\begin{aligned} \kappa &= \oint_L \vec{v}_s(\mathbf{r},t).d\vec{l} \quad L \equiv \text{circulation contour in superfluid} \\ \Rightarrow \kappa &= \int_A [\nabla \times \vec{v}_s(\mathbf{r},t)].d\vec{A}\Big|_{\text{Stokes theorem}} \\ \Rightarrow \kappa &= 0 \quad \because (\nabla \times \vec{v}_s(\mathbf{r},t)) = 0 \quad \text{using EQN. [1.3.14]} \end{aligned} \tag{2.1.1}$$

This result of zero circulation then implies an irrotational nature to superfluids: an idea corroborated famously by the Andronikashvilli experiment [Andronikashvilli 1946] where an oscillating pile of disks "entrained" the normal component and left the superfluid component at rest. However in 1950, an experiment conducted by D.V.Osborne rotated a cylindrical bucket containing He II where both the normal

and the superfluid components were found to be moving with the same angular velocity [Osborne 1950]. Central to understanding this apparent contradiction between the experimental evidence of rotation in a superfluid and its theoretical prediction of irrotationality lies in looking at the region inside the integration contour of the superfluid as *multiply connected*. The discontinuous *holes* in the superfluid are regions where $\nabla \times \vec{v}_s(\mathbf{r}, t) \neq 0$. These holes give rise to the concept of **vortex core**: a hole in the superfluid — either empty of fluid or containing normal fluid — that has cylindrical symmetry and is surrounded by superfluid matter experiencing irrotational flow, once again, with cylindrical symmetry.

This lets us rewrite the circulation (using EQN. [1.3.11]) as –

$$\kappa = \oint_L \vec{v}_s(\mathbf{r}, t).d\vec{l} = \frac{\hbar}{m} \oint_L \nabla\gamma_0(\mathbf{r}, t).d\vec{l} = \frac{\hbar}{m}[\Delta\gamma_0(\mathbf{r}, t)]_L \qquad [2.1.2]$$

Here, $[\Delta\gamma_0(\mathbf{r}, t)]$ is the change in the phase angle $\gamma_0(\mathbf{r}, t)$ (of the condensate wave function, $\psi_0(\mathbf{r}, t)$) after going around the contour L. This is because $\nabla\gamma(\mathbf{r}, t)$ can be understood as the gradient pointing in the direction of phase change along the continuously degenerate curve of equipotential.

Thus $\Delta\gamma_0(\mathbf{r}, t) = 2\pi k$ [$k \in \mathbb{Z}$], with the zero value corresponding to the Landau criterion of superfluidity and the multiples of 2π giving the non-zero circulation.

Using this idea, the circulation in EQN. [2.1.2] can be expressed as –

$$\kappa \sim k\frac{h}{m}\Big|_{k\in\mathbb{Z}} \qquad [2.1.3]$$

The circulation of the flow is therefore *quantized* in units of the quantum of circulation, h/m. Also, the quantum number k corresponds to the *topological winding number* for the phase $\gamma_0(\mathbf{r}, t)$ around the closed loop, i.e., it counts the number of times that $\gamma_0(\mathbf{r}, t)$ winds through 2π on going around any closed path.

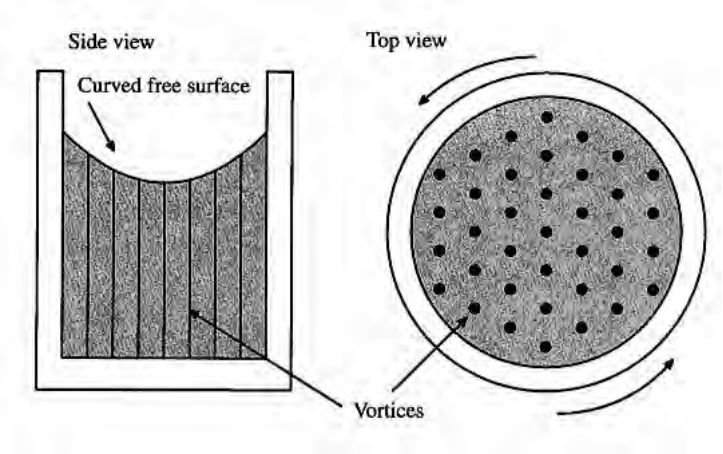

Figure 2.1.1: Schematic representation of superfluid in a rotating cylinder. A dense array of vortices develop and the free surface becomes curved due to usual centrifugal effect.[7]

Thus we understand that although simply connected regions in the bulk prevent superfluid flow, the presence of many multiply connected regions of *quantized vortex lines* (a cylindrical extension to the vortex core) in the macroscopic bulk of the superfluid can lead to rotation. In fact, the free surface of a rotating ^{4}He superfluid becomes curved due to the normal rotational centrifugal force as seen in FIG. 2.1.1

Considering a streamline located at a radius r from the centre of an isolated vortex line: due to the cylindrical symmetry of the vortex structure, one can infer that the circulation κ (at an instant of time t) can be expressed as $\kappa = \oint_L \vec{v}_s(\mathbf{r},t).d\vec{l} = 2\pi r v_\phi$. Thus we have the linear velocity $\vec{v}_s(\mathbf{r},t)$, angular velocity $\vec{\Omega}_s(\mathbf{r},t)$ and correspondingly, the angular momentum $\vec{L}(\mathbf{r},t)$ of the fluid at a given distance from the vortex core as –

$$\vec{v}_s(\mathbf{r},t) \equiv v_\phi\hat{\phi} = \frac{\kappa}{2\pi r}\hat{\phi} = \left|\frac{k\hbar}{mr}\right|\hat{\phi} \Rightarrow v_s = \frac{k\hbar}{mr} \qquad [2.1.4]$$

$$\Rightarrow (\vec{\Omega}_s \times \mathbf{r}) \equiv \Omega_s\hat{\mathbf{z}} \times r\hat{\mathbf{r}} \equiv \Omega_s r\hat{\phi} = \left|\frac{k\hbar}{mr}\right|\hat{\phi} \Rightarrow \Omega_s r = v_s$$

$$\Rightarrow \vec{L} = r\hat{\mathbf{r}} \times \underbrace{m\vec{v}_s}_{\text{linear momentum}} \equiv r\hat{\mathbf{r}} \times mv_\phi\hat{\phi} = mv_\phi r\hat{z} = k\hbar\hat{\mathbf{z}} \qquad [2.1.5]$$

[7] Picture simulated with `Adobe Illustrator CS5` (originally sourced from [Annett 2004])

This shows that, in addition to the circulation, both the angular velocity and angular momentum of the fluid around the vortex line are quantized.

Each individual vortex contributes h/m to the overall circulation of the fluid and thus we have the net circulation of the fluid given as –

$$\begin{aligned} \kappa_{\text{total}} &= \frac{h}{m} N_\nu \quad \text{where} \quad N_\nu = \sum \text{vortices in rotating fluid} \\ \text{Also } \kappa_{\text{total}} &= \oint_L \vec{v}_s . d\vec{l} \equiv \oint_L (\vec{\Omega}_s \times \vec{R}) . d\vec{l} = 2\pi R^2 \Omega_s \\ \Rightarrow \frac{N_\nu}{\pi R^2} &= \frac{2m\Omega_s}{h} : \text{Feynman-Osanger relation [Feynman 1972]} \quad [2.1.6] \end{aligned}$$

where R is the radius of the cylinder and Ω_s is the angular speed of rotation. This gives an indication of the number of vortices per unit area in the rotating superfluid. As represented in FIG. 2.1.1, at small rotations rates in helium, vortices are formed into quite well ordered triangular arrays — an idea first proposed by Tkachenko [Tkachenko 1966] in 1966. The inter vortex spacing d_ν is then taken to be –

$$d_\nu = \sqrt{\frac{h}{\sqrt{3} m \Omega_s}} \qquad [2.1.7]$$

When the length scales get larger than this inter vortex spacing d_ν, the superposition of the flow patterns of all the vortex lines result in the superfluid flow resembling a rigid body rotation.

2.2 Single vortex line in superfluids

The existence of quantized vortices were independently predicted by Richard Feynman [Feynman 1955] and Alexei Abrikosov [Abrikosov 1957] in the early 1950s, however the first experimental evidence of quantized vortex lines in superfluid He II was recorded by Henry Hall and Joe Vinen [Hall and Vinen 1956] in 1956.

A straight vortex line can be obtained as a cylindrical solution to the time independent Gross Pitaevskii field equation in EQN. [1.3.7] with the absence of an external

potential field $V_{\text{ext}}(\mathbf{r}) = 0$. This solution can be expressed as –

$$\mu\psi_0(\mathbf{r}) = \left[-\frac{\hbar^2}{2m}\nabla^2 + g|\psi_0(\mathbf{r})|^2\right]\psi_0(\mathbf{r}) \qquad [2.2.1]$$

It can be seen that the solution minimizes the energy density $E[\psi_0]$ as expressed in EQN. [1.3.5], taken along with the chemical potential μ as –

$$E[\psi_0] \equiv \int \mathrm{d}^3\mathbf{r}\left\{\left(\frac{\hbar^2}{2m}\right)|\nabla\psi_0(\mathbf{r})|^2 - \mu|\psi_0(\mathbf{r})|^2 + \frac{g}{2}|\psi_0(\mathbf{r})|^4\right\} \qquad [2.2.2]$$

Decomposing $\psi_0(\mathbf{r})$ into cylindrically symmetric polar components as $\psi_0(\mathbf{r}) = \rho_0(\mathbf{r})e^{i\gamma_0(\mathbf{r})}$, the real and imaginary parts of EQN. [2.2.1] (in the absence of an external potential field $V_{\text{ext}}(\mathbf{r}) = 0$) read as –

$$\begin{aligned}\left\{-\frac{\hbar^2}{2m}\left[\nabla^2 - (\nabla\gamma_0(\mathbf{r}))^2\right] - \mu + g\rho_0^2(\mathbf{r})\right\}\rho_0(\mathbf{r}) = 0 \quad &: \text{Real Part}\\ 2\nabla\rho_0(\mathbf{r}).\nabla\gamma_0(\mathbf{r}) + \rho_0(\mathbf{r})\nabla^2\gamma_0(\mathbf{r}) = 0 \quad &: \text{Imaginary Part}\end{aligned}$$

In this case, it can be verified that when the Imaginary part of the Gross Pitaevskii equation is re-expressed as $\nabla.\Big(\rho_0^2(\mathbf{r})\nabla\gamma_0(\mathbf{r})\Big) = 0$, it is indeed equivalent to the conservation of superflow particle current density $j_s(\mathbf{r})$, i.e., $\nabla.j_s(\mathbf{r}) = 0$ where we have taken $j_s(\mathbf{r}) \equiv -\dfrac{i\hbar}{2m}\left(\psi_0^*(\mathbf{r})\nabla\psi_0(\mathbf{r}) - \psi_0(\mathbf{r})\nabla\psi_0^*(\mathbf{r})\right) \equiv \rho_0^2(\mathbf{r})\nabla\gamma_0(\mathbf{r})$. This current conservation is ensured by a purely circular flow in which $\rho_0(\mathbf{r}) = \rho_0(r)$ and $\gamma_0(\mathbf{r}) = k\theta\Big|_{k\in\mathbb{N}^0}$ where r measures the radial distance from the cylindrical axis and θ is the azimuthal angle.

Under such a prescription, the Real part of Gross Pitaevskii equation can then re-expressed as –

$$\left\{-\frac{\hbar^2}{2m}\left[\frac{\mathrm{d}^2}{\mathrm{d}r^2} + \frac{1}{r}\frac{\mathrm{d}}{\mathrm{d}r} - \left(\frac{k^2}{r^2}\right)\right] - \mu + g\rho_0^2(r)\right\}\rho_0(r) = 0 \qquad [2.2.3]$$

The ground state $[\psi_0]_{GS}$, which corresponds to time $t = 0$, of the Gross Pitaevskii theory has an order parameter — seen in §. 1.3.3 — given by –

$$\psi_0(\mathbf{r},t)\Big|_{t=0} = \psi_0(\mathbf{r})e^{i\frac{\mu}{\hbar}t}\Big|_{t=0} \equiv \Big|[\psi_0]_{GS}\Big| \equiv \frac{\psi_{GS}}{\sqrt{2}} \equiv \sqrt{n_0} \equiv \sqrt{\frac{\mu}{g}} \qquad [2.2.4]$$

The quantized vortices can be thought of as excitation states of the theory, effectively saying that the real and imaginary part of the order parameter $\psi_0(\mathbf{r}) = \rho_0(\mathbf{r})e^{i\gamma_0(\mathbf{r})} = \rho_0(r)e^{ik\theta}$ can be individually decomposed into their ground state values and the perturbations upon them, viz. –

$$\begin{aligned} \rho_0(\mathbf{r}) &= \rho_{0GS}(\mathbf{r}) + \delta\rho(\mathbf{r}) \Rightarrow \rho_0 = \rho_{0GS} + \delta\rho \\ \gamma_0(\mathbf{r}) &= \gamma_{0GS}(\mathbf{r}) + \delta\gamma(\mathbf{r}) \Rightarrow \gamma_0 = \gamma_{0GS} + \delta\gamma \sim \theta_{GS} + \delta\theta \end{aligned} \qquad [2.2.5]$$

Adding to this, one then defines the temperature dependent *coherence length* or *healing length* as the length scale at which the condensate density (amplitude) fluctuation $\delta\rho$ and phase (angular) fluctuations $\delta\gamma$ in the condensate are removed by the interaction between condensed particles. Generally speaking — expressed in terms of the field as $\xi^2(T) = \psi_0/\nabla^2\psi_0$ — the coherence length for radial/size fluctuations can de shown to be $\xi = \hbar/\sqrt{2mn_0g} \equiv \sqrt{\hbar/2m\mu}$ (with $\hbar\mu = n_0 g$) whereas the coherence length for phase/angular fluctuation becomes infinite (a detailed discussion into the perturbative effects and subsequent Nambu-Goldstone modes can be found in [Kleinert 1990])

With this at hand, a new dimensionless variable $\eta = r/\xi$ and consequently $\rho_0(r) = \sqrt{n_0}f(\eta)$ can be defined, such that EQN. [2.2.3] gets written as –

$$\Big\{ -\Big[\frac{\mathrm{d}^2}{\mathrm{d}\eta^2} + \frac{1}{\eta}\frac{\mathrm{d}}{\mathrm{d}\eta} - \Big(\frac{k^2}{\eta^2}\Big)\Big] + \Big(f^2(\eta) - 1\Big)\Big\} f(\eta) = 0 \qquad [2.2.6]$$

This equation is then the dimensionless expression of the time independent Gross Pitaevskii equation (with a spherically symmetric, cylindrical polar coordinate ansatz for the order parameter).

CASE I $\eta \ll 1 \Rightarrow r \ll \xi$

Linearising EQN. [2.2.6] by neglecting terms of higher power, i.e., ignoring $f^3(\eta)$ to understand the asymptotic behaviour of $f(\eta)$ as $\eta \longrightarrow 0$, we get the linearised time independent Gross Pitaevskii equation as –

$$\eta^2 \frac{\mathrm{d}^2 f(\eta)}{\mathrm{d}\eta^2} + \eta \frac{\mathrm{d}f(\eta)}{\mathrm{d}\eta} + \left(\eta^2 - k^2\right) f(\eta) = 0 \qquad [2.2.7]$$

This is a standard second-order ordinary differential equation of a special kind with polynomial solutions called *Bessel functions of order* k. The generic solution is of the form $f(\eta) = c_1 J_k(\eta) + c_2 Y_k(\eta)$ where $J_k(\eta)$ and $Y_k(\eta)$ are Bessel functions of the first and second kind respectively. In the asymptotic limit as $\eta \longrightarrow 0$, the Bessel function of first kind $J_k(\eta) \sim \eta^k$, where as the Bessel function of the second kind $Y_k(\eta)$ is divergent. Thus the general solution has the coefficient of $Y_k(\eta)$, i.e., $c_2 = 0$ in order to make meaningful physical result for a system with no source or sink at $\eta \sim 0$. This solution is then given as ($\eta \ll 1 \Rightarrow r \ll \xi$) –

$$f(\eta)\Big|_{\eta \longrightarrow 0} = c_1 J_k(\eta) \propto \eta^k \qquad [2.2.8]$$

Including the phase factor of $e^{ik\theta}$, we have the order parameter expressed as –

$$\psi_0(\mathbf{r}) = \rho_0(\mathbf{r}) e^{i\gamma_0(\mathbf{r})} = \sqrt{n_0} f(\eta) e^{ik\theta} = \Big([\psi_0(\mathbf{r})]_{GS}\Big) \eta^k e^{ik\bar{\theta}} \sim \left(\eta e^{i\bar{\theta}}\right)^k \qquad [2.2.9]$$

Thus the complex field $\psi_0(\mathbf{r})$ is effectively the solution with winding number k. However, the phase $\gamma_0(\mathbf{r}) = 0$ for $k = 0$, i.e., it is *clamped*, implying that $[\psi_0(\mathbf{r})]_{GS} \equiv \sqrt{n_0}$ (n_0 as the condensate particle density) and $f(\eta) = 1$. This is exactly the ground state solution and has no variation in condensate density. In case of $k \neq 0$, the $\eta \longrightarrow 0$ regime $f(\eta) \sim \eta^k$ and equivalently $\psi_0(\mathbf{r}) \sim (\eta e^{i\bar{\theta}})^k$ is said to correspond to the solution of the k-th order in the complex mapping $\eta e^{i\bar{\theta}} \longrightarrow \psi_0$ of the Gross Pitaevskii EQN. [2.2.1].

Also, with $\eta \longrightarrow 0$, the radial distance r from the *vortex core* decreases, subsequently increasing the superfluid velocity v_s. This is in line with $v_s \propto r^{-1}$ as seen from the Feynman-Osanger relation in EQN. [2.1.6].

CASE II $\eta \gg 1 \Rightarrow r \gg \xi$

In general the order parameter $\psi_0(\mathbf{r})$ is expected to remain constant as the radial distance r from the vortex core increases and thus in the large r limit or equivalently $\eta \gg 1$ the solution to EQN. [2.2.6] must asymptotically approach a (finite) non-negative constant value, say a_0. In this case, a series solution in $1/\eta$ to the dimensionless equation in $f(\eta)$ in the large η regime is found to be –

$$f(\eta)\Big|_{\eta\gg1} \sim 1 - \frac{k^2}{2\eta^2} + \mathcal{O}\left(\frac{1}{\eta^4}\right) + \dots \qquad [2.2.10]$$

Physically, looking at the condensate wave function as –

$$\psi_0(\mathbf{r}) = \sqrt{n_0} f(\eta) e^{ik\theta} \sim [\psi_0(\mathbf{r})]_{GS}\left(1 - \frac{k^2\xi^2}{2r^2} + \cdots\right)e^{ik\bar{\theta}} \qquad [2.2.11]$$

one can identify $\sqrt{n_0}f(\eta)$ ($\equiv [\psi_0(\mathbf{r})]_{GS}.f(\eta)$) as the condensate density in the state of quantum coherence. With η getting larger and larger, the condensate wave function gets identified with the order parameter (in line with the Bogoliubov method) such that, $|[\psi_0(\mathbf{r})]_{GS}|^2 = n_0$ and $f(\eta) \xrightarrow{\text{identified}} 1$.

The complete solution to the differential equation in EQN. [2.2.6] is obtained upon numerically integrating inwards [Yamamoto 2010-2011] and is represented in FIG. 2.2.1 below.

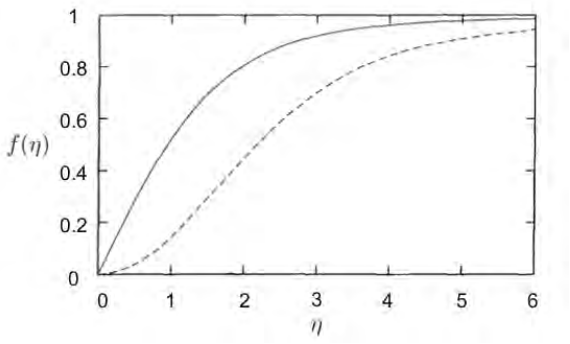

Figure 2.2.1: Vortex solutions ($k = 1$, solid line; $k = 2$, dashed line) of the Gross Pitaevskii equation as a function of the radial coordinate $\eta \equiv r/\xi$. The density of the gas is given by $n_0(r) = n_0 f(\eta)^2$. [8]

[8] Picture sourced from [Yamamoto 2010-2011]

2.3 Energy of the vortex line

To study the energy of the vortex lines, we can explore the consequence of Derrick's no-existence theorem from the general theory of solitonic physics that states: suppose, if, for an arbitrary non-vacuum finite energy field configuration $\psi(x)$, the energy functional $E[\psi]$ has no stationary point, then the theory has no static solutions of the field equation with finite energy other than the vacuum [Manton and Sutcliffe 2004]. This is to say that the excited states of such a theory are not time stable solutions. In the current context, this no-existence theorem has the contrary implication based on a scaling argument: if $\psi_0(\vec{x})$ is the solution of the differential equation EQN. [2.2.1], then the rescaled solution given as $\psi_\delta(\vec{x}) = e^\delta.\psi_0(\mathbf{r})$ must extremize the energy $E[\psi_0]$ of EQN. [2.2.2] for $\delta = 0$. Thus we have –

$$\begin{aligned} E[\psi_\delta] &= \int \mathrm{d}^3\mathbf{r}\Big\{\Big(\frac{\hbar^2}{2m}\Big)|\nabla\psi_\delta(\mathbf{r})|^2 - \mu|\psi_\delta(\mathbf{r})|^2 + \frac{g}{2}|\psi_\delta(\mathbf{r})|^4\Big\} \\ \Rightarrow E[\psi_0] &= \int \mathrm{d}^3\mathbf{r}\Big\{\Big(\frac{\hbar^2}{2m}\Big)e^{2\delta}|\nabla\psi_0(\mathbf{r})|^2 - e^{2\delta}\mu|\psi_0(\mathbf{r})|^2 + \\ &\qquad e^{4\delta}\frac{g}{2}|\psi_0(\mathbf{r})|^4\Big\} \end{aligned} \tag{2.3.1}$$

Setting the derivative with respect to δ equal to zero at $\delta = 0$ gives –

$$\begin{aligned} \int \mathrm{d}^3\mathbf{r}\Big[\Big(\frac{\hbar^2}{2m}\Big)|\nabla\psi_0(\mathbf{r})|^2 - \mu|\psi_0(\mathbf{r})|^2 + e^{2\delta}g|\psi_0(\mathbf{r})|^4\Big]2e^\delta(\partial\delta) &= 0\Big|_{\delta=0} \\ \Rightarrow \int \mathrm{d}^3\mathbf{r}\Big[\Big(\frac{\hbar^2}{2m}\Big)|\nabla\psi_0(\mathbf{r})|^2 - \mu|\psi_0(\mathbf{r})|^2 + g|\psi_0(\mathbf{r})|^4\Big] &= 0 \end{aligned} \tag{2.3.2}$$

Subtracting EQN. [2.3.2] from EQN. [2.3.1] for $\delta = 0$ we see that the energy of a solution of the field equation is $E[\psi_0] = -\int \mathrm{d}^3\mathbf{r}\,\frac{g}{2}|\psi_0(\mathbf{r})|^4$.

Most of this energy is due to the asymptotic regime where the wave function $\psi_0 \longrightarrow \left|[\psi_0]_{GS}\right| \sim \frac{\psi_{GS}}{\sqrt{2}} \equiv \sqrt{n_0} \equiv \sqrt{\frac{\mu}{g}}$, and is equal to the *condensation energy* given as $E_{n_0}^{\text{cond}} = -\frac{g}{2}\int \mathrm{d}^3\mathbf{r}\,|[\psi_0]_{GS}|^4 \equiv -\int \mathrm{d}^3\mathbf{r}\,\left(\frac{\mu^2}{2g}\right)$, — in line with what was seen in EQN. [1.3.6]. Subtracting this background energy from $E[\psi_0]$ we find the *additional energy of the vortex line* as –

$$E_\nu = -\frac{g}{2}\int \mathrm{d}^3\mathbf{r}\,\left(|\psi_0|^4 - |[\psi_0]_{GS}|^4\right) \qquad [2.3.3]$$

which can then be recast in cylindrical polar coordinates (r, θ, z) as –

$$\begin{aligned} E_\nu &= 2\pi\xi^3\bar{L}\left(\frac{\mu^2}{2g}\right)\int_0^\infty \eta\,\mathrm{d}\eta\left(1-[f(\eta)]^4\right) \text{ expressing in reduced} \\ &\quad \text{units of } \eta = \frac{r}{\xi},\ \bar{L} = \frac{L}{\xi} \text{ and } f(\eta) = \frac{\rho(r)}{\sqrt{n_0}} \end{aligned} \qquad [2.3.4]$$

CASE I $\quad \eta \ll 1 \Rightarrow r \ll \xi$

In the small η regime, the behaviour of $f(\eta)$ — as seen from EQN. [2.2.8] when inserted into EQN. [2.3.4] — leads to an expression of the form – $E_\nu \approx \pi\xi^3\bar{L}\left(\frac{\mu^2}{2g}\right)\eta^2$.

CASE II $\quad \eta \gg 1 \Rightarrow r \gg \xi$

It can be seen, due to the factor of η in the integrand, the additional energy of the vortex line come mainly from the large η regime, i.e., from the far zone around the cylindrical axial line. Inserting, the leading $f(\eta)$ asymptotic behaviour of EQN. [2.2.10] in the EQN. [2.3.4] we have $E_\nu \approx 4\pi\xi^3\bar{L}k^2\left(\frac{\mu^2}{2g}\right)\int^\infty \frac{\mathrm{d}\eta}{\eta}$ ignoring $\mathcal{O}\left(1/\eta^4\right)$.

This integral is logarithmically divergent for large η: an immediate conclusion is that a single vortex line can have a finite energy only in a finite container. If this container is cylindrical of radius $\bar{R} \equiv R/\xi$, the integral is finite and becomes $E_\nu \approx 4\pi\xi^3\bar{L}k^2\left(\frac{\mu^2}{2g}\right)\ln\left(\bar{R}\right)$

Thus from the two regimes, we can see that close to the origin, the energy of the vortex line grows as η^2, however on increasing η, the rate of growth slows down rapidly and settles at the asymptotic rate $4\pi\xi^3\bar{L}k^2\left(\frac{\mu^2}{2g}\right)\ln\left(\bar{R}\right)$. The proper inclusion of the non-asymptotic behaviour gives a finite correction to this asymptotic **energy of the vortex line per unit length**, [Kleinert 2008] (in a container of radius $R \equiv \bar{R}.\xi$)

$$\frac{E_\nu}{L} \approx 4\pi\xi^2k^2\left(\frac{\mu^2}{2g}\right)\left[\ln\left(\frac{R}{\xi}\right)+0.385\right] \qquad [2.3.5]$$

In the expression above, the lowest vortex line c, gives rise to the concept of a *vortex core* whose radius r_c can be estimated with an expression of the form $r_c = \xi e^{-c} \approx 0.68\,\xi$. It is closer to this radial core where the behaviour of $f(\eta) \sim \eta^k$ and correspondingly the vortex line energy grows as η^2. Moving away and till reaching the asymptotic value of $4\pi\xi^3\bar{L}k^2\left(\frac{\mu^2}{2g}\right)\ln\left(\bar{R}\right)$, the energy of the vortex line is given as EQN. [2.3.5].

At this point, it is worth mentioning in passing, some important features in the story of the vortex line energy –

1. The energy density $E[\psi_0]_{GS}$ given in EQN. [1.3.5] in the absence of an external potential $V_{\text{ext}} = 0$ and condensation energy E_{no}^{cond}, can be approximated in the *hydrodynamic limit* (also called *London limit*) as –
   $E[\psi_0]_{\text{hydro}} = \frac{\hbar^2}{2m}\int \mathrm{d}^3\mathbf{r}\left\{n_0|\nabla\gamma_0(\mathbf{r})|^2\right\}$ since $[\psi_0(\mathbf{r})]_{GS} = \sqrt{n_0}e^{i\gamma_0(\mathbf{r})}$.
   However, with $v_s(\mathbf{r}) = \frac{\hbar}{m}\nabla\gamma_0(\mathbf{r}) \equiv \frac{k\hbar}{m}(\nabla\theta) \equiv \frac{k\hbar}{mr}\hat{e}_\theta$, we have,
   $E[\psi_0]_{\text{hydro}} \equiv \frac{n_0k^2\hbar^2}{2m}\int\frac{\mathrm{d}^3\mathbf{r}}{r^2} = \int \mathrm{d}^3\mathbf{r}\,\mathcal{E}(\mathbf{r})$, where the hydrodynamic kinetic energy density of the vortex line is represented as being taken as –
   $\mathcal{E}(\mathbf{r}) = \frac{n_0k^2\hbar^2}{2mr^2} \equiv \frac{1}{2}\left[n_0m\right]v_s^2(\mathbf{r})$.
   A comparison of the expression for $E[\psi_0]_{\text{hydro}}$ to the vortex line energy expression $E_\nu \approx \xi^2k^2\left(\frac{\mu^2}{2g}\right)\int\frac{\mathrm{d}\mathbf{r}}{r}$ (with $\xi = \hbar/\sqrt{2m\mu}$) shows that the dominant contribution to the vortex line energy is mainly due to the *hydrodynamic energy of the superflow* around the line.

2. For the major portion of the fluid the limiting hydrodynamic expressions give an accurate description; it is only in the neighbourhood of the vortex line, i.e., $r \leq \xi$, the energy density expression $\mathcal{E}(\mathbf{r})$ differs due to the gradient of the field $|\psi_0(\mathbf{r})|$, i.e., to say that the velocity field closer to the core of the vortex line mimics a solid rotator (scaling as r/ξ) rather than diverging as $1/r$. This then establishes a cut-off in the energy integration scheme at the core radius ($r_c \sim \xi$) and effectively speaking, one can regard the complete lack of any superflow up to the radius ($r_c \sim \xi$) of the vortex tubes. Following that distance, there is a sudden onset of idealised flow outside r_c moving with the limiting velocity, $v_s(\mathbf{r})$ of EQN. [1.3.11].

3. Although vortices are massless fluid configurations, relative motion of a vortex with respect to the local superfluid induces small additional irrotational flow which contributes to the kinetic energy of the system as given by EQN. [2.3.5] and imparts an *effective mass to the vortex*. For practical purposes this effective mass is negligible; however when included, the kinetic energy (per unit length) associated with the vortex flow (with velocity $\vec{v}_\nu$) is then given as –

$$\frac{E_\nu}{L} \approx \frac{1}{2}\vec{v}_\nu^2 \rho_s \pi \xi^2 + 4\pi\xi^2 k^2 \left(\frac{\mu^2}{2g}\right)\left[\ln\left(\frac{R}{\xi}\right) + 0.385\right] \qquad [2.3.6]$$

The coefficient of $\vec{v}_\nu^2/2$ in the first term on the right hand side may be interpreted as the effective mass m^* (per unit length of the vortex), which is equal to the mass per unit length of the fluid displaced by the vortex core $m^* = \rho_s \pi \xi^2$. The second term is independent of $\vec{v}_\nu$ and has the usual form of the energy of a single vortex, *cf.* EQN. [2.3.5].

Adéjà vu is usually a glitch in the Matrix.
It happens when they change something.
Trinity in The Matrix, 1999

3

Glitchings in Pulsars

The rotational energy of a pulsar has been shown to have a very gradual and largely predictable decrease, predominantly though, due to the magnetic dipole radiation causing a decrease in the spin periods of pulsars [Gold 1968]. The stellar modelling of radio pulsars predict a long-time tendency to approach an inherent *death line* where the pulsations get completely turned off. However, certain timing irregularities are observed in the rotational velocities of pulsars.

A stochastic timing irregularity is the sudden increase in the rotation velocity without any change in the pulsed electromagnetic emission. This spectacular increase in rotation velocity is commonly referred to as a **glitch**. The period of gradual recovery that follows the glitch lasts anything from days to years and during this time, the observed periodicity slows to a period close to what was observed before the glitch.

The precise physics underlying the glitching mechanism is currently not completely understood and there are many models forwarded as an explanation (reviewed in §. 3.1). However, according to the conventional belief, glitching is a behaviour seen due to some internal process within the pulsar's matter — as opposed to the external factors that determine the gradual decrease in the rotational frequency of pulsars.

It should be mentioned that other intrinsically motivated, stochastic timing irregularities are found to be present along with glitches in pulsar observations. These *timing noises* exhibit a fairly continuous, erratic and non-standard behaviour, potentially also having their origins in the neutron star's internal constitution and/or the magnetospheric disturbances in its atmosphere. A description of this type of irregularity is beyond the scope of this dissertation and is not attempted here.

3.1 Pulsar glitches and Glitch mechanisms: A review

3.1.1 Phenomenological Introduction

Glitches are the discrete, randomly timed, positive jumps in the spin rate of pulsars — superposed on their gradual spin-down behaviour — as observed historically in the Vela pulsar [PSR B0833-45] in 1969 [Radhakrishnan and Jackson 1969] and more recently in anomalous X-ray pulsars (e.g., [Kapsi et al. 2007]) and accreting neutron stars [Galloway et al. 2007]. A current estimate finds about 315 glitch events observed in 102 pulsars [Melatos et al. 2008; Yuan et al. 2010; Espinoza et al. 2011]. As reviewed in detail in [Eysden 2011], 54 pulsars are known to have glitched only once, whereas 6 pulsars have glitched more than 10 times [Melatos et al. 2008; Espinoza et al. 2011] with the most famous ones being: the Crab Pulsar (27 times) [Wong et al. 2001], PSR J1740-3015 (23 times) [Zou et al. 2008], PSR J0537-6910 (20 times) [Middleditch et al. 2006], Vela (17 times) [Dodson et al. 2007] and PSR J1341-6220 (12 times) [Wang et al. 2000].

These glitches are usually measured as a *fractional increase* in angular velocity; typically of the order of $\Delta\Omega/\Omega \sim 10^{-9}$ to 10^{-6}, with the smallest glitch having $\Delta\Omega/\Omega \sim 8 \times 10^{-12}$ [PSR B1821-24][Cognard and Backer 2004] and the largest being $\Delta\Omega/\Omega \sim 6 \times 10^{-5}$ [PSR J164710.2-455216] [Israel et al. 2007].

The characteristic time scales over which this fractional increase in angular velocity takes place often ranges from a few minutes to a few hours: with the most constrained observation of less than ~ 30s in Vela [Dodson et al. 2007]. Following the glitch, the spin-down rate ($\dot{\Omega}$) tries to reach an equilibrium value (in line with its pre-glitch value) in a process called **glitch recovery** that can take months or even years.

Although, quite typically in most pulsars, the post-glitch value of the spin-down rate tends to almost match its pre-glitch value (a fact evident by the slightly decreased spin-down rate $\Delta\dot{\Omega}$: the largest decrease being $\Delta\dot{\Omega}/\dot{\Omega} \sim -2.7 \times 10^{-3}$ [PSR J1825-0935] [Shabanova 2005]), in some cases like the glitches occurring in the Crab Pulsar [PSR B0531+21] the post-glitch value is higher [Lyne et al. 1993] (the largest $\Delta\dot{\Omega}/\dot{\Omega} \sim 1.11$ seen in [PSR J2301+5852] [Kapsi and Gavriil 2003]).

A typical example of such a glitch is shown in FIG. 3.1.1.

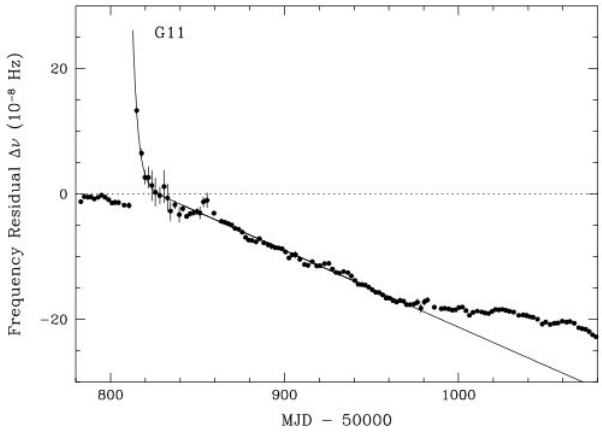

Figure 3.1.1: Glitch $\frac{\Delta\Omega}{\Omega} \sim 9 \times 10^{-9}$ observed in the Crab pulsar by Wong et al. [9]

[9]Picture sourced from [Wong et al. 2001]

3.1.2 Glitch Mechanisms

Following the increased observations of pulsar glitches, several initial ideas were proposed to explain their origin. These ranged from magnetospheric instabilities, pulsar disturbance by a planet, hydrodynamic instabilities or collisions of in-falling massive objects (a review of these early models is made in [Ruderman 1972]). Fundamentally though, as the structure of the pulsed radiation beam remained unaltered by the glitch, the probable cause of pulsar glitchings came to be thought of as an internal stellar process rather than an external one. The first, most probable, and convincing theory was offered with the idea of *starquakes* as proposed by Malvin Ruderman in 1969 [Ruderman 1969]. The explanation offered was as follows: As a result of centrifugal forces, rotating neutron stars are not spherical but rather oblate spheres. If the star were purely fluid, a deceleration of its rotation would entail a readjustment of the stellar shape to a more spherical configuration. However, a solid crust would prevents such readjustments and consequently the star would remains more oblate. The spin-down of the star would then builds up stress in the crust making it crack at some critical value, followed closely by a stellar shape-readjustment to reduce the deformation. This readjustment would cause a decrease in the moment of inertia of the star, effectively, causing an increase in rotational frequency to conserve angular momentum. Observationally though, the photon beam generated by the magnetic field (anchored to the crust) would responds to the spin-up of the crust and accordingly generates the pulsar glitch.

This model was consistent with the glitches observed in the Crab pulsar and explained the weak glitch activity of young pulsars by the fact that the internal temperatures were still too high for the crust to store a large stress. However, for the Vela pulsar, with a *relaxation time* (time between two successive starquakes) $\tau \sim 10^4$ years, the glitch amplitude was calculated to be $\Delta\Omega/\Omega \sim 10^{-9}$: about three orders of magnitude smaller than those observed. Moreover, as pointed out by Gordon Baym & David Pines in 1971 [Baym and Pines 1971], the amount of mechanical energy ΔE that would need to be transferred to the crust per glitch would be in excess of 10^{36}J. Thus the actual time required for this accumulation of this energy in the crust — and then the subsequent glitching —would end up being

inconsistent with the frequency of observed glitches in most pulsar (~ 5/decade). This came to become the main discrepancy of the starquake model.

The ineffectiveness of the starquake model to perfectly describe pulsar glitches necessitated other models to be developed and explored. Very soon after abandoning the starquake model, superfluidity in the interior of neutron stars came to be extended to explain the glitching phenomenon. As has been reviewed in §. 1.2.3, neutron superfluid was theorised to be present in the interior regions of the neutron star and subsequently the long relaxation time scales between glitch events: a fact describable by only considering a superfluid interior as opposed to a solid or normal fluid one. This laid observational confirmation to the superfluid hypothesis. A superfluid flow nucleates the formation of quantized vortices, as has been seen in detail in §. 2.1, and this then formed the basic premise upon which many plausible explanatory theories of pulsar glitches were formulated.

A central tenant to most of these theories remained the bifurcation of the loosely flowing star's internal superfluid region and the crust (colloquially, taken to include the mutually coupled and co-rotating solid outer crust, the electrically charged plasma permeating the inner regions of the neutron star and the external magnetosphere) into two separate differentially rotating layers (more on this in §. 3.2). The superfluid was viewed as an angular momentum reservoir due to the spin-down rate of the superfluid being slower than that of the crust. The resultant differential rotation between the two layers would at some point during coupling transfer angular momentum from the superfluid to the crust and thereby spin the crust up causing a glitch. Much debate and differences originate from this point further regarding the actual physics underlying this phenomenon, for example, the specific cause and location of the coupling within the star, the actual angular momentum transfer process and its cause, the physical chemistry of the star and its superfluid content, etc. Multiple attempts have been made to answer these questions: each offering a different theoretical model with observational support, however, no concurrent model currently exists that forwards a conclusive and comprehensive explanation.

A brief developmental review is provided in this section, outlining some of the more tenable models put forth, relying on similar attempts made in [McDonald 2007; Chamel and Haensel 2008; Eysden 2011] along with the other articles/papers sourced on the subject (references appended alongside).

Beginning with the work of John Negele and Dominique Vautherin in 1973, the inner crust of neutron stars was considered to contain a neutron superfluid interpenetrating the Coulomb lattice of neutron-rich nuclear clusters [Negele and Vautherin 1973]. With this idea, Phillip Anderson & Naoki Itoh in 1975 proposed pulsar glitches as a natural macroscopic outcome of the interaction between quantized neutron vortex lines (nucleated in the rotational charged superfluid) and the crustal lattice bound normal matter [Anderson and Itoh 1975]. This pinning interaction was expected to bind vortices to the normal component of the star preserving the superfluid vorticity and retaining its angular momentum. The pulsar's spin-down by emission of electromagnetic and gravitational radiation increased the hydrodynamical lift (Magnus force) exerted on the vortices — equalling it to the pinning force on the vortex lines — and thereby causing the vortices to detached from the lattice. This freedom initiated an angular momentum transfer from the superfluid component to the normal crustal component of the star under the action of drag forces. In the same paper, Phillip Anderson & Naoki Itoh suggested that pulsar glitches are entirely dictated by the dynamics of pinning and unpinning of neutron superfluid vortices attached to/between the nuclear pinning sites of the lattice-bound nuclear clusters of the neutron star crust: an analogous idea to the phenomenon of flux pinning seen in type II superconductors. Historically, the underlying physical dynamics of these vortices then went on to form the basis of almost all of the proposed theories of pulsar glitching mechanism. Generically though, most explanations fell within the heading of a crust-driven or core-driven phenomena, leading to the observed pulsar glitches.

The crust-driven approach found its basis in the crust-fracture model proposed by Malvin Ruderman in 1976 [Ruderman 1976] (extended in 1991 [Ruderman 1991]) that looked at strong crustal vortex pinning and the subsequent mechanical stress-fracturing of the crust generated due to vortex migration as the cause of the angular momentum transfer. This vortex migration (creep) along the radial direction away from the rotational axis was considered a consequence of the frictionally-

motivated weak coupling between the neutron superfluid (containing the quantized vortex lines) and the normal charged component (strongly coupled to the magnetically braked solid crust) during the typical spin-down of the neutron crust. The differential rotation of the two layers then consequentially induced an increasing Magnus force on the vortices producing crustal stresses and the subsequent crust fracture, *before* the sudden unpinning of the vortices. In this model, the angular momentum transfer from the superfluid to the crust during the glitch allowed for a larger spin-up than that due solely to a stellar-shape readjustment. However, Ali Alpar et al. in 1982, [Alpar et al. 1982] showed that the crust breaking mechanism was not plausible as the global pinning forces were contained by stronger gravitational forces as compared to elasticity. Their work lead to the belief that the catastrophic unpinning of a large number of vortices from the lattice represent a coherent model for pulsar glitching. The mechanics of this spontaneous unpinning of inhomogeneously distributed vortex line assembly (effectively, accumulated and depleted regions of vortex line density within the neutron star) was demonstrated by in 1988 by K. S. Cheng et al. [Cheng et al. 1988] as a plausible mechanism for initiation of glitches.

Based on the work furthered by Ali Alpar et al. in 1993, [Alpar et al. 1993], the same year, Ali Alpar and David Pines [Alpar and Pines 1993] proposed a phenomenological model ascribing the glitch in Vela pulsar to vortex trap/discharge regions (capacitors) within the neutron star. Utilizing the approach of the vortex-creep model (reviewed in §. 3.2), the gradual movement of vortices through the superfluid interior was believed to lead on to an inhomogeneous density distribution of the vortex-array assembly; leading in effect to resistive regions (vortex devoid regions) and capacitive regions (vortex accumulated regions). The charged plasma encircling the vortices (continuous vortex-current) in the capacitive regions was thought to then 'discharge" onto the resistive regions in the event of a glitch. This explained the permanent change in the subsequent spin-down rates in some pulsars as reduction of moment of inertia due to new capacitive regions being formed.

A physical microscopic picture of the capacitor model was furthered by Y. Mochizuki et. al in 1995, [Mochizuki and Izuyama 1995] referring to self-trapped, strongly pinned vortices in the frontier regions of pulsars causing collective unpinning

leading to a glitch. However, the difficulty of explaining vortex unpinning and re-pinning continued to exist in this approach.

A more recent approach along this line continues to exist with the work of Lila Warszawski & Andrew Melatos where self-organised critical processes [Warszawski and Melatos 2008] or coherent noise processes [Melatos and Warszawski 2009] from stochastic physics of condensed matter systems are employed to further the unpinning avalanches of superfluid vortex arrays.

Building on Malvin Ruderman's original starquake model, Bennett Link & Richard Epstein in 1996 extended their thermal glitch model [Link and Epstein 1996], where the vortex-creep rate of radial outward migration of vortices was considered as a thermally motivated response to starquakes. The subsequent glitch following the vortex-creep (that led onto increased crustal stress and eventual fracture) differed from the crust-fracture model in terms of its post-glitch internal energy release: an argument that led to the suggestion by Michelle Larson & Bennett Link in 2002, that the observation of thermal X-ray emissions of glitching pulsars could constraint the glitching mechanism [Larson and Link 2002].

In keeping with the crust-driven approach, in 2002, Nils Andersson, Gregory Comer and Reinhard Prix proposed the superfluid two-stream instability model as an explanation of pulsar glitching [Andersson et al. 2002]. It was based on Kelvin-Helmholtz instability between the neutron superfluid and the conglomeration of charged particles (inter-permeating the neutron superfluid) in the crust; provided the coupling through entrainment effect was considered sufficiently strong.

Alongside to this, the idea of core-driven processes found its proponent in the flux tube model advanced by Malvin Ruderman, Tianhua Zhu and Kaiyouin Chen in 1998 [Ruderman et al. 1998], where the interaction between the superfluid vortices and magnetic flux tubes (formed by coexisting superconducting protons) in the core resulted in an expanding core vortex array and thereby caused increased crustal stresses leading to fractures. These magnetically motivated flux tubes were believed to have a configuration and number (10^{13}/vortex) that caused such a strong entanglement with the neutron vortices that with the spin-down of the pulsar, the radially-outwards vortex-creep would initiates a flux tube drag. It was this drag that was believed to stress the crust and with the strong pinning regime

of the vortices, it led to starquakes and fracturing of the crust into plates. The subsequent equatorial migration of these plates and pinned vortices resulted in the spin-down of the superfluid causing a characteristic glitch. Interestingly, this model explained the observed increase in the post-glitch spin-down rate seen in some pulsars like Crab by looking at the electromagnetic interaction between the electrically-conductive crustal plate movement and the magnetic field configuration: the electromagnetic torque acting on the pulsar increased in relation to the angle between the magnetic and rotation axes. In 2000, L. M. Franco et al. [Franco et al. 2000] showed — independent of vortex pinning — the stellar oscillation and precession following starquake would lead to subsequent increase in angular deviation of magnetic and rotational axes upon reaching new equilibrium state.

A different explanation to this main idea of vortex array expansion was proposed in the flux annihilation model of Armen Sedrakian and James Cordes in 1999 [Sedrakian and Cordes 1999] wherein the proton flux tubes cohabiting with the superfluid vortex in the core got annihilated at the crust-core boundary, leading to the outward radial migration of the vortices and subsequent glitching.

Later in the year 2000, Brandon Carter, David Langlois and David Sedrakian [Carter et al. 2000] proposed an alternative approach to explain pulsar glitching with their theory of centrifugal buoyancy mode. They employed the concept of the centrifugal buoyancy forces arising in the superfluid due to differential rotation as the cause of strong pressure gradients that crack the crust leading to momentum transfer (effectively, a glitch). This mechanism has been unique in that, it remains effective independent of the vortex motion and proton superconductivity. In particular, even if the neutron vortices were not considered pinned to the crust, this model demonstrated crustal stresses of similar magnitudes to those obtained in the pinned case. In 2006, Nicolas Chamel *&* Brandon Carter [Chamel and Carter 2006] extended to show that the entrainment effect caused by the neutron superfluid and the normal crust have no reflection on the magnitude of the stress, despite an increase in crustal stresses due to the stratification.

In all these models reviewed here, there remains an inconclusive description of the underlying physics of pulsars, for example, the strength of the vortex pinning forces and the type of superconductivity in the core — both equally controversial

issues. Again, the superfluid vortices and their extension through the inner crust region could be a density dependent phenomena, with certain regions being non-superfluid all together. This raises some unanswered question about the superfluid vortex array arrangement as well as the magnetic flux tubes of type II superconducting protons. However, as it stands today, despite these open questions most explanations of the pulsar glitch mechanism rely heavily on the observational evidence of the post-glitch relaxation time scales, as is reviewed in the next section.

3.2 Post-glitch recovery physics

The *two-component model* of stellar interior advanced by Gordon Baym, David Pines, Christopher Pethick and Malvin Ruderman in 1969 [Baym et al. 1969a] to understand post-glitch recovery physics of pulsars consisted of the magnetically braked solid crust (coupled to the electrically charged plasma in the interior region and co-rotating together with it at the observed angular velocity of the pulsar) and the internal charge-neutral neutron superfluid core having differential rotation rate.

Historically, this was the first consolidated attempt to offer a plausible explanation for pulsar glitching soon after the first glitch observation was made in Vela pulsar. It incorporated the idea of superfluidity in the neutron star interior — as had already been established by that point of time — in a remarkable manner to explain the origin and dynamics of pulsar glitchings.

The characteristic features of this model, which has been the basis of all subsequent lines of thought, deserves a special mention at the very outset –

1. The two-component model proposed the stratification of the neutron star as a solid nuclear-lattice crustal shell (quasi-spherical) and an interior region dominated by neutron superfluid matter (with a possible solid core). The superfluid was also thought to contain $\sim 1\%$ to 5% impurities in the form of charged plasma of protons and electrons, which then could lead to formation of superconducting protons and charged electron plasma. This picture would still be in line with what has been reviewed in §. 1.1.1, with the exception of stating such a clear bifurcation of the two density regimes.

2. The core magnetic field of neutron stars was believed to drive the strong coupling between the electrically charged plasma in its interior region and the solid lattice-bound nuclear clusters of crustal nuclei, hence leading to a co-rotation on very long time scales (of the order of the pulsar-age) [Eaason 1979]. This then explained the long term spin-down of the pulsars through electromagnetic radiation losses.

3. The charged plasma (of the interior) and the solid crust were thought to be further coupled to the magnetosphere, leading to a co-rotation at the observed angular frequency of the pulsar. Contrastingly, the neutron superfluid being charge neutral had a differential rotation rate independent to the pulsar's rotation.

4. The explanation to the glitching phenomena understood as a characteristic spin-up of the solid crust, rested on two major assumptions: (i) the strong core magnetic fields helped communicate the crust spin-up to the electrically charged plasma of the interior on a rapid time scale of ~ 100s and (ii) the response of the neutron superfluid to the crust speed-up was considerably slower on a time scale of years due to the weak coupling between the normal and superfluid components. The actual mechanism for the spin-up though was considered to be starquakes occurring in the solid crust.

5. The presence of such a configuration of superfluid interior (neutron superfluid, along with superconducting protons, charged ionic plasma and solid core) and a solid lattice crust gave post-glitch relaxation times of the order of months or years as actually seen in Vela or Crab pulsars — a leading suggestion towards glitches being associated with the neutron superfluid in the core [Baym et al. 1969b]. With the two-component model all other configurations viz., normal fluid-filled interior or solely neutron superfluid interior (devoid of proton-electron mixture) gave post-glitch relaxation times much smaller than what was observed (10^{-7}s to 10^{-17}s as compared to observed $\sim 10^{7}$s) [Lyne and Graham-Smith 2006].

Based on the two-component model of Baym et al. (1969) [Baym et al. 1969a] to understand the post-glitch behaviour of a pulsar, the normal component (including the solid crust and the charged plasma of the interior) having moment of inertia I_c was considered to be weakly coupled to the neutron superfluid with moment of inertia I_s. The normal component being magnetically strongly coupled, rotated with the observed pulsar rotation velocity of $\Omega_c(t)$ where as the superfluid that was assumed to rotate quasi-uniformly had an angular velocity of Ω_s. The important coupling parameter between the two components was τ_c, and was referred to as the relaxation time scale for frictional dissipation.

With this at hand, the equation of motion for the crustal component was shown to be given as (a detailed derivation can be found in [Shapiro and Teukolsky 1983]) $\Omega_c = \Omega_0(t) + \Delta\Omega_0[Qe^{-t/\tau} + 1 - Q]$, where $\Delta\Omega_0$ was the absolute magnitude of the glitch, Q was the *healing parameter* — roughly explaining to what degree the post-glitch angular velocity of the crust (in effect, the pulsar) relaxes back toward its extrapolated value and regarded statistically as $Q = (\sum_{n=1}^{N} \Delta\Omega_n)/\Delta\Omega_0$ (for N time scales) — and $\tau = \tau_c I_s/(I_c + I_s)$. Typically thought, if one considered $\Delta\Omega_p$ as the permanent change in the orbital velocity Ω, then when $\Delta\Omega_p \longrightarrow 0$, $Q \longrightarrow 1$.

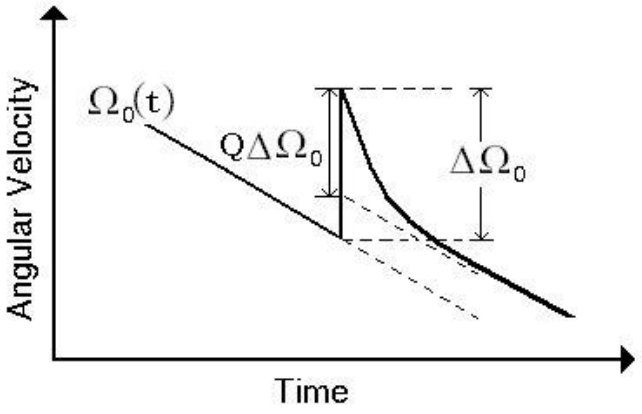

Figure 3.2.1: Typical pulsar response to a glitch represented in the time dependence of the pulsar angular velocity, Ω_c, according to the two-component model. [10]

This clearly showed that the two-component model gave an exponential decay rate of the pulsar rotational velocity in the post-glitch regime. A typical practice

[10] Picture simulated with `Adobe Illustrator CS5`

that followed, was to mathematically fit the observational data of the pulsar glitch to an exponential curve in order to obtain the values of the coupling constant, τ and the healing parameter, Q, e.g., in 1971, Paul Boynton et al. [Boynton et al. 1971] fitted the glitch data of the Crab Pulsar (end of September 1969) to obtain the healing parameter $Q = 0.9$ and a coupling constant of $4 < \tau < 16$ days. It was expected that the values of Q and τ would remain consistent for all observed glitches on a given pulsar and this fact was held as a true test of any glitch model for a considerable time that followed.

The major observational dissidence to the two-component model came about through the power spectrum analysis of timing fluctuations of pulsar timing data done by Paul Boynton in 1981 [Boynton 1981], and later in the same year by George Downs with his work on the pulsar timing observation of Vela [Downs 1981]. Also, the observational existence of multiple time scales in the post-glitch recovery of Crab and Vela could not be accounted for by the simple two-component model.

In light of this new observational evidence, Ali Alpar, Phillip Anderson, David Pines and Jacob Shaham proposed the **vortex-creep model** in 1984 to explain the post-glitch relaxation mechanism [Alpar et al. 1984b; Alpar et al. 1984c] utilizing the idea of quantized vortices nucleated in rotating superfluid (*cf.* §. 2.1). In a concurrent paper the same year, Ali Alpar, Stephen Langer and James Sauls [Alpar et al. 1984a] showed that due to the superfluid vortex lines being spontaneously magnetised by the dragged proton supercurrent around them in the core regions of the neutron star, the coupling of the superfluid core to the normal component (solid crust and charged plasma) is on a time scale of merely $\sim$ 400 P(s) (P being the stellar rotation period): an unrealistic estimation of the rotational equilibrium times (effectively, the post-glitch relaxation time scales) with any simplistic two-component model being considered. However; with the already prevalent pulsar glitch constraint condition, $I_p/I \ll \Delta\dot{\Omega}/\dot{\Omega} \sim 10^{-2}$, where I_p represented the moment of inertia of the dynamically *pinned* inner crustal superfluid part and I, the total moment of inertia of all stellar-components coupled to the outer crust on time scales shorter than the glitch resolution (shown by [Alpar et al. 1981]), the superfluid core was seen to contain most of the moment of inertia of the star: hence acting like an angular momentum reservoir from where the superfluid vortex dynamics could feed the outer crust during glitches.

The vortex-creep model built up from the general idea of quantized superfluid vortices being *pinned* to the lattice-bound nuclear clusters found in the inner crust of neutron stars in a density-dependent, dynamic and energetically favoured manner (Phillip Anderson *&* Naoki Itoh [Anderson and Itoh 1975], Malvin Ruderman [Ruderman 1976] and Ali Alpar [Alpar 1977]). The general understanding was that vortex-pinning constrained the angular momentum of the superfluid leading to a lag between the angular rotation rates of the chargeless crustal superfluid and the charged normal-matter of the crust. This is due to the charged normal matter tending to spin-up (spin-down) under the influence of an electromagnetic external torque. This lag determined the dynamics of the hydrodynamic lift (magnus) force and the pinning force experienced by the inner-crust superfluid vortices leading to different pinning scenarios: ranging from perfect pinning regime with strongly-pinned inner-crust superfluid vortices (frozen vorticity) to the imperfect pinning regime with radially-outward gradual vortex-creep, all the way to the sudden and catastrophic unpinning of a large number of vortices ($\sim 10^7$ to 10^{14} out of $\sim 10^{18}$ in total) causing free angular momentum transfer of stored vorticity from the inner-crust superfluid to observable normal crust (magnetically strongly coupled outer-crust and charged plasma of the interior) — a characteristic giant glitch.

Bennett Link and Richard Epstein [Link and Epstein 1991] calculated the activation energy for vortex unpinning by looking at the stationary vortex-configuration energetics in the density dependent interstitial pinning regions ($\rho \lesssim 10^{13}$ g cm^{-3}) and the nuclear pinning regions ($\rho \gtrsim 10^{13}$ g cm^{-3}) of the stellar crust. Their work considering the idea of vortex line tension and values of pinning parameters of Epstein *&* Baym [Baym and Epstein 1988], found the interstitial pinning regions to favour stronger pinning (effectively, a continuous breakaway regime of vortex-creep over many pinning sites), where as the nuclear pinning regions favoured weaker pinning (effectively, single-site independent breakaway of vortices).

In the post-glitch recovery period, the vortex-creep mechanism was thought of as the steady dislocation of the inner-crust superfluid vortices — hopping through different crystal lattice pinning sites — and this limiting creep rate was found to be a highly temperature dependent phenomenon [Blandford et al. 1993], i.e., the thermal creep of vortex line against the pinning energy barriers. Interestingly

enough, in 1993, Bennett Link et al. [Link et al. 1993] suggested that the vortex-creep could be initiated due to quantum tunnelling, even at zero temperature. The vortex-creep model quite successfully predicted the nature of the creep to evolve from a linear regime to a non linear regime as the pulsar aged and cooled, i.e., in older pulsars (like Vela) the post-glitch dynamic response of the crustal-pinned superfluid moment of inertia was non linear [Alpar et al. 1993; Alpar et al. 1996]. However, the global hydrodynamics of the process was not clearly evident in the workings of the theory.

With a resounding body of observational data on post-glitch recovery of pulsars, many inconsistencies and irregularities have been found to reside in the vortex-creep model. A few of the main lines of objections (including alternative explanations) are mentioned here below –

1. Any confirmation of the relaxation times being age and temperature dependent in the linear regime is beset with the problem of making comparison of relaxation time data from pulsars of different ages; the relaxation time scales that are observationally available viz., minutes to years, correspond to different layers of the pinned superfluid for pulsars of different ages and temperature. Also, if hydrodynamic processes like linear Ekman pumping ($\Delta\Omega/\Omega \ll 1$) in the stellar interior (assuming a viscous process independent of glitch amplitude and small post-glitch perturbation of flow) are considered responsible for the glitch recovery process, the recovery time scale response should be uniform for all glitches in a given pulsar [Eaason 1979; Abney and Epstein 1996]. However, counter evidence from Crab and Vela pulsars [Alpar et al. 1993; Alpar et al. 1996; Dodson et al. 2002] and less heavily studies pulsars [Peralta 2007] are observationally forwarded.

2. Conventionally, multiple time scales of glitch recovery ($\tau \sim 0.3$ days to 300 days) are needed to account for the multiple exponential fitting of high resolution glitch recovery data (e.g., [Dodson et al. 2002]), which is then attributed to the different density dependent variation in vortex-pinning strength (effectively, vortex-creep) in the stellar interior [Alpar et al. 1993; Alpar et al. 1996; Sedrakian and Cordes 2002]. This approach fails to make proper connection with the equation of state or transport coefficients of bulk

nuclear matter, and hence harder to test against a nuclear stellar theory or via terrestrial experiments. Moreover, the linear relation between the $\Delta\Omega_p$ (permanent Ω increase) and $\Delta\Omega_0$ implied by the vortex-creep model is inconsistent with a stochastic process [Jones 2002].

3. The recovery regime of some pulsars like Vela being monotonic and quasi-exponential are explained by the vortex-creep model, however, the Crab pulsar consistently *overshoots* during recovery to a below steady-state angular velocity level, before asymptotically rising again [Wong et al. 2001]. This implies a failure of the vortex unpinning to homogeneously distribute the angular momentum throughout the star indicating the presence of a certain amount of perpetual differential rotation between the superfluid and normal component even during recovery.

4. A different approach to the thermally activated vortex-creep model was presented in the idea of co-rotation of unpinned vortices under weak drag forces extended by Peter Jones in [Jones 1990; Jones 1991; Jones 1992]. It was suggested there that the maximum pinning force was small due to the vortex rigidity and highly dissipative Kelvin mode vortex excitations. This implied a co-rotating picture involving the neutron superfluid and its vortices, wherein the vortices are subjected to resistive dissipation due to the vortex-core and nuclear lattice interactions. Moreover, in 2006, Bennett Link [Link 2006] demonstrated that strong pinning of vortices (as required by the vortex-creep model) is not consistent with long-period pulsar precession observations. Recent observations of long-period precession in pulsars, e.g., RX J0720.4-3125 [Haberl et al. 2006], further suggests a very weakly-dragged picture of neutron vortices [Link and Cutler 2002; Shaham 1977].

5. Various other hydrodynamic models based on averaged vortex microphysics have also been proposed as an alternative to the vortex-creep model, viz., [Glampedakis and Andersson 2009; Andersson et al. 2012b; Sidery et al. 2010] and [Haskell et al. 2012] (building on the work of Pierre Pizzochero [Pizzochero 2011]).

With the different methods of the post-glitch physics described above, many ambiguities continue to be prevalent in formulating a theoretically consistent and observationally coherent model. Apart from the ad hoc initial glitch mechanism itself, the models reviewed here make many implicit assumptions e.g., the crust-core disconnection through a normal fluid layer between sub-nuclear s-wave ($\sim {}^4$He) and supra-nuclear p-wave ($\sim {}^3$He) neutron superfluids [Jones 1990]: an assumption countered by the microscopic calculations [Zuo et al. 2004] suggesting a continuous vortex line. However, recent work into the non-dissipative entrainment coupling between the neutron superfluid and crustal lattice has raised questions about the core superfluidity as an influence in glitches [Andersson et al. 2012a]. Typically, any explanation of the pulsar glitches based on crustal vortex unpinning would now have to address the crust-core disconnection during a glitch; a difficult endeavour if the singlet pairing gap allowed neutron superfluid to reach far into the core subsequently raising question about the behaviour of superfluid vortices across the interface. Also, the exact microscopic nature of the proton superconductor in the core is in itself a matter of debate [Jones 2006]; [Sedrakian 2005]. The conventional understanding is that the entrained proton in the core form a type II superconductor and magnetize the superfluid vortices present there, whereas the crustal vortices remain unmagnetised [Alpar et al. 1984a]. However, the positive identification of pulsar long-term precession model favour a type I proton superconductor in the core [Link 2003] and thereby decouple the core from the crust completely. This necessitates some new physics to describe the short time scale crust-core coupling condition of pinned superfluid vortices in the vortex-creep model. As an ending comment to this chapter, it deserves to be mentioned that although suggestive, the vortex theory of glitches in itself is yet to be unequivocally confirmed with observational confidence — keeping the origin of these stellar spin-ups a very open and exciting question to answer.

To them, I said, the truth would be literally nothing but the shadows of the images.

Plato, 342 BCE.

4

Holographic Superfluids

4.1 Introduction and Motivation

Within the last two decades it has been conjectured: effective theories of gravity that live in some specific spacetime backgrounds share an *equivalence* with a certain class of quantum field theories that are defined at the conformal boundary of that space with dimension lower by one or more. This has helped in extracting the complicated physics of real world systems (manifestly, the gauge theories on the boundary) using a correspondingly holographic dual description (gravity theories in the bulk). Historically, the first realisation of the Holographic principle — proposed in 1994 by Gerald 't Hoooft ['t Hooft 1993], Charles Thorn [Thorn 1994] and Leonard Susskind [Susskind 1994] — was in the AdS/CFT conjecture of Juan Maldacena in 1998 in which $\mathcal{N} = 4$ supersymmetric Yang-Mills theory was considered dual to the type II-B superstring theory in $AdS_5 \times S^5$ [Maldacena 1998]. Till date this remains one of the best examples of the gauge/gravity duality and over

time with the works of Stephen Gubser, Igor Klebanov, Alexander Polyakov, Edward Witten, Sean Hartnoll, Christopher Herzog, Gary Horowitz, Thomas Hertog and Subir Sachdev amongst others (*cf.* [Gubser et al. 1998; Witten 1998; Klebanov and Witten 1999; Gubser 2008; Hartnoll and Herzog 2008; Hartnoll et al. 2008; Hartnoll 2009; Sachdev 2010]) found applications to a whole universe of strongly coupled quantum field theoretical systems (e.g., RHIC physics, condensed matter systems, QGP hydrodynamics) being studied in the weakly coupled gravitational background. In the interest of this review, we would like to look at the development of one such application to describe the physics of superfluids, in other words, a Holographic superfluid description.

Before venturing further into the development of the subject, it would be in line here to mention some of the subject-literature references that are currently available to permit a detailed study. Within the universe of material available on AdS/CFT correspondence, a few accessible physical introduction to the subject (with emphasis on condensed matter systems) can be seen in [Zwiebach 2004; Papadimitriou and Skenderis 2007; Nastase 2007; Balasubramanian and McGreevy 2008; Albash 2010; Pires 2010; Polchinski 2010; Horowitz 2011]. More specifically, an introduction to the principles of holography applied to superfluids (or superconductors) can be found with [Herzog et al. 2009; Hertog 2009; Horowitz 2010; Keränen 2011; Sachdev 2012], which when read together, offer a brilliant insight into the workings of the theory.

In an attempt to construct a systematic review of holographic superfluids, the aforesaid references (along with references mentioned alongside text through this chapter) have been consulted to collect, organize and present the subject matter from the available literature in the field. The basic schema employed here is to provide a comprehensive and tractable overview of the dynamics of superfluid vortices in this gauge/gravity picture, motivated in part as an attempt to answer the original question of pulsar glitches.

A first step along the way would be in presenting a short heuristic picture of the workings of the AdS/CFT conjecture from a stand alone perspective. Amongst others, an excellent lecture introduction to the AdS/CFT correspondence can be found in [Papantonopoulos 2011, chapter 3] and [Maldacena 2011].

4.1.1 AdS/CFT correspondence

The AdS/CFT correspondence is a statement of the equivalence of all the physics in an asymptotic Anti de Sitter (AdS) spacetime to the quantum field theory (QFT) on the boundary. The bulk AdS_{d+1} dimensional space provides for a black hole (BH) where the geometry of the space gets deformed in the presence of the BH, but *asymptotically* is restored to the original AdS space. This can be expressed in terms of the metric describing a Schwarzschild BH inside an AdS_{d+1} spacetime as seen below –

$$\mathrm{d}s^2 = -\left(1 + \frac{r^2}{L^2} - \frac{2gM}{r^{d-2}}\right)\mathrm{d}t^2 + \left(1 + \frac{r^2}{L^2} - \frac{2gM}{r^{d-2}}\right)^{-1}\mathrm{d}r^2 + r^2\,\mathrm{d}\Omega_{d-1}^2 \qquad [4.1.1]$$

where t is the time coordinate, r is the radial coordinate, $\mathrm{d}\Omega_{d-1}^2$ is the metric on S^{d-2}, $g \sim G_{\mathrm{N}}^{(d+1)}/L^{d-1}$ is Newton constant $G_{\mathrm{N}}^{(d+1)}$ expressed in terms of AdS radius L and M is the mass of the BH. The parameter $2gM \sim r_0^{d-2}$ is connected with the presence of a BH: in fact, as $L \longrightarrow \infty$, the metric is identical to a Schwarzschild BH in $d+1$ dimensional Minkowski space with r_0 being identified with the Schwarzschild radius r_s. Moreover, in the asymptotic limit $r \gg r_o(\sim 2gM) \Rightarrow r_0/r \ll 1$, the metric can be seen to be identical to an AdS_{d+1} metric with AdS radius L.

The Schwarzschild radius for an AdS BH r_+ is determined by letting the coefficient of $\mathrm{d}t^2 = 0$, and it turns out to be a function of the Schwarzschild radius in Minkowski space $r_0 \sim 2gM$ at fixed AdS scale L, i.e., a function of the BH mass. Also, the Hawking temperature for small BH ($r_+ \ll L$) scales as $T_{\mathrm{BH}} \propto r_+^{-1}$ as expected as for small BH, implying the effect of AdS curvature is negligible. However, in case of large BH ($r_+ \gg L$) the Hawking temperature $T_{\mathrm{BH}} \sim r_+$, implying the large black holes have temperature growing with size.

The boundary of the $d+1$ dimensional AdS space can be established at large fixed r, i.e., $r \gg L$ and the metric in EQN. [4.1.1] can be rescaled as being given by $\mathrm{d}s^2 \simeq \frac{r^2}{L^2}\left[-(\mathrm{d}t)^2 + L^2\,\mathrm{d}\Omega_{d-1}^2\right]$ evidently the boundary $\mathbf{R} \times S^{d-1}$ with L being the radius of S^{d-1}. This boundary shows the isometries of AdS space that are identical

to the conformal group SO(2, d) in d dimensions, implying that the boundary QFT is in fact a conformal field theory (CFT).

The standard CFT picture maps operator on the plane $\mathbf{R}^d$ acting on the field theory vacuum to create states of the system on the cylinder $\mathbf{R} \times \mathrm{S}^{d-1}$ — a property independent of the AdS/CFT correspondence. The dimension of the operator, e.g., scaling dimension Δ, directly corresponds to the energy of the corresponding field theory state created: an operator $\hat{\mathcal{O}}(t, \mathbf{x}) = e^{iHt - iP_i x_i} \hat{\mathcal{O}}(0) e^{-iHt + iP_i x_i}$ with scaling dimension $\Delta_{\mathcal{O}}$ — under standard Schrödinger algebra taken as $[D, \hat{\mathcal{O}}(0)] = i\Delta_{\mathcal{O}} \hat{\mathcal{O}}(0)$ — leads to field theory state $|\phi_{\mathcal{O}}\rangle = e^{-H} \mathcal{O}^\dagger |0\rangle$, such that $H|\phi_{\mathcal{O}}\rangle = e^{-H} \Delta_{\mathcal{O}} \mathcal{O}^\dagger |0\rangle = \Delta_{\mathcal{O}} |\phi_{\mathcal{O}}\rangle$. The AdS/CFT conjecture then relates this field theory state on the cylinder (the conformal boundary of AdS space) to the bulk theory state in the AdS space of the Schwarzschild BH in terms of the metric $\mathrm{d}s^2$ in EQN. [4.1.1] with $2gM/r^{d-2} \ll 1$ and $L = 1$.

In the bulk theory residing in the AdS space, at large energies, gravity (or effectively, BH) provides for the entropy — relating to the entropy of the boundary CFT — with massless particles at finite temperature (taken as $S_{\mathrm{YM}} \sim c V_{d-1} T_{\mathrm{BH}}^{d-1} \sim c L^{d-1} T_{\mathrm{BH}}^{d-1}$, where c is the effective number of fields in the theory and $V_{d-1} \sim L^{d-1}$ is the volume of S^{d-1}). This is saying that for large BH of mass M in AdS space with Schwarzschild radius $r_+ \gg L$ and Hawking temperature $T_{\mathrm{BH}} \sim r_+$, the entropy $S_{\mathrm{BH}} \sim \dfrac{\mathrm{A}_{\mathrm{horizon}}}{g} \sim \dfrac{r_+^{d-1}}{g} \sim \dfrac{T_{\mathrm{BH}}^{d-1}}{g} \sim \dfrac{L^{d-1}}{G_{\mathrm{N}}^{(d+1)}} T_{\mathrm{BH}}^{d-1}$ (where $G_{\mathrm{N}}^{(d+1)}$ measures the coupling of gravity in $d+1$ dimensions AdS space and hence effectively, the nonlinear perturbative interactions among gravitons). Thus we have $S_{\mathrm{BH}} \sim S_{\mathrm{YM}}$ with the effect that $c \propto 1/G_{\mathrm{N}}^{(d+1)}$: a clear indication that for weakly-coupled bulk theories we require a large number of fields in the CFT.

Quite typically, in large N gauge theories with gauge group SU(N) (living on the boundary), the perturbative expansions in $1/N$ and $g_{\mathrm{YM}}^2 N \equiv \lambda$ ('t Hooft coupling) resemble the loop expansions in string theory in terms of the string coupling $g_s = 1/N$. Moreover, the Feynman diagrams can be considered as planar in the limit $N \longrightarrow \infty$ with leading corrections ($\propto 1/N^2$) imposed in taking N as finite and they seem to resemble the surface that represent interactive strings. This is where the precise AdS/CFT correspondence lies: 0n the AdS side, the parameter set is represented in the dimensionless string coupling g_s, the string length l_s and the

AdS curvature radius L, where as on the CFT side, the set includes the rank N of the gauge group and the dimensionless coupling constant g_{YM}.

The identification of the parameter-sets on the two sides then establishes the limitation on the applicability of the AdS/CFT, viz. –

$$g_s = g_{\text{YM}}^2 \quad (L/l_s)^{D-p-3} \sim g_{\text{YM}}^2 N = \lambda \qquad [4.1.2]$$

where D refers to the total spacetime dimensions and N refers to the number of D_p branes wrapped around a p-dimensional compact space employed in describing the gravitational size of a system of D_p branes in string theory. This is in keeping with the $\mathcal{N} = 4$ original supersymmetric SU(N) Yang-Mills theory (arising on a set of N coincident D3 branes) coupling to a type II-B superstring theory on $\text{AdS}_5 \times \text{S}^5$ (gravitational background created by the D3 branes) in the low energy limit.

Thus we can say that for the *gravity approximation* — a weakly-coupled bulk gravity theory acting as the dual description in the AdS/CFT correspondence — we require a weak string coupling $g_s \longrightarrow 0$ (implying small quantum string corrections) and a large $N \longrightarrow \infty$ of the SU(N) boundary gauge theory with the 't Hooft coupling $\lambda \equiv g_{\text{YM}}^2 N$ as large and $\lambda \gg 1$. In the opposite picture, where $\lambda \equiv g_{\text{YM}}^2 N \ll 1$ we have a weakly coupled boundary gauge theory that can be studied perturbatively in AdS/CFT. The *duality* of AdS/CFT is in the two descriptions of the underlying physics (gauge perturbative theory and gravitational approximation) in the AdS_{d+1} space that are applicable in two separate regimes ($\lambda \ll 1$ and $\lambda \gg 1$). This is saying that the weak coupling calculations in bulk gravity theory ($g_s \longrightarrow 0$) is *equivalent* to the strong coupling ($\lambda \equiv g_{\text{YM}}^2 N$ being large and $\lambda \gg 1$) calculations in the boundary gauge theory and vice versa.

The pedagogical methodology of AdS/CFT can be understood as the correspondence between the bulk gravity theory in AdS_{d+1} space and the corresponding CFT theory living on the boundary of this AdS_{d+1} space, e.g., $\mathbf{R} \times \text{S}^{d-1}$. The introduction of bulk scalar fields ϕ^I (I indexing the different types of scalar field) and bulk gauge fields A_μ affects the AdS space geometry only very slightly. Typically, the bulk scalar fields ϕ^I are considered to be the *external* sources/fields to some operator $\hat{\mathcal{O}}_I$ in the CFT with conformal dimension Δ_I. The bulk gauge fields A_μ

couple to the conserved currents J^μ of the global symmetry in the CFT. Also, the CFT metric h_{ij} is the induced part of the AdS metric $g_{\mu\nu}$ and any perturbation of this CFT metric creates the boundary stress-energy tensor operator, $\hat{T_{\mu\nu}}$.

Thus in effect, in AdS/CFT, the AdS fields act as sources whose boundary values provide for the initial perturbations creating the CFT operators. More formally, the statement of the correspondence[11] is: assuming the boundary of the AdS space occurs at some small *holographic* radius $z \sim 1/r$ with $z = \epsilon$ (the BH horizon is then taken as $z_{\rm H} \sim 1/r_+$), the effective action for the boundary CFT (also referred to as the *energy functional*, or simply, the logarithm of the partition function) with the source perturbations $\phi^I(\epsilon)$, $A_i(\epsilon)$ and metric $h_{ij}(\epsilon)$ is exactly identical to the bulk gravity **onshell** action with boundary conditions $\phi^I(\epsilon) = \phi^I$, $A_i(\epsilon) = A_i$ and $g_{ij}(\epsilon) = h_{ij}$. In terms of a formula, one can express this as –

$$\Gamma = -\log\left\langle \exp\left[\int_{S^d} \mathrm{d}^d x\sqrt{h}\left(\phi^I\hat{\mathcal{O}}_I + A_a\hat{J}^a + \delta h_{ij}\hat{T}^{ij}\right)\right]\right\rangle_{\rm CFT} = \underbrace{\mathbf{S}_{\rm bulk}[\phi^I, A_a, h_{ij}]}_{\text{on-shell gravity action}} \quad [4.1.3]$$

This statement effectively says that; given the boundary conditions of the bulk fields, we can get a gravity action which when looked at from the holographic point of view is equivalent to the effective action of the CFT: with the boundary value of bulk fields acting as external fields for the CFT operators. The effective CFT action then helps compute the various quantities in the field theory including free energy, n-point correlation functions, renormalisation group (RG) flow equation (deriving macroscopic behaviour from the microcanonical model) etc.

With this approach, there are two problems which deserve to be mentioned here. The first deals with the divergence of the on-shell bulk gravity action as one con-

[11]The correspondence stated here is the **low-energy** approximation of the full AdS/CFT correspondence. Strictly speaking, when we consider the AdS side being described by string theory, the correspondence is expressed as the correspondence between the string partition function in the bulk AdS_{d+1} and the d dimensional boundary CFT generating function -

$$\begin{aligned} \mathcal{Z}_{\rm AdS}[\phi^I, A_a, h_{ij}]_{\rm string} &= \mathcal{Z}_{\rm CFT}[\phi^I, A_a, h_{ij}] \\ \Rightarrow \int_{\phi^I, A_a} \mathcal{D}\phi e^{-\mathbf{S}_{\rm string}} &= \left\langle \exp\left[\int_{S^d} \mathrm{d}^d x\sqrt{h}\left(\phi^I\hat{\mathcal{O}}_I + A_a\hat{J}^a + \delta h_{ij}\hat{T}^{ij}\right)\right]\right\rangle_{\rm CFT} \end{aligned}$$

siders $z = \epsilon \longrightarrow 0$ (this is in saying that the boundary of the asymptotic AdS space is now at spatial infinity), where as the second problem is in the divergent/zero-valued asymptotic behaviour of the AdS fields when one considers the gauge choice of the metric with *orthogonal* $z = \epsilon \longrightarrow 0$: $\phi^I \Big|_{\epsilon \longrightarrow 0} \longrightarrow z^{-\Delta_I + d}\varphi$, $A_a \Big|_{\epsilon \longrightarrow 0} \longrightarrow \tilde{A}_a$ and $h_{ij} \Big|_{\epsilon \longrightarrow 0} \longrightarrow z^{-2}\tilde{h}_{ij}$ where φ_I, $\tilde{A}_a$ and $\tilde{h}_{ij}$ are the z-independent part of the bulk fields. The process of elimination of divergences in the bulk on-shell gravity action is called *holographic renormalisation*. A good reference to the prescriptive formalism of can be found in [Boer et al. 2000; Skenderis 2002; Bianchi et al. 2002].

In passing it would be in line to briefly mention the physical reasoning behind justifying the $\text{AdS}_{d+1}/\text{CFT}_d$ correspondence despite the apparent dimensional miss match. Essentially, the RG flow can be geometricised in certain quantum field theories and necessitates an extra dimension to quantify the RG flow scale. In the AdS/CFT perspective, this can be viewed as the extra spatial dimension of the gravity theory living in the bulk. The two-point correlation function $\left\langle \hat{\mathcal{O}}_\phi(x)\hat{\mathcal{O}}_\phi(x') \right\rangle$ for local boundary field operator $\hat{\mathcal{O}}_\phi(x)$ perturbing the field theory at two separate boundary coordinates ($x, x' \in \mathbf{R} \times \text{S}^{d-1}$) can be computed from the asymptotic boundary value of the bulk field ϕ with the *conformal* radial coordinate $r \longrightarrow \infty$. This effectively says that when the boundary point x and x' are *close* to each other (or energy scale is large: UV), the asymptotic $\phi \Big|_{r \longrightarrow \infty}$ behaviour of the bulk field is governed by the gravitational background *close* to the boundary, where as when the boundary points are *widely* separated (or energy scale is small: IR), the asymptotic $\phi \Big|_{r \longrightarrow \infty}$ behaviour of the bulk field is governed by the gravitational background further *away* from the boundary (inside the bulk). A UV divergence in the field theory corresponds to the asymptotic spacetime boundary, where as the IR cut-off of the theory relates to the region in the interior of the bulk. This then establishes the extra bulk radial dimension r as the energy scale of boundary field theory: a fact quite visibly pointed out in [McGreevy 2010] when considering the RG flow equation involving coupling constant g as a function of the RG scale u to be *local* in scale, i.e., the beta function $\beta[g(u)] = u\partial_u g(u)$ is completely determined by the coupling constant evaluated at the energy scale u, without looking at the UV/IR energy divergent regimes.

4.1.2 Motivation towards gravity duals in superfluids

Any second-order quantum phase transition in a condensed matter system; much like the concept of superfluidity discussed earlier, requires the presence of a temperature scale and a condensate field. In constructing a dual gravitational theory in the AdS/CFT approach, quite typically, the role of temperature is provided for by a black hole (BH) in the bulk and the condensate is described by a bulk scalar field (coupled to gravity). As seen in §. 4.1.1, the temperature $T_{\rm BH}$ of massive ($r_+ \gg L$) planar BH scales linearly with their horizon radius r_+, i.e., $T_{\rm BH} \sim r_+$: implying large BH have positive specific heat in addition to having total energy ($E_{\rm BH} \sim r_+^3 V \sim T_{\rm BH}^3 V$) and entropy ($S_{\rm BH} \sim A \sim r_+^2 V \sim T_{\rm BH}^2 V$) within the AdS volume,$V$, effectively, akin to a non-gravitational thermal system. Moreover, the critical-temperature dependent ($T_D < T_c$) phase transition of superfluidity requires a non-zero condensate (refer §. 1.2.1), which in the dual picture can be thought of as a static non-zero scalar field outside the BH: a **black hole hair**. An instant objection is presented in the famous *no hair* theorem — originally extended in 1971 by John Wheeler and Remo Ruffini [Ruffini and Wheeler 1971] — that trivializes certain matter fields outside the BH by thinking of the external matter as in-falling or radiating-out to infinity in the asymptotically flat case. This no-hair conjecture, however, since has been countered within the framework of SU(2) Einstein-Yang-Mills (EYM) theory with a whole arsenal of BH configurations giving rise to hairs, viz., black holes with Skyrme, dilatonic black holes, Yang-Mills-Higgs hair etc. (a more detailed discussion on this issue can be found in [Bekenstein 1996; Heusler 1996]). Fundamentally though as it stands, many nonlinear theories do permit the formation of non-trivial black hole hair and it is with one of those that we could begin to look at superfluidity in this dual framework.

Interestingly enough, an argument against AdS black holes developing scalar hair was presented in 2006 by Thomas Hertog [Hertog 2006] in which he numerically demonstrated that static AdS black holes do not develop spherical scalar hairs if the scalar field theory coupled to gravity is in obedience of the Positive Energy Theorem (PET) of general relativity — a condition that if violated would lead to negative masses of asymptotically flat spacetime (effectively, asymptotic AdS),

destabilizing it and making the approach in itself unacceptable. The real scalar fields studied there were taken to have an arbitrary potential (including negative extrema) and hence in keeping with saying that such (asymptotically) negative potential-extremum tending scalar fields were *neutral* asymptotic AdS scalar-hair solutions of the coupled field equations. A solution to this apparent problem was offered Steven Gubser in 2008 when he proposed that a *charged* scalar field coupled to a *charged* BH had the ability to produce temperature-dependent scalar hair [Gubser 2008].

To appreciate the solution to the no-hair dilemma offered by Steven Gubser [Gubser 2008], one can consider an Einstein Hilbert lagrangian $\mathcal{L}_{\text{EH}} = R + 6/L^2$ with negative cosmological constant, $\Lambda = -3/L^2$ (hence AdS solutions with AdS radius L) coupled to a standard Abelian Higgs lagrangian $\mathcal{L}_{\text{AB}} = -\frac{1}{4}F_{\mu\nu}F^{\mu\nu} - |(\partial_\mu - iqA_\mu)\Psi|^2 - V(|\Psi|)$ with a Maxwell gauge field A_μ and charged complex scalar field Ψ (mass: m, charge: q) having potential $V(|\Psi|) = m^2|\Psi|^2$ (ignoring the $|\Psi|^4$ term) in four spacetime dimensions. Quite typically, the effective mass of the scalar field in such a configuration is $m^2_{\text{eff}} = m^2 + q^2 g^{tt} A_t^2$. This raises the idea that m^2_{eff} can becomes sufficiently negative near the horizon: the last term g^{tt} (looking at the metric of AdS_4 space) being negative outside the horizon and diverging to $-\infty$ near it, any non-zero A_t can make m^2_{eff} sufficiently negative (tachyonic mode) to destabilize the scalar field Ψ outside the BH horizon by the process of spontaneous symmetry breaking. This could then be viewed as the metastable perturbative Nambu-Goldstone modes seen in condensate systems like superfluids, i.e., $\Psi \neq 0$ outside the BH horizon. In fact, even if $A_t = 0$ to begin with, a large enough charge q sets the electric field $E_i = -F_{0i}$ outside the horizon to be large (in effect, A_t rises from 0 to a finite value very quickly) and considering a small $m^2 > 0$, one could yet have $m^2_{\text{eff}} < 0$. Moreover, Gubser demonstrated that in $T_{\text{BH}} \longrightarrow 0$ regime, the Reissner Nordström BH solutions of the coupled field equations in AdS_4 present g_{tt} with double zeros at the *extremal horizon*: a place where the lowering of temperature and effectively the mass M of the static, charged BH reaches a minimal configuration compatible with its charge Q, in essence making $|g^{tt}|$ larger.

The geometry of the asymptotic space here plays an important role in understanding the physics at the conformal boundary where the dual gauge theory exists : the *constant* scalar curvature of the space implies the *constancy* of m^2_{eff} — be it positive or negative. Thus, considering an asymptotic flat space with positive curvature (fixed metric $\mathrm{d}\Omega^2 \in \mathbb{S}^2$ and $L \longrightarrow \infty$), one can imagine that as the temperature of a maximally charged BH, $T_{\text{BH}} \longrightarrow 0$ (correspondingly the mass, M being reduced), any strongly charged particle created at the BH horizon (Schwinger mechanism) escapes the gravitational attraction — owing to the strong electrostatic repulsion of the BH and begins to journey outwards unrestrictedly. The instability is countered by the BH in the *superradiance* of charged particles, thereby reducing its charge-to-mass ratio up to the point at which the created particles cannot escape the gravitational well any more. This regenerative mechanism maintains stability of the scalar wave function at infinity, effectively maintaining its stability in the near horizon limit to counter the onset of any tachyonic-instability led symmetry breaking and scalar hair formation outside BH horizons. However, in case of an asymptotic AdS space with positive curvature (e.g., $\text{AdS}_2 \times \text{S}^2$), the confinement boundary of L makes normal ($m^2 > 0$) particles necessarily contain within the volume (irrespective of their charge) as the conformal boundary of the space is inaccessible to them and the tachyonic modes ($m^2 < 0$) could get perfectly reflected at the boundary: in both cases, they would settle into a condensate outside the BH horizon.

In what follows through the next section, we look at the systematic extension of the model of Steven Gubser as has been applied to holographically study the phenomenon of superfluidity. A few important aspects are taken into consideration in defining a comprehensive gravity dual model of superfluids and they deserve a special mention –

1. The idea of conformal (scale) invariance in a CFT (living in Minkowski space) implies that in the absence of any other scales, all non-zero temperature are effectively equivalent under scaling arguments. A requirement of temperature-dependent phase transitions in superfluids then necessitates the use of a different scale (like the chemical potential μ) with which to quantify the functional dependence of the dimensionless measure of con-

densate, i.e., $\sqrt{\langle\mathcal{O}\rangle}/\mu$ as a function of T/μ. This is in keeping with wanting to study systems that have a non-vanishing charge density (sourced by turning on the chemical potential in the dual field theory) and temperature.

Also, the statement in the AdS/CFT correspondence relates to a unique position of one-to-many mapping between the AdS gravity theories and multiple CFT: an idea that goes to say: the quantization of the gauge field A_μ in $\text{AdS}_{(3+1)}$ with Dirichlet or Neumann boundary conditions of $A_\mu \longrightarrow [a_\mu]_{\text{fixed}}$ and $A_\mu \longrightarrow [a_\mu]_{\text{dynamic}}$ respectively implies different dual CFTs — under S generator of SL(2,$\mathbb{Z}$) — each with a different global U(1) [Witten 2007]. This then leads to utilizing the appropriate boundary conditions when solving for the excitation spectrum in the field theory viz., superfluid vortex solutions.

2. In the context of superfluidity, the boundary value of the bulk scalar field $[\psi_{\text{bulk}}]_{\text{boundary}}$ mapping to the non-trivial vacuum expectation value (vev) of a charged boundary operator $\left\langle\hat{\mathcal{O}}\right\rangle$ (effectively, the condensate) corresponds to normalizable modes that can be thought of as the saddle points of the action (for fixed boundary conditions) — with the quanta occupying such modes having a dual description in the Hilbert space of the boundary theory [Balasubramanian et al. 1999]. However, the boundary values of the bulk U(1) gauge field $[(A_\mu)_{\text{bulk}}]_{\text{boundary}}$ that map to fixed background values of the boundary gauge field, correspond to non normalizable modes. This is in effect saying that the bulk modes are non-fluctuating and present a classical background for the propagation of bulk excitations. On considering $[(A_0)_{\text{bulk}}]_{\text{boundary}}$ corresponding to the fixed chemical potential μ of the conformal asymptotic AdS boundary condensed matter system, one can effectively regard the presence of a source Reissner Nordström charged BH in the bulk.

3. A more general approach to what is undertaken here would be to look at the different temperature regimes (with respect to chemical potential) separately when studying the transition from *non-formation* of scalar hair at large T to *condensation* of the scalar field at small T. In the high temperature regime (equivalently, the finite temperature CFT living of the asymptotic AdS boundary), an increased bulk temperature of the system causes the

coordinate distance between the BH horizon and asymptotic AdS boundary to reduce. This makes sure that no potential energy gain can compensate for the steep gradient in fall of the scalar $\psi \longrightarrow 0$ going from bulk to boundary, effectively meaning a vanishing scalar at large temperature. However, as the temperature is lowered (or the chemical potential raised, with respect to the ratio μ/T), the scalar field begins to condense outside the BH forming a scalar hair and it is in this region where the most interesting physics lies. The solution to determining the correct thermal state of the boundary CFT is effectively a problem of solving the bulk equations of motion for the lowest free energy states.

4. The Breitenlohner Freedman (BF) bound [Breitenlohner and Freedman 1982] takes the tachyonic states $m_\psi^2 < 0$ of the fields in the AdS$_{d+1}$ space to cause an instability of the ambient geometry *only* in the limit of a highly negative threshold of the order of the reciprocal of the AdS radius L squared. In other words, for AdS$_{d+1}$ bulk field with negative mass-squared parameter m_ψ^2, the stability bound can be expressed as $m^2L^2 > -d^2/4$. As it will be seen, many bulk field theories have the masses in the limits: $1-d^2/4 > m_\psi^2 L^2 > -d^2/4$, leading to *both* expression for the scaling dimension ($\Delta_\pm$) of conformal operator $\hat{\mathcal{O}}_\psi$ that emerges from the constraint equation $m_\psi^2 L^2 = (\Delta - d)\Delta$ as valid: choosing one or the other then corresponds to two different boundary theories differentiated by the dimension of the operator $\hat{\mathcal{O}}_\psi$.

In passing, it should be mentioned that there have been applications of the alternative regime of AdS/CFT to try construct a string theory with branes as a dual to the standard condensate field theory. These present interesting ideas about the large N degrees of freedom in embedding the holographic dual model in string/M theories. It remains beyond the scope of this dissertation to review such attempts, but a good starting point is found in [Gauntlett et al. 2009; Ammon et al. 2009; Gubser et al. 2010].

4.2 Holographic superfluid model

As an extension of the bulk theory of Steven Gubser [Gubser 2008], Sean Hartnoll, Christopher Herzog and Garry Horowitz [Hartnoll et al. 2008] first proposed a consistent holographic description of superconductors in 2008 where they looked at a simpler version with charge neutrality of the BH in the bulk. Their model showed the presence of a critical-temperature (T_c) dependent scale of superconductivity with second-order phase transitions that are critical for an effective description of the specific condensed matter system.

The original model of superconductivity from a gauge/gravity dual perspective, was continued in line of work by Christopher Herzog, Pavel Kotvin and Dam Son who went on to propose the holographic model of superfluidity in 2009 [Herzog et al. 2009]. They studied the relativistic low-temperature frictionless flow to conclude that the first-order superfluid-normal phase transition occurs as the superfluid current is changed. A subsequent second-order phase transition is mediated on by the increase in the temperature of the system. In this section, we review the holographic superfluid model studied by Christopher Herzog et al. and highlight some of the major salient features.

Typically, to holographically model a superfluid one considers a model of gravity (standard Einstein Hilbert action) in an asymptotically AdS space in $d+1 \equiv 3+1$ dimensions coupled to a $U(1)$ gauge field A_μ and a minimally coupled charged complex scalar field ψ_0 (mass: m_{ψ_0} being small and charge: q) with potential $V(|\psi_0|)$. This approach provides for bulk AdS Schwarzschild BH (decoupled solution to the Einstein Hilbert lagrangian) that develops scalar hair (solution to the Abelian Higgs lagrangian) at the horizon of the AdS space; the Ads space itself is taken to be the conformal boundary on which the $d \equiv 2+1$ CFT (global U(1) gauge superfluid theory) resides.

The effective field action for the holographic dual theory of superfluid in AdS_{3+1} can be given as an expression of the form –

$$\mathbf{S}_{\text{AdS}} = \int \mathrm{d}^4x\sqrt{-g}\Big[\frac{1}{2\kappa_4^2}\underbrace{\Big(R+\frac{6}{L^2}\Big)}_{\mathcal{L}_{\text{EH}}} - \underbrace{\Big(|D_\mu\psi_0|^2+\frac{1}{4}F_{\mu\nu}F^{\mu\nu}+\frac{2}{L^2}|\psi_0|^2\Big)}_{\mathcal{L}_{\text{MS}}}\Big] \tag{4.2.1}$$

where $g_{\mu\nu}$ is the metric of the AdS_{3+1} space with $g = \det[g_{\mu\nu}]$ and $\sqrt{-g}$ defining the volume element $\kappa_4^2 = 8\pi G_N^{(3+1)}$ with $G_N^{(3+1)}$ being the gravitational Newton constant in $(d+1 \equiv 3+1)$ dimensions, R is the Ricci curvature of the space with cosmological constant Λ. The negative cosmological constant Λ defines the asymptotic AdS radius L via the relation $\Lambda = -d(d-1)/L^2 \equiv -6/L^2\Big|_{d=3}$. In the Maxwell Scalar lagrangian, $\mathcal{L}_{\text{MS}}$, the gauge covariant derivatives of ψ_0 is given as $D_\mu\psi_0 \equiv \partial_\mu\psi_0 - iqA_\mu\psi_0$, the gauge invariant antisymmetric field tensor as $F_{\mu\nu} = \partial_\mu A_\nu - \partial_\nu A_\mu$ and the scalar field potential is taken as $V(|\psi_0|) \equiv m_{\psi_0}^2|\psi_0|^2$, with the scalar $m_{\psi_0}^2 = -2/L^2$. It is noted here that $m^2L^2 > m_{\text{BF}}^2L^2 \equiv -9/4$ for scalars in AdS_{3+1} in line with the Breitenlohner-Freedman stability bound.

In the U(1) gauge theory coupled to a complex scalar field, the Euler Lagrange equations of motion exhibit a gauge redundancy, i.e., the gauge transformation for an infinitesimal $\alpha(x)$ in this theory can be expressed as $\psi_0 \longrightarrow \psi_0 e^{i\alpha(x)} \equiv \psi_0 + i\alpha(x)\psi_0 + \mathcal{O}(\alpha(x)^2)$, $\bar{\psi}_0 \longrightarrow \bar{\psi}_0 e^{-i\alpha(x)} \equiv \bar{\psi}_0 - i\alpha(x)\bar{\psi}_0 + \mathcal{O}(\alpha(x)^2)$ and for the four potential $A_\mu \longrightarrow A_\mu + \partial_\mu\alpha(x)$, where $\partial_\mu\alpha(x)$ shifts the value of the gauge field in a spacetime dependent manner.

Decoupled Probe Limit

Redefining the fields as $\psi_0 \longrightarrow \tilde{\psi}_0/q$ and $A_\mu \longrightarrow \tilde{A}_\mu/q$, one can consider the Maxwell Scalar sector to decouple from gravity in the limit $q \longrightarrow \infty$, effectively saying that the backreaction of matter fields are suppressed in the *probe* limit of $q^2 \ll \kappa_4^2$ thereby simplifying the problem and yet retaining the nonlinear physics. In this framework; with $\tilde{D}_\mu\psi_0 \equiv \partial_\mu\tilde{\psi}_0 - i\tilde{A}_\mu\psi_0$ and $\tilde{F}_{\mu\nu} = \partial_\mu\tilde{A}_\nu - \partial_\nu\tilde{A}_\mu$ (dropping

the tilde for transcriptional convenience from here forth) the action is –

$$\mathbf{S}_{\text{AdS}} = \int \mathrm{d}^4x\sqrt{-g}\Big[\frac{1}{2\kappa_4^2}\left(R+\frac{6}{L^2}\right) - \frac{1}{q^2}\left(|\tilde{D}_\mu\psi_0|^2 + \frac{1}{4}\tilde{F}_{\mu\nu}\tilde{F}^{\mu\nu} + \frac{2}{L^2}|\tilde{\psi}_0|^2\right)\Big] \quad [4.2.2]$$

4.2.1 Gravitational background

The Einstein field equation (EFE) for the gravitational dual model coupled to matter in an AdS_{3+1} space can be expressed in the standard form as being given by $G_{\mu\nu} + \frac{1}{2}g_{\mu\nu}\Lambda - \kappa_4^2 T_{\mu\nu} = 0$, where $G_{\mu\nu} \equiv R_{\mu\nu} - \frac{1}{2}g_{\mu\nu}R$, $\Lambda \equiv -6/L^2$ is the cosmological constant and $\kappa_4^2 \equiv 8\pi G_{\text{N}}^{(3+1)}$ (with $c=1$). An alternate form of the EFE may be expressed as $R_{\mu\nu} - \frac{1}{2}g_{\mu\nu}\left(R-\Lambda\right) = \kappa_4^2 T_{\mu\nu}$. Effectively, in the decoupled probe limit one can consider the gravitational background as separate from the matter content of the theory, i.e., $\kappa_4^2 T_{\mu\nu} \longrightarrow 0$. This then gives the typical AdS Schwarzschild BH solution (in 3+1 dimensions) as the metric solution –

$$\begin{aligned} \mathrm{d}s^2 &= \frac{L^2}{z^2}\left[-f(z)\,\mathrm{d}t^2 + \underbrace{\mathrm{d}r^2 + r^2\,\mathrm{d}\theta^2}_{\mathrm{d}\mathbf{x}^2\text{: flat metric of }\mathbf{R}^2}\right] + \frac{L^2}{z^2}\frac{1}{f(z)}\,\mathrm{d}z^2 \quad [4.2.3] \\ \text{where } f(z) &= 1 - \left(\frac{z}{z_h}\right)^{d=3} \equiv f(\tilde{z}) = 1 - \tilde{z}^3\Big|_{z\sim z/z_h} \end{aligned}$$

The metric has a signature $[-+++]$ with coordinates as (t, z, r, θ), where t, is the time, (r, θ) forms a plane and z is the *holographic* radial coordinate for the asymptotically $\text{AdS}_{(3+1)}$ spacetimes with the AdS boundary occurring at $z=0$ and the BH horizon at $z=z_h$. Importantly, as we would like our bulk theory — extended to the conformal boundary — to be dual to a finite temperature theory (a non-zero critical temperature T_c), we look at the Euclidean regime with compact time $it \in [0, 1/T]$, where T defines the Hawking temperature of the large ($1/z \gg L$) BH, i.e., $T_{\text{BH}} = \dfrac{\hbar\kappa}{2\pi} \sim \dfrac{1}{4\pi}f'(z)\Big|_{z=z_h} \sim \dfrac{3}{4\pi z_h}$: in line with the idea of T_{BH} scaling like the radius for large BH. This temperature is typically identified as the temperature in the dual CFT.

To obtain the free energy in the dual field theory one can adopt the standard AdS/CFT prescription of first evaluating the Euclidean on-shell action with the inclusion of the $z = \epsilon$ cut off to exclude the divergence of the original action i.e., the boundary counter terms that cancels off the divergence of the original action[12].

Upon doing so, the *regularised* Euclidean gravity action in the current framework of an asymptotic AdS_{3+1} space is found out to be –

$$[\mathbf{S}_{\text{EH}}]_{\text{reg}} = -\frac{4\pi^2 L^2}{3^3 G_{\text{N}}} T_{\text{BH}}^2 \quad \times \underbrace{\left[\int \mathrm{d}^2 x\right]}_{\text{2-volume of boundary CFT with flat metric in } \mathbb{R}^2} \qquad \text{refer [McGreevy 2010]}$$

The basic AdS/CFT dictionary gives an estimate for the boundary field theory partition function for the on-shell gravity action, and subsequent free energy $\mathcal{F}$, as seen in –

$$\mathcal{Z}_{\text{CFT}}[h_{ij}] = e^{-[\mathbf{S}_{\text{EH}}]_{\text{reg}}} \Rightarrow \mathcal{F} = -T_{\text{BH}} \log \mathcal{Z} = T_{\text{BH}} [\mathbf{S}_{\text{EH}}]_{\text{reg}} = -\frac{4\pi^2 L^2}{3^3 G_{\text{N}}} T_{\text{BH}}^3 \left[\int \mathrm{d}^2 x\right]$$

where h_{ij} is the induced metric on the *regularized boundary* at $z = \epsilon$. With a fixed background metric in the CFT, we can regard h_{ij} as the Minkowski metric $\eta_{\mu\nu}$ for $\mu \in \mathbb{N}_2 \bigcup 0$.

Utilizing this free energy then, we can estimate the expectation value of the free energy, $\langle E_{\text{BH}} \rangle$ and entropy, $\langle S_{\text{BH}} \rangle$ as being given by –

$$\begin{aligned} \langle E_{\text{BH}} \rangle &= -\frac{\partial}{\partial \beta} \log \mathcal{Z}_{\text{CFT}} \Big|_{\beta = 1/T_{\text{BH}}} = \frac{8\pi^2 L^2}{3^3 G_{\text{N}}} T_{\text{BH}}^3 \left[\int \mathrm{d}^2 x\right] \\ \text{and } \langle S_{\text{BH}} \rangle &= -\frac{\partial F}{\partial T_{\text{BH}}} = \frac{4\pi L^2}{9 G_{\text{N}}} T_{\text{BH}}^2 \left[\int \mathrm{d}^2 x\right] \end{aligned}$$

Using the definition of $T_{\text{BH}} = 3/(4\pi z_h)$, the definition of the expectation value of the CFT entropy gives –

$$\langle S_{\text{BH}} \rangle = \frac{A}{4 G_{\text{N}}} \quad \text{with } A = \frac{L^2}{z_h^2} \int \mathrm{d}^2 x = \frac{16\pi^2 L^2 T_{\text{BH}}^2}{9} \int \mathrm{d}^2 x$$

[12]The regularisation of the gravitational action requires the inclusion of the boundary Hawking-Gibbons term to ensures the validity of the variational principle in the spacetime with conformal boundary [Gibbons and Hawking 1977].

which is in line with the Bekenstein-Hawking entropy, showing that boundary thermodynamic quantities are those of a 2+1 dimensional CFT.

4.2.2 Scalar field decomposition and Gauge transformation

The Euler Lagrange equation of motion for variation in the bulk scalar field ψ_0 ($\bar{\psi_0}$) and the gauge field A_μ from the action $\mathbf{S}_{\text{AdS}}$ in EQN. [4.2.2] is given as –

$$\begin{aligned} \frac{1}{\sqrt{-g}} D_\mu \left\{ \sqrt{-g} g^{\mu\nu} D_\nu \psi_0 \right\} &= m^2_{\psi_0} \psi_0 \quad \left[\frac{1}{\sqrt{-g}} \bar{D}_\mu \left\{ \sqrt{-g} g^{\mu\nu} \overline{D_\nu \psi_0} \right\} = m^2_{\psi_0} \bar{\psi}_0 \right] \\ \frac{1}{\sqrt{-g}} \partial_\nu \left\{ \sqrt{-g} g^{\nu\alpha} g^{\mu\beta} F_{\alpha\beta} \right\} &= g^{\mu\beta} \left\{ D_\beta \psi_0 (i\bar{\psi_0}) - \overline{D_\beta \psi_0} (i\psi_0) \right\} \end{aligned} \qquad [4.2.4]$$

The variational equations in the minimally coupled charged complex scalar field ψ_0, with negative mass m_{ψ_0} are functionally equivalent to the standard Klein Gordon picture for real fields and the variation in the gauge field A_μ is effectively the restatement of Maxwell EM equations in the presence of a source term. The Noether conserved current $j^{(0)}_\mu$ is identified with the source current $j_\mu \equiv (\rho, \vec{j})$ defined as $i \left[\bar{\psi_0} (D_\mu \psi_0) - \psi_0 (\overline{D_\mu \psi_0}) \right]$ with ρ as the charge density and $\vec{j}$ as the current density for the U(1) gauge field A_μ. The conservation of charge is given by the continuity equation, $\partial^\mu j_\mu = 0$.

At this point we make a few assumptions to simply the problem under study: (**a**) the minimally-coupled, charged complex scalar field expressed as two real fields, $\rho_0(x)$ and $\gamma_0(x)$, is taken to be $\psi_0(x) = \dfrac{\rho_0(x)}{\sqrt{2}} e^{i\gamma_0(x)}$ (**b**) the U(1) gauge symmetry $A_\mu \longrightarrow A_\mu + \partial_\mu \alpha(x)$ allows to identify $\alpha(x) \leftrightarrow \gamma_0(x)$.

These conditions — considered together — help in expressing the matter lagrangian $\mathcal{L}_{\text{MS}}$ in EQN. [4.2.1] as –

$$\mathcal{L}_{\text{matter}} = -\frac{\sqrt{-g}}{q^2} \left\{ \frac{g^{\mu\mu}}{2} (\partial_\mu \rho_0)^2 + \frac{g^{\mu\mu} \rho_0^2}{2} A_\mu^2 + \frac{1}{4} F_{\mu\nu} F^{\mu\nu} + \frac{m^2_{\psi_0}}{2} \rho_0^2 \right\} \qquad [4.2.5]$$

With this formulation at hand, it can be seen that the perturbative quadratic lagrangian has the perturbative modes that correspond to a vector Bosonic field

A_μ with mass $g^{\mu\mu}\rho_0$ and a scalar Higgs field $\rho_0(x)$ with *effective mass* taken as $m^2_{\text{eff}} = m^2_{\psi_0} + g^{\mu\mu}A^2_\mu$.

The gauge transformation results in the massless mode (Nambu Goldstone Boson) $\delta\gamma$ to be *eaten up* by the gauge transformed vector Bosonic field A_μ, thereby acquiring mass. This is the essence of Higgs Mechanism in the bulk theory. The absence of $\gamma_0(x)$ in the matter lagrangian in EQN. [4.2.5] implies the arbitrariness of the field $\gamma_0(x)$, i.e., a gauge degree of freedom.

Adding further additional constraints, (**c**) we demand the solution minimizing the Euclidean on-shell action to be translationally [in space (r, θ)] and temporally [in time t] invariant, i.e., $\partial_i \sim 0 \quad \forall i \in (r, \theta)$ and $\partial_t \sim 0$, such that we are left with the two fields $\psi_0(x) \equiv \frac{\rho_0(x)}{\sqrt{2}} e^{i\gamma_0(x)} \xrightarrow{\textit{fourier}} \frac{\rho_0(z)}{\sqrt{2}} e^i k_\mu x^\mu$ $\Big[$with $x^\mu \equiv (t, r, \theta)$ and $k_\mu x^\mu \equiv -\omega t + \vec{k}\cdot\vec{x}\Big]$ and $A_\mu(x) \sim A_\mu(z)$. Also, (**d**) we can have – up to pure gauge consideration – $A_r(z) = A_\theta(z) = 0$ and utilize a *radial AdS gauge* such that $A_z(z) = 0$. This then constrains the physical degrees of freedom of the vector Bosonic field to $A_\mu(x) \longrightarrow A_t(z)$: a single degree of expression.

With the ansatz conditions (**a**) – (**d**) implemented we have the Euler Lagrange equations of motion for the scalar field $\psi_0(x) \sim \rho_0(z)/\sqrt{2}$ and gauge field $A_\mu(x) \sim A_t(z)$ in the bulk AdS_{3+1} space with fixed non-reacting background metric $\mathrm{d}s^2$ of EQN. [4.2.3] (utilizing the field EQN. [4.2.4]) reduced to the coupled ordinary differential equations studied by Sean Hartnoll, Christopher Herzog and Garry Horowitz in [Hartnoll et al. 2008].

The bulk equations of motions can expressed as –

$$\begin{aligned} z^4\partial_z\left[\frac{f(z)}{z^2}\partial_z\rho_0(z)\right] &= \left[-\frac{z^2}{f(z)}A_t^2(z) + m^2_{\psi_0}L^2\right]\rho_0(z) \\ f(z)\partial_z\Big[\partial_z A_t(z)\Big] &= \frac{\rho_0^2(z)}{z^2}A_t(z) \end{aligned} \qquad [4.2.6]$$

Boundary Regularisation Conditions

The boundary conditions required to solve these coupled ordinary differential equations are the regularity conditions at the AdS boundary ($z \longrightarrow 0$) and the

BH horizon $z \longrightarrow z_h$ within the 3+1 dimensional bulk. At the BH horizon, where $z \longrightarrow z_h \Rightarrow z \longrightarrow 1 \Rightarrow f(\tilde{z}) \longrightarrow 0$, the regularity of the gauge field $A_\mu(x) \sim A_t(z) = 0$ based on $A_\mu A^\mu = -g^{tt}A_t^2(z) = \dfrac{z^2}{L^2}\dfrac{A_t^2(z)}{f(z)}$ being finite. Also, the scalar field $\psi_0(x) \equiv \rho_0(z \longrightarrow z_h)$ being finite, requires (based on EQN. [4.2.6] being probed at $z \longrightarrow z_h$ regime) the regularity condition –

$$\Big[\partial_z f(z)\partial_z \rho_0(z)\Big]\Big|_{z=z_h} + \frac{L^2 m_{\psi_0}^2}{z_h^2}\rho_0(z)\Big|_{z=z_h} = 0 \qquad [4.2.7]$$

At the other end along the AdS conformal boundary $z \longrightarrow 0$ in the 2+1 dimensional conformal cover. This translates to the regularisation of the scalar field $\psi_0(z)$ and the gauge field $A_t(z)$ as $z \longrightarrow 0 \Rightarrow z \longrightarrow 0 \Rightarrow f(\tilde{z}) \longrightarrow 1$. Effectively, this can be expressed as –

$$\partial_z\Big[\partial_z\rho_0(z)\Big] - \frac{2}{z}\partial_z\rho_0(z) + \frac{2}{z^2}\rho_0(z) = 0 \text{ and } \partial_z\Big[\partial_z A_t(z)\Big] - \frac{L^2}{z^2}\Big[\rho_0^2(z)A_t(z)\Big] = 0$$

The solution to these equations represent the asymptotic AdS boundary behaviour of the fields and can be given in a Frobenius type power series in z [Herzog et al. 2009] as –

$$\begin{aligned} A_\mu(x) \equiv [A_t(z)]_{\text{bound}} &= (a_\mu + \mathcal{O}\left(z^2\right)) + z\left(b_\mu + \mathcal{O}(z^2)\right) \\ \sqrt{2}\psi_0(x) \equiv [\rho_0(z)]_{\text{bound}} &= z^{\Delta_-}\left(\tilde{\rho}_-(z) + \mathcal{O}(z^2)\right) + z^{\Delta_+}\left(\tilde{\rho}_+(z) + \mathcal{O}(z^2)\right) \end{aligned} \qquad [4.2.8]$$

The boundary values of the fields have various interpretations in the dual field theory. For the bulk U(1) gauge field $A_\mu(x) \equiv A_t(z)$, $a_0 = \mu$ is the chemical potential and $a_i = -[v_s]_i$ is the superfluid velocity of the dual field theory, where as $b_0 \sim -\rho$ is proportional to the charge density and $b_i = \vec{j}$ are the charge currents of the boundary field theory.

For the scalar field $\psi_0(x) \equiv \rho_0(z)/\sqrt{2}$, there exists an ambiguity [Klebanov and Witten 1999]. The solution for $\rho_0(z)$ at the AdS boundary admits two normalizable modes with $\Delta \equiv \Delta_\pm = \dfrac{3}{2} \pm \sqrt{\dfrac{9}{4} + L^2 m_{\psi_0}^2} \Rightarrow \Delta_\pm \in \mathbb{N}_2 \; \forall \; m_{\psi_0}^2 = -2/L^2$ and $\Delta_- + \Delta_+ = d$. In keeping with the Breitenlohner-Freedman stability bound:

$-d^2/4 < m_{\psi_0} L^2 < 1 - d^2/4$, both $\Delta_\pm$ modes are acceptable, however when m_{ψ_0} is larger than that, only Δ_+ mode is permitted.

Typically, when $\tilde{\rho}_-(z)$is identified as the source leading to $\left\langle \hat{\mathcal{O}}_- \right\rangle$ in the boundary CFT, it turns out that U(1) is explicitly broken as $\left\langle \hat{\mathcal{O}}_- \right\rangle \sim \tilde{\rho}_+(z)$. This is to say that as $z \longrightarrow 0$, the solution proportional to z^{Δ_-} grows and as a boundary condition must be set to zero. Thus effectively, the *vacuum expectation value* of the operator of dimension Δ_+ is $\tilde{\rho}_+(z)$ when we consider the source $\tilde{\rho}_-(z)$ switched off. Similarly, when the source is considered as $\tilde{\rho}_+(z)$ (being turned off), the vacuum expectation value of the operator of dimension Δ_- is $\tilde{\rho}_-(z)$. Only one of these vacuum expectation values is non-zero at a time and the two different gauge theories are related to each other via a Legendre transformation.

With parameters constrained, the only true freedom resides in the boundary CFT temperature T (identified with T_{BH}) and the chemical potential μ (identified with the boundary value of the bulk gauge field $A_t(z) \xrightarrow{z \longrightarrow 0} a_0 \equiv \mu$). Based on numerical solutions as computed by [Keränen 2011] (as seen in FIG. 4.2.1) it can be seen that above a certain ratio of $T/|\mu|$ the scalar field condenses, having non-zero value of $\rho_0(z)$ for normalized $z/z_h \in [0, 1]$ (i.e., outside the BH horizon).

In keeping with the standard procedure of holographic renormalization, the on-shell action with equations of motion given in EQN. [4.2.6] with the inclusion of the $z = \epsilon$ cut off to exclude the divergence of the matter action $[\mathbf{S}_{\text{MS}}]$ gives the regularised on-shell action as –

$$\begin{aligned}[\mathbf{S}_{\text{MS}}]_{\text{regular}} &= -\frac{1}{2q^2}\int \mathrm{d}^4x\sqrt{-g}\Big\{\frac{1}{\sqrt{-g}}\partial_z\Big(\sqrt{-g}A_t(z)F^{zt}\Big) + \\ &\quad \frac{1}{\sqrt{-g}}\partial_z\Big(\sqrt{-g}g^{zz}\rho_0(x)\partial_z\rho_0(x)\Big) - A_t(z)A^t(z)\rho_0^2(x)\Big\}\end{aligned}$$

This then has an expression of the form (using the explicit definition of the metric $\mathrm{d}s^2$ from EQN. [4.2.3]) –

$$\begin{aligned}[\mathbf{S}_{\text{MS}}]_{\text{regular}} &= -\frac{1}{2q^2}\int \mathrm{d}^3x\Big[f(z)\left(A_t(z)\partial_z A_t(z) + \frac{1}{z^2}\rho_0(z)\partial_z\rho_0(z)\right)\Big|_{z=\epsilon} \\ &\quad + \int_\epsilon^{z_h \equiv 1} \mathrm{d}z\frac{rL^2}{z^2}\left(A_t(z)A^t(z)\rho_0^2(z)\right)\Big] \qquad [4.2.9]\end{aligned}$$

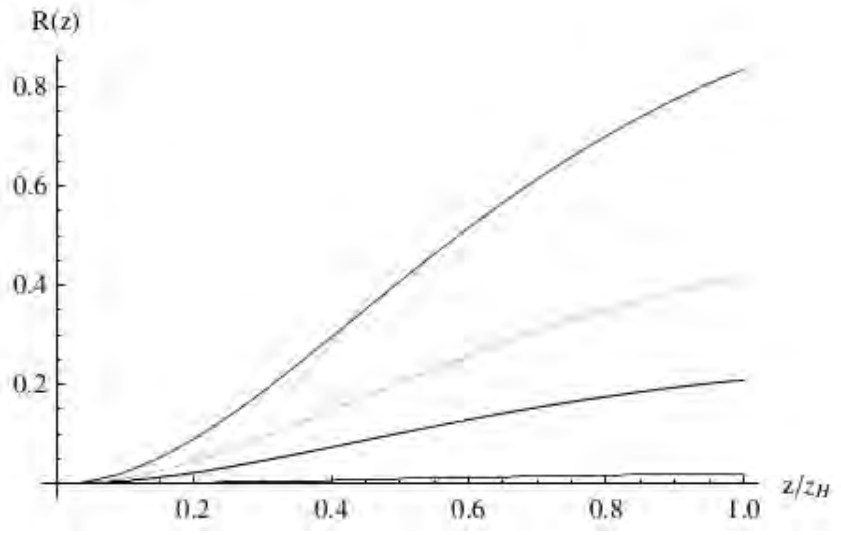

Figure 4.2.1: Scalar field $\psi_0(x) \sim \rho_0(z)$ (represented as R(z) in the original figure above) profiles corresponding to different values of ratio $T/|\mu|$ (0.24607, 0.24601, 0.24583 and 0.24508 in going from the bottom to top) indicating condensate profile. [13]

Consider the asymptotic boundary AdS space conditions discussed above – with the boundary gauge field $A_\mu(x) \equiv A_t(z) = a_0 + b_0 z$ (treating $a_0 \equiv \mu$ as fixed, i.e., $\delta A_t(z \longrightarrow 0) = 0$ effectively working in the grand canonical ensemble of the CFT) and the boundary scalar field $\rho_0(z) = \tilde{\rho}_-(z) z^{\Delta_-} + \tilde{\rho}_+(z) z^{\Delta_+}$ with a boundary choice such that $\tilde{\rho}_- \longrightarrow 0 \Rightarrow \left\langle \hat{\mathcal{O}}_- \right\rangle \sim \tilde{\rho}_+ \sim 0$, making the background variation in $\rho_0(z) = 0$. This quantization routine is referred to as $\hat{\mathcal{O}}_-$ quantization and it transforms to $\hat{\mathcal{O}}_+$ quantization under Legendre transforms. Under these conditions, the boundary divergence in the on-shell regularised action is corrected by the addition of the term generically expressed as $[\Delta \mathbf{S}]^{(\pm)}_{\text{boundary}} = -\frac{1}{2q^2} \int_\partial \left[\sqrt{h}(d - \Delta_\pm) \rho_0^2(z) \right]_{\text{boundary}}$ (with h_{ij} being the induced metric at the boundary) that leads to a *renormalised* on-shell action (with Euclidean continuation of compact time $it \in [0, T]$) as –

$$[\mathbf{S}_{\text{MS}}]^{(\pm)}_{\text{renorm}} = -\frac{1}{2q^2} \int \mathrm{d}^3 x \Big[\Big(-\mu\rho \pm \hat{\mathcal{O}}_- \hat{\mathcal{O}}_+ + \int_0^{z_h \equiv 1} \mathrm{d}z \frac{rL^2}{z^2 f(z)} \left(A_t^2(z) \rho_0^2(z) \right) \Big] \tag{4.2.10}$$

As seen before, the AdS/CFT dictionary free energy estimate (from the boundary

[13] Image sourced from [Keränen 2011, p. 41].

field theory partition function for the renormalised on-shell matter action) is –

$$\mathcal{Z}_{\text{CFT}}\Big[[A_t]_{\text{bound}}, [\rho_0(z)]_{\text{bound}}\Big] = e^{-[\mathbf{S}_{\text{MS}}]^{(\pm)}_{\text{renorm}}} \Rightarrow \mathcal{F}^{\pm} = -T_{\text{BH}} \log \mathcal{Z} = -T_{\text{BH}}[\mathbf{S}_{\text{MS}}]^{(\pm)}_{\text{renorm}}$$

Thus, free energy of the dual field theory can be defined as –

$$\mathcal{F}^{\pm} = \frac{1}{2q^2}\Big[\Big(-\mu\rho + \pm\hat{\mathcal{O}}_-\hat{\mathcal{O}}_+\Big) + \int_0^{z_h \equiv 1} \mathrm{d}z \frac{L^2}{z^2 f(z)} \Big(A_t^2(z)\rho_0^2(z)\Big)\Big] \int \mathrm{d}^2x \quad [4.2.11]$$

with the Legendre transforms as $\partial\mathcal{F}^-/\partial\hat{\mathcal{O}}_- = -\hat{\mathcal{O}}_+$ and $\partial\mathcal{F}^+/\partial\hat{\mathcal{O}}_+ = \hat{\mathcal{O}}_-$; implying that the free energy is extremised such that the physical solutions permit only one non-zero $\tilde{\rho}_{\pm}(z)$: $\mathcal{F}_-$ sits where $\hat{\mathcal{O}}_+$ vanishes and vice versa.

An interesting quantity to look at is the free energy difference between condensed and uncondensed phases: $\Delta\mathcal{F}^{\pm} = \mathcal{F}^{\pm}_{\text{condensed}} - \mathcal{F}^{\pm}_{\text{uncondensed}}$. In the uncondensed phase, $\tilde{\rho}_{\pm}(z) = 0 \Rightarrow \hat{\mathcal{O}}_{\pm} = 0$ and hence considering $\Delta\mathcal{F}^{\pm} < 0$, we can deduce the thermodynamic favourability of the condensed phase (non vanishing scalar profile). The free energy as a function of $T/|\mu|$ can be computed by evaluating EQN. [4.2.11] with fields, $A_\mu(x) \equiv A_t(z)$ and $\psi_0(x) = \rho_0(z)/\sqrt{2}$ as solutions to the equations of motion in EQN. [4.2.6]. With this prescription, the free energy difference is found to be –

$$\Delta\mathcal{F}^{\pm} = T^3 \frac{g(T/|\mu|)}{q^2} \int \mathrm{d}^2x \quad \textit{cf.} \text{ [Keränen 2011, p. 42]}$$

The profile when numerically computed, indicates a clear thermodynamic preference of scalar condensation as seen in FIG. 4.2.2. Alongside in the figure, is $\Delta\mathcal{F}^-/T^3(\langle\hat{\mathcal{O}}_-\rangle)$ profile where the characteristic behaviour of a second order phase transition system is clearly evident: a smooth transition from maxima at the origin (non-zero condensate) in $T < T_c$ regime to minima at the origin in $T > T_c$ regime.

A detailed numerical working can be found in [Herzog et al. 2009] where depending on the different input parameters with regard to chemical potential μ (or superfluid velocity ξ_i as done in [Hartnoll et al. 2008]), the mean field scaling near phase transition temperatures in observed as $\langle\hat{\mathcal{O}}\rangle \propto \sqrt{1 - T/T_c}$: a typical feature of phase transition systems with critical points. It is also been pointed out that the critical temperature for the phase transition (and hence non-zero vev of the

dual CFT operators) is estimated for $\langle \hat{\mathcal{O}}_- \rangle$ as $T_c = 0.213\mu$, while for $\langle \hat{\mathcal{O}}_+ \rangle$ it is $T_c = 0.587\mu$ [Herzog et al. 2009].

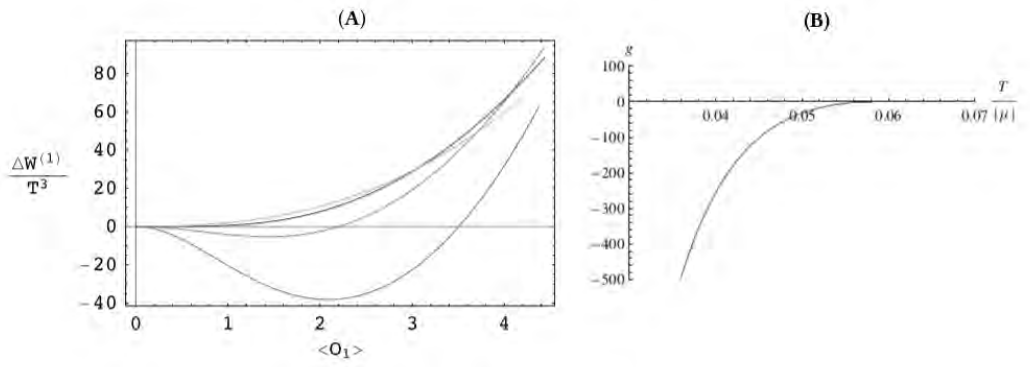

Figure 4.2.2: [A] represents the normalised $\Delta\mathcal{F}^-/T^3$ (represented as $\Delta W^{(1)}/T^3$ in the original figure above) as a function of $\langle \hat{\mathcal{O}}_- \rangle$ (represented as $\langle O_1 \rangle$) for $\mu = -1$ and temperature (going from top to bottom) as T being 0.35, 0.30, 0.25 and 0.20: indicating a second order smooth phase transition. [B] shows the parametrised factor profile of $g(T/|\mu|)$, where below $T_c \simeq 4.065\mu$, a non vanishing scalar solution is thermodynamically favoured. [14]

With all this information at hand, we now have the formulation of the basic holographic superfluid model as proposed by Sean Hartnoll et al. [Hartnoll et al. 2008] and subsequently extended by many others. The next step would be in trying to look at the formation of excited states in the bulk theory which are mapped to vortex like solitonic solutions in the boundary CFT. Achieving such topologically conserved solutions helps propose an alternative theoretical framework within which we could attempt to look at the dynamics of these vortices as a plausible answer to the question of pulsar dynamics.

4.3 Holographic vortex solutions

Quite typically, in any Abelian Higgs (AH) set-up like the bulk AdS gravity coupled Maxwell scalar field theory, the spontaneous symmetry breaking causes the scalar field to have a non-zero ground state of its wave function/order parameter. As seen in §. 4.2, using the AdS/CFT dual interpretation the choice of $\psi_0(x) \xrightarrow{z \longrightarrow 0}$

[14] Image sourced from [Franco et al. 2010, p. 17] (FIG. A) and [Keränen 2011, p. 42] (FIG. B)

$0 \approx \tilde{\rho}_{\pm} \longrightarrow 0$ implies setting any sources explicitly breaking the U(1) gauge symmetry to zero and looking at $\langle\hat{\mathcal{O}}_{\mp}\rangle_{\text{vev}}$. This along with $A_\mu(x) \xrightarrow{z\longrightarrow 0} a_0 \equiv \mu(\neq 0)$ defines the non-zero chemical potential required to induce a non-zero $\langle\hat{\mathcal{O}}_{\mp}\rangle_{\text{vev}}$ at $T < T_c(\mu)$, leading in effect to superfluidity (akin with $|[\psi_0]_{\text{ground state}}| \equiv \psi_{\text{GS}} \neq 0$ as $\mu > 0$ and $T < T_c$, *cf.* §. 1.3.2). In 3+1 dimensions, the AH set-up admits topologically stable *soliton* solutions with field energy density concentrated along tubes of finite width. These structures have quantized magnetic field encasement and an energy per unit length ratio equal to an integral multiple of a basic unit. Imposing *translational invariance* along a particular direction causes the vortices or flux tubes to be parallel to one another and essentially restricts the study to 2+1 dimensions. Given the $\text{AdS}_{3+1}/\text{CFT}_{2+1}$ conjecture employed, this then forms an interesting restriction pertaining to the current study.

Looking at spatially dependent solutions on the (r, θ) plane (in line with thinking that the superfluid velocity, $[v_s]_{(r,\theta)}$ identified with the boundary behaviour of the bulk gauge field $A_\mu(x)$ component a_i is turned on, *cf.* EQN. [4.2.8]) the vortex ansatz solution for modelling holographic superfluids can be taken as –

$$\begin{aligned} \psi_0(x) &\equiv \frac{\rho_0(z,r)}{\sqrt{2}L} e^{i\gamma_0(\theta)} \text{ where } \gamma_0(\theta) = k\theta \text{ with } \theta \in [0, 2\pi) \text{ and } k \in \mathbb{Z} \\ A_\mu(x) &\equiv [A_t(z,r),\ A_\theta(z,r)] \end{aligned} \qquad [4.3.1]$$

This ansatz has certain salient features: (**a**) the holographic radial gauge is employed as before, i.e., $A_z(x) = 0$ and $A_r(x)$ is taken to be zero; (**b**) the cylindrical symmetry makes all gauge invariant quantities independent of θ, with the characteristic exception of the field $\gamma_0(\theta)$ — being a normalizable mode — making the superfluid velocity profile dynamic, i.e., to say that fixing $\gamma_0(\theta)$ by hand *explicitly* breaks the U(1) gauge symmetry [Appendix B in Keränen et al. 2010b]; (**c**) the metric line element $\mathrm{d}s^2$ is as defined in EQN. [4.2.3] with the metric tensor $g_{\mu\nu}$ and scalar field mass $m^2_{\psi_0} = -2/L^2$ and (**d**) the static vortices imply time invariant construction i.e., $\partial_t \sim 0$.

With these consideration the Euler Lagrange equations of motion in EQN. [4.2.4] (ignoring the gravitational field equation in the decoupled probe limit with back-reaction to gravity ignored) can be expressed as –

$$z^2\partial_z\left(\frac{f(z)}{z^2}\partial_z\rho_0(z,r)\right)+\frac{1}{r}\partial_r\Big(r\ \partial_r\rho_0(z,r)\Big)$$
$$+\left(\frac{A_t^2(z,r)}{[f(z)]^2}-\frac{[A_\theta(z,r)-k]^2}{r^2}-\frac{m^2}{z^2}\right)\rho_0(z,r)=0 \quad [4.3.2]$$

$$\partial_z\Big(f(z)\partial_z A_\theta(z,r)\Big)+r\partial_r\left(\frac{1}{r}\partial_r A_\theta(z,r)\right)-\frac{\rho_0^2(z,r)}{z^2}\Big(A_\theta(z,r)-k\Big)=0 \quad [4.3.3]$$

$$f(z)\partial_z^2 A_t(z,r)+\frac{1}{r}\partial_r\Big(r\ \partial_r A_t(z,r)\Big)-\frac{\rho_0^2(z,r)}{z^2}A_t(z,r)=0 \quad [4.3.4]$$

The regularity of the vortex solutions of the bulk equation of motions given in the set EQN. [4.3.2] – EQN. [4.3.4] can be studied by considering certain boundary conditions imposed on their behaviour near the BH horizon and the asymptotic boundary regime as they approach the conformally flat space (asymptotically AdS spacetime). A detailed explanation/justification for these boundary conditions can be found in [Albash and Johnson 2009] and along a similar line in [Domenech et al. 2010; Keränen et al. 2010b].

REGULARITY CONDITIONS OF VORTEX SOLUTIONS

BH BOUNDARY BEHAVIOUR

The finiteness of the effective scalar mass m^2_{eff} ($\sim g^{tt}A_t^2$) implies the BH horizon i.e., $z=z_h\equiv\tilde{z}\longrightarrow 1$ (or setting $z_h=1$), equivalently $f(z)\longrightarrow 0$ makes the term $A_t(z=1,r)=0$. Moreover, at the BH horizon, regularity of the vortex solutions are imposed by constraint equations –

$$\Big[-3\partial_z\rho_0(z,r)+\partial_r^2\rho_0(z,r)+\frac{1}{r}\partial_r\rho_0(z,r)$$
$$-\frac{1}{r^2}\rho_0(z,r)\left[A_\theta(z,r)-k\right]^2+2\rho_0(z,r) \;=\; 0\Big]\Big|_{z=z_h}$$
$$\text{and}\ \Big[-3\partial_z A_\theta(z,r)-\rho_0^2(z,r)\left[A_\theta(z,r)-k\right]$$
$$+\left(\partial_r^2 A_\theta(z,r)-\frac{1}{r}\partial_r A_\theta(z,r)\right) \;=\; 0\Big]\Big|_{z=z_h}$$

Vortex core boundary behaviour

At $r = 0$, in the vortex core region, we impose the following conditions: **(i)** scalar field $\rho_0(z, r = 0) = 0 \forall k \neq 0$ to maintain normal phase within the vortex core and keep the bulk electric charge at the vortex core zero (i.e., $\mathcal{Q} = \int \mathrm{d}^3x j_0(x) \xrightarrow{r\longrightarrow 0} 0$, with $j_0(x)$ being charge density), **(ii)** gauge field $\partial_r A_t(z, r = 0) = 0$ so that there is no contribution to the radial electric field, i.e., $\mathbf{E}_i(x) = -\partial_r A_t(x) \longrightarrow 0$ for $r \longrightarrow 0$, and **(iii)** $\partial_r \rho_0(z, r = 0) = 0 \; \forall \; k = 0$ and $A_\theta(z, r = 0) = 0$.

Asymptotic boundary behaviour

The boundary conditions at the AdS boundary determines the external sources turned on in the dual field theory as seen in § 4.3. With this consideration, the regularity conditions can be expressed as: **(i)** $A_t(z = 0, r) \equiv a_0(z = 0) = \mu$, the chemical potential of the boundary CFT, **(ii)** $A_\theta(z \longrightarrow 0, r) = a_\theta(r) = \frac{1}{2}\mathrm{B}r^2$ (B, being external rotation or external fixed magnetic field) as the boundary magnetic field $\mathbf{B}_z = (\partial_r A_\theta)/r \longrightarrow 0$, and **(iii)** for the scalar field, $\rho_0(z, r)$: $\rho_0(0, r) = 0$ (Dirichlet b.c.) or $\partial_z \rho_0(0, r) = 0$ (Neumann b.c.) correspond to two different boundary theories with different scaling dimensions of the condensing scalar operator, either $\langle \hat{\mathcal{O}}_+ \rangle$ or $\langle \hat{\mathcal{O}}_- \rangle$ respectively.

An additional consideration is in the size of the cylindrical radius R such that $r \leq R$, as the vortex energy per unit length diverges with $\xi \sim r \ll R|_{\longrightarrow\infty}$ (compare with EQN. [2.3.5]). Effectively, at $r = R$: $\partial_r \rho_0(z, R) = 0$, $\partial_r A_t(z, R) = 0$ and $A_\theta(z, R) = \frac{1}{2}\mathrm{B}R^2$ are the constraints.

4.3.1 Numerical simulations and Analysis

The holographic vortex equations of motion in EQN. [4.3.2] – EQN. [4.3.4] are a set of inhomogeneous coupled nonlinear partial differential equations that do not present a straightforward analytic solution. Numerically, they have been solved using various numerical recipes involving different boundary constraints, e.g., Ville Keränen et al. [Keränen et al. 2010b] employed an angular gauge field $A_\theta(z = 0, r) = 0$ and used the Gauss Seidel relaxation scheme where the system was placed in a finite box of radius L, with $(z, r) \in [0, 1] \times [0, L]$ and discretized

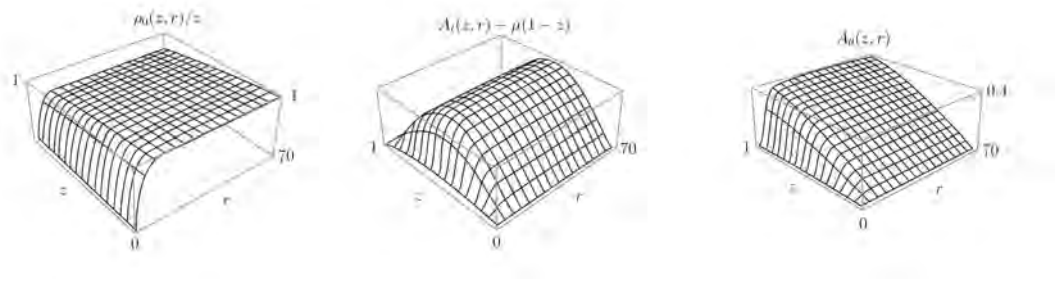

(a) Typical bulk field profiles for the $\langle\hat{\mathcal{O}}_-\rangle$ condensate

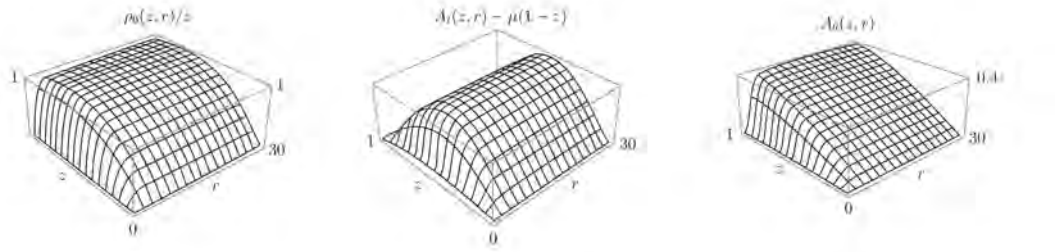

(b) Typical bulk field profiles for the $\langle\hat{\mathcal{O}}_+\rangle$ condensate

Figure 4.3.1: Typical bulk field profiles with $\rho_0(z,r)/z \leftrightarrow \langle\hat{\mathcal{O}}_\pm\rangle$ based on Dirichlet/Neumann boundary conditions respectively and condensate ($T/T_c \simeq 0.9$). For visualisation purposes, the linear background (as in the homogeneous case of $A_\mu(z) \equiv A_t(z) \sim \mu - \rho z$ as $z \longrightarrow 0$) is subtracted from A_t. In keeping with current context, the labelling is modified with current coordinate and variable convention. [15]

along both axis; turning derivative equations into finite difference equations (details of the numerical procedure found in [Keränen et al. 2010a]). The typical bulk field profiles calculated by Ville Keränen et al. [Keränen et al. 2010b] for both the $\langle\hat{\mathcal{O}}_-\rangle$ and $\langle\hat{\mathcal{O}}_+\rangle$ condensate with $T/T_c \simeq 0.9$ are shown in FIG. 4.3.1a and FIG. 4.3.1b respectively.

Separately, Oriol Domnènech et al. [Domenech et al. 2010] employed a numerical computation scheme (initiated using COMSOL MULTIPHYSICS[16] 3.4 package) of the holographic vortex equations with the angular gauge field, $A_\theta(z=0,r) = \frac{1}{2}\mathrm{B}r^2$ along with the other boundary conditions detailed above. In their model, the mass of the scalar field $m_{\psi_0} = 0$ that related to the dimension of the corresponding boundary condensate $\langle\hat{\mathcal{O}}\rangle$, effectively permitting only the Δ_+ modes.

[15] Modified on `Adobe Illustrator CS5`, sourced originally from [Keränen et al. 2010b, p. 10]

[16] www.comsol.com

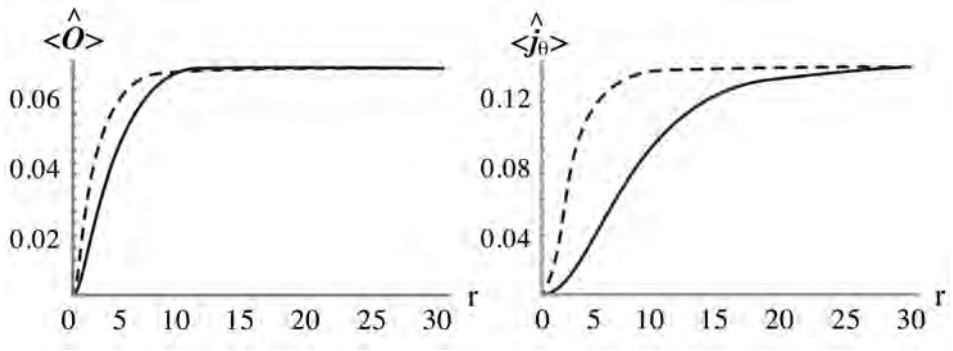

Figure 4.3.2: Expectation values of condensate $\langle\hat{\mathcal{O}}\rangle$ and the azimuthal current $\langle\hat{j_\theta}\rangle$ (up to a factor of $1/q^2$) as functions of r from the holographic model in the $k = 1$ superfluid vortex solution for $d = 2 + 1$, with a choice of $T/T_c = 0.3$ and B$= 0$. The dashed lines show the comparative profiles in the classical Ginzburg Landau model (or equivalently the Gross Pitaevskii model); all in units of $\mu = 1$. [17]

As typically expected with the AdS/CFT prescription, $\left\langle\hat{\mathcal{O}}_\Delta(r)\right\rangle = \frac{1}{\Delta}\tilde{z}^{1-\Delta}\partial_z\psi_0(z,r)\Big|_{z=0}$ where $\Delta := \{\Delta_-, \Delta_+\}$ is the dimension of the operator related to the mass $m^2_{\psi_0}$ of the scalar field as seen $m^2_{\psi_0}L^2 = \Delta(\Delta - d)\Big|_{d=3}$. Moreover, the free energy of the system [Montull et al. 2009] can be seen to be (in line with §. 4.2.2) –

$$\frac{\mathcal{F}[T_{\text{BH}}, \text{B}, \mu]}{T_{\text{BH}}} = [\mathbb{S}_{\text{AdS}}]_{\text{Euclidean}} + \frac{\pi}{T_{\text{BH}}}\int_0^R \mathrm{d}r r A_t(z,r)\partial_z A_t(z,r)\Big|_{z=0}$$

With this at hand, the expectation value of the azimuthal current can be found out to be $\left\langle\hat{j_\theta}(r)\right\rangle = \frac{\delta\mathcal{F}}{\delta A^\theta}\Big|_{z=0} \simeq \frac{\partial_z A_\theta(z,\theta)}{r}\Big|_{z=0}$. The FIG. 4.3.2 represents the order parameter $\langle\hat{\mathcal{O}}(r)\rangle$ and the current $\langle\hat{j_\theta}(r)\rangle$ as functions of r for $k = 1$ vortex solution obtained in the numerical analysis of Oriol Domnènech et al. [Domenech et al. 2010].

The dual boundary theory has the condensate operator $\hat{\mathcal{O}}(r)$ from the AdS/CFT prescription in line with the expectations of $[\psi(r,\theta)]_{\text{vortex solution}}$ in the standard Gross Pitaevskii superfluidity model, i.e., $\langle\hat{\mathcal{O}}(r)\rangle \equiv [\psi_0(z=0,r)]_{\text{boundary}} \leftrightarrow [\psi_0(r,\theta)]_{\text{GP}}$ This can be seen in the power law function fitted to the $\langle\hat{\mathcal{O}}_\pm(r)\rangle$ from the inhomogeneous vortex solutions found using the dual AdS/CFT description.

[17] Modified on `Adobe Illustrator CS5`, originally from [Domenech et al. 2010, p. 12]

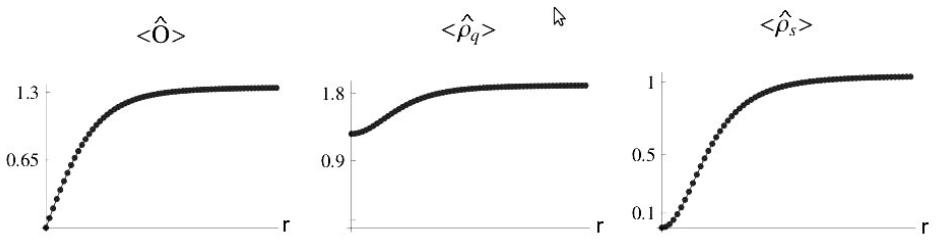

Figure 4.3.3: Typical radial profile for expectation values of the condensate $\left\langle \hat{\mathcal{O}}_{-} \right\rangle$ (represented here as $\langle \hat{\mathrm{O}} \rangle$), the charge density $\langle \hat{\rho_q} \rangle$ and the superfluid density $\langle \hat{\rho_s} \rangle$ (for $T/T_c \approx 0.9$. In keeping with current context, the labelling is modified with current coordinate convention. [18]

In line with the work of identifying characteristic scale lengths of the problem, Ville Keränen et al. [Keränen et al. 2010b] showed that (*cf.* FIG. 4.3.3) –

$$\langle \hat{\mathcal{O}}_{\pm}(r \longrightarrow \infty) \rangle = e^{i\theta} \left| \langle \hat{\mathcal{O}}_{\pm}(r \longrightarrow \infty) \rangle \right| \left(1 - \frac{\xi_{\text{tail}}^2}{2r^2} + \cdots \right) \text{ for the tail region}$$

$$\text{and } \langle \hat{\mathcal{O}}_{\pm}(r \longrightarrow 0) \rangle = e^{i\theta} \left| \langle \hat{\mathcal{O}}_{\pm}(r \longrightarrow \infty) \rangle \right| \frac{r}{\xi_{\text{core}}} \text{ for the slope region}$$

where $\left| \langle \hat{\mathcal{O}}_{\pm}(r \longrightarrow \infty) \rangle \right| \leftrightarrow \left| [\psi_0(r, \theta)]_{\text{GS}} \right|$, the ground condensate state of the GP theory. This quite neatly ties in with the GP model where based on the regime of $\eta \equiv r/\xi$, the condensate wave function has power law behaviour as seen in §. 2.2. On comparison with EQN. [2.2.9] and EQN. [2.2.11] — with the winding number taken as $k = 1$ — it is natural to identify the **coherence length** of vortices, ξ (or effectively, the vortex radius size, $r_c = \xi e^{-c} \approx 0.68\,\xi$) with the term ξ_{core} here. An important point here relates ξ_{core} to the inverse of Fermi momentum, $p_{\mathcal{F}}$ (as most of the physics of the matter within the core healing length is in normal phase), where as ξ_{tail} is identified with the inverse energy gap of superfluid state of matter. This implies that the ratio of the two length scales is important when trying to understand the transfer between the weakly coupled BCS superconductor regime ($\xi_{\text{tail}} \gg \xi_{\text{core}}$) and strongly coupled BEC condensation states ($\xi_{\text{tail}} \sim \xi_{\text{core}}$) through a BCS-BEC crossover [Sensarma et al. 2006] as is found within neutron star layers. This could have an important part to play in understanding the different coupling regimes required to support the vortex pinning theories of pulsar glitches.

[18] Image sourced from [Keränen et al. 2010b, p. 12]

In the $z \longrightarrow 0$ regime, $A_t(z,r) = a_0(z,r) + b_0(z,r)z \equiv \mu - \rho(r)z$, with $-\rho$ being proportional to the charge density (*cf.* §. 4.2.2) and with this understanding, it is easy to see that $\langle\hat{\rho}_q(r)\rangle_{\text{boundary}} \equiv [\rho(z \longrightarrow 0)]_{\text{bulk}}$ leads to the identification, $\langle\hat{\rho}_q(r)\rangle = \langle\hat{\rho}_q(0)\rangle + \Big(\langle\hat{\rho}_q(r \longrightarrow \infty)\rangle - \langle\hat{\rho}_q(0)\rangle\Big)\left(1 - \frac{\xi_q^2}{r^2} + \cdots\right)$ with the value $\langle\hat{\rho}_q(r \longrightarrow \infty)\rangle \equiv qn_0$, the condensate charge density in the ground state of $[\psi_0(\mathbf{r})]_{\text{GP}}$ and ξ_q as the characteristic **charge density coherence length**. This length scale helps understand the nontrivial information of density depletion (the fraction of charged matter in the condensate) in the vortex core as function of temperature. This is a good indication (when compared with a standard field theoretical analogue) of trying to probe the microscopic physics of condensate looking at the solitonic cores. In [Keränen et al. 2010b], it was pointed out that based on the choice of the dual gauge theory, a comparison of the density depletions in nonrelativistic settings — solitonic cores at zero temperature have zero charge density as the condensate vanishes, where as the BCS solitonic cores have finite number density of cold atoms despite the loss of condensate — reveals $\hat{\mathcal{O}}_-$ as a BEC superfluid and $\hat{\mathcal{O}}_+$ as a BCS superfluid: another important consequence towards a better description of the holographic superfluid model.

The boundary value of the derivative of the angular gauge field $A_\theta(z \longrightarrow 0, r)$ can be identified with the current $\langle\hat{j}_\theta(r)\rangle$ in the boundary theory. This boundary current when fit to a power law series, presents a similar comparison to the concept of superfluid current density $j^i = \rho_s[v_s]^i$, where $[v_s]$ is the superfluid velocity and ρ_s is understood as the superfluid mass density ($\sim mn_0$ as $r \longrightarrow \infty$). With the identification of $\langle\hat{\mathcal{O}}\rangle$ as the condensate wave function $[\psi_0(r,\theta)]_{\text{GP}}$, the term $\gamma_0(\theta) = k\theta$ becomes identified with the phase of the condensate, implying that $[v_s]^i \leftrightarrow (\hbar/m)\partial^i\gamma_0(\theta) \Rightarrow [v_s]^\theta \propto k/(mr)$ (*cf.* EQN. [1.3.11]). Thus, the superfluid density as extracted from the holographic theory, i.e., $\langle\hat{\rho}_s(r)\rangle \sim m\partial_z A_\theta/k$ presents the third scale of **superfluid density coherence length** (ξ_s), taken as $\langle\hat{\rho}_s(r)\rangle = \langle\hat{\rho}_s(r \longrightarrow \infty)\rangle\left(1 - \frac{\xi_s^2}{r^2} + \cdots\right)$, where $\langle\hat{\rho}_s(r \longrightarrow \infty)\rangle \leftrightarrow \rho_s \equiv mn_0$ is the superfluid mass density in the GP field theory.

In the holographic dual theory — in line with the work of Oriol Domènech et al. [Domenech et al. 2010] — as seen in the $\langle\hat{\mathcal{O}}\rangle$ and $\langle\hat{j}_\theta\rangle$ profiles of FIG. 4.3.2, (**a**) the value of $\xi_{\text{GP}} \sim \xi_{\text{core}}$ can be estimated from the value of $\left\langle\hat{\mathcal{O}}(r)\right\rangle$ (depending on the scaling dimension) as seen above and (**b**) the identification of $\langle\hat{j}_\theta(r)\rangle = \partial_z A_\theta/r \leftrightarrow [j^\theta(r)] = \rho_s(r)[v_s(r)]^\theta \sim n_0(r)k/r$ from where the coupling g_{GP} could be extracted based on the relation $\hbar\mu = n_0(r)g_{\text{GP}}$. The estimated parameters of ξ_{GP} and g_{GP} then help calculate the condensate and current measurements of the classical GP theory in a standard way. A comparison of the classical and holographic results reveals the strength of the duality applied to superfluid study, e.g., Oriol Domènech et al. found (for a superconducting model of Ginzburg Landau) that for $d = 3$ at $T/T_c = 0.3$, $\xi_{GL} \simeq 1.1\mu^{-1}$ and $b_{\text{GL}} \equiv g_{\text{GP}}/2 = 3.3\mu$. Their numerical work confirmed that as $T \simeq T_c$, the holographic model imitated the GL theory in its prediction of condensate and current densities despite having a characteristic difference in the vortex sizes, $\xi > \xi_{\text{GP}}$.

4.4 Free energy configuration of vortex lines

A strong indication of the validity of applying AdS/CFT techniques to study superfluids is in looking at the vortex line energy per unit length. If the energy profile of the excited vortex states in the holographic superfluid model show the characteristic logarithmic divergence for the vortex core radius $\xi \sim r \ll R|_{\longrightarrow\infty}$ with R being the cylindrical sample radius under study (*cf.* EQN. [2.3.3]), then this dual gauge/gravity approach could be taken as a theoretical framework from where a lot of interesting physics of superfluid phenomenon can be potentially extracted. Motivated by this reasoning, this section attempts to look at reviewing the free energy configuration of holographic vortices in line with the works of [Keränen et al. 2010b; Montull et al. 2009].

According to standard methods, the AdS/CFT dictionary identifies the free energy of the boundary CFT with the renormalised Euclidean on-shell action in the bulk AdS as $\mathcal{F} = -T_{\text{BH}}[\mathbf{S}_{\text{EUCLIDEAN}}]_{\text{renorm}}$. The first step along the holographic renormalization routine for inhomogeneous solitonic (vortex) solutions of the field equation is in identifying the Lorentzian on-shell action of the solution (with the AdS

boundary $z = \epsilon$ cut-off and the IR (long distance) cut-off at radial distance $r = R_c$). Thus, in the decoupled probe limit (ignoring gravitational backreaction) with the matter action $\mathbf{S}_{\text{MS}}$ of EQN. [4.2.2], a background metric $\mathrm{d}s^2|_{L=1}$ of EQN. [4.2.3] and vortex ansatz solutions of EQN. [4.3.1] we have –

$$\begin{aligned}[\mathbf{S}_{\text{MS}}]_{\text{on-shell}} \;=\; & \int \mathrm{d}t \int_{\epsilon}^{z_h \equiv 1} \mathrm{d}z \int_0^{2\pi} \mathrm{d}\theta \int_0^{R_c} r\,\mathrm{d}r \Big(-\frac{f(z)}{z^2}|\partial_z \psi_0|^2 - \frac{1}{z^2}|\partial_r \psi_0|^2 \\ & + \frac{1}{f(z) z^2} A_t^2 |\psi_0|^2 - \frac{m^2}{z^4}|\psi_0|^2 - \frac{1}{2r^2}(\partial_r A_\theta)^2 + \frac{1}{2}(\partial_z A_t)^2 \\ & + \frac{1}{2f(z)}(\partial_r A_t)^2 - \frac{f(z)}{2r^2}(\partial_z A_\theta)^2 - \frac{1}{z r^2}|\partial_\theta \psi_0 - i A_\theta \psi_0|^2 \Big) \quad [4.4.1]\end{aligned}$$

As is evident here, once the counter term of $[\mathbf{S}]_{\text{counter}} = -\int \mathrm{d}^3x \frac{|\psi_0|^2}{\epsilon^3}$ is added to regularize the on-shell divergences, there remains in the regularised action a *divergence* due to integration over r, i.e., the leading terms in the free energy would become divergent as $R_c \longrightarrow \infty$: a typical large r effect where the AdS boundary gauge fields and scalar fields are considered spatially homogeneous and translationally invariant as $r \longrightarrow \infty$ in the CFT regime (*cf.* §. 4.2.2).

This comparison lets us view the behaviour of the scalar $\psi_0(z, r, \theta) \sim \sqrt{2}\rho_0(z, r)e^{ik\theta}$ and gauge fields in the excited vortex state as being perturbatively given by: $\rho_0(z, r) = \rho_0^{(0)}(z) + \delta\rho_0(z)/r^2 + \cdots$, $A_t(z, r) = A_t^{(0)}(z) + \delta A_t(z)/r^2 + \cdots$ and $A_\theta = A_\theta^{(0)}(z) + \delta A_\theta(z)/r^2 + \cdots$. With this implementation it can be clearly seen that the leading term in A_θ, i.e., $A_\theta^{(0)}$ leads to logarithmic divergence in the last two terms of the EQN. [4.4.1], while the sub-leading term $\delta A_\theta(z)/r^2$ makes a finite contribution. Moreover, with the vortex equations of motion in EQN. [4.3.2] – EQN. [4.3.4] and the AdS boundary conditions in §. 4.3, it can be verified (utilizing some mathematical labour) that the contributions coming from the leading (and sub-leading) perturbative bulk field terms (of $A_t(z, r)$ and $\rho_0(z, r)$) in the regularized on-shell action $[\mathbf{S}]_{\text{regular}}$ stated above are vanishing. This is due to them being identified with the equations of motion (hence on-shell criterion) or being proportional to a vanishing boundary constraints.

As an effect of this, when looking at the difference between the regularised action in an excited vortex state and a spatially homogeneous, translationally invariant state of spontaneous symmetry breaking (ground state) in the holographic model, we have an expression of the form (neglecting all finite contribution terms in the $r \longrightarrow \infty$ limit) –

$$\begin{aligned}
[\Delta\mathbf{S}]_{\text{renorm}} &\approx -\int \mathrm{d}^4x \left[\frac{1}{2z^2}(\rho_0^{(0)})^2(A_\theta^{(0)}-k)^2 + \frac{f(z)}{2}(\partial_z A_\theta^{(0)})^2\right] \\
&\equiv \lim_{\epsilon\longrightarrow 0}\Big\{ -\int_0^{2\pi}\mathrm{d}\theta\int_\xi^{R_c} r\,\mathrm{d}r\int \mathrm{d}t\int_\epsilon^{z_h\equiv 1}\mathrm{d}z\Big[\frac{k}{2}\partial_z\Big(f(z)\partial_z A_\theta^{(0)}\Big) \\
&\quad -\frac{1}{2}\partial_z\left(f(z)A_\theta^{(0)}\partial_z A_\theta^{(0)}\right)\Big]\Big\} \\
&\approx -\frac{k\pi}{T_{\text{BH}}}\ln\left(\frac{R_c}{\xi}\right)\Big[\partial_z A_\theta^{(0)}\Big|_{z\longrightarrow 0} + \underbrace{\cancelto{0}{f(z)A_\theta^{(0)}\partial_z A_\theta^{(0)}}}_{\text{boundary constraint at } z\longrightarrow 0}\Big]
\end{aligned}$$

where in the second step, the asymptotic behaviour ($z \longrightarrow 0$ and $r \longrightarrow \infty$) of the field equations is considered, $\partial_z(f(z)\partial_z A_\theta^{(0)}) - (\rho_0^{(0)}/z)^2(A_\theta^{(0)} - k) = 0$ (*cf.* [Appendix C, Keränen et al. 2010b]) and the in the last step a Euclidean compactification of time with period $\beta = 1/T_{\text{BH}}$ is regarded. With this at hand, one can write the difference in free energy between the ground superfluid state and the first excitation state, effectively the vortex free energy as (taking $A_\theta^{(0)} \sim A_\theta$): $\mathcal{F}_{\text{vortex}} \approx -T_{\text{BH}}\underbrace{[\Delta\mathbf{S}]_{\text{renorm}}}_{\text{Euclidean}} = k\pi\ln\left(\frac{R_c}{\xi}\right)\partial_z A_\theta\Big|_{z\longrightarrow 0}$ leading to the expression –

$$\Rightarrow \mathcal{F}_{\text{vortex}} \approx \frac{k^2\pi\rho_s(r\longrightarrow\infty)}{m}\ln\left(\frac{R_c}{\xi}\right) \qquad [4.4.2]$$

where the superfluid density ρ_s identified with the boundary expectation value $\langle\hat{\rho}_s(r)\rangle$ in the holographic picture is defined as $\rho_s \simeq (m/k)\partial_z A_\theta\Big|_{z\longrightarrow 0}$ at $r \longrightarrow \infty$ on the boundary and ξ is the length scale of vortex core size, $\xi \sim r_c$.

As has been seen in §. 2.2, the energy of a vortex line (per unit length) associated with the superfluid flow in EQN. [2.3.5] in the absence of the ambient flow causing vortex line motion, i.e., $\vec{v}_n = 0$ is given as: $\frac{E_\nu}{L} \approx 4\pi\xi^2k^2\left(\frac{\mu^2}{2g}\right)\ln\left(\frac{R}{\xi}\right) \approx \pi\rho_s(x)\kappa^2\ln\left(\frac{R}{\xi}\right)$, with $\xi = \sqrt{\frac{\hbar}{2m\mu}}$, $\hbar\mu = n_0 g$ and $\rho_s(r) = mn_0(r)$.

This then lets the vortex free energy (in the classical case) be identified as –

$$\mathcal{F}_{\kappa} \approx \frac{k^2 \pi \rho_s(r)}{m} \ln\left(\frac{R}{\xi}\right) \qquad [4.4.3]$$

when we identify $n_0(r)$ with the condensate particle density of the ground state, i.e., $|[\psi_0(r)]_{GS}|$, leading to the vortex energy per unit length effectively being the free energy difference of vortex excitations from ground state vacuum.

Within the definitions of AdS/CFT at the asymptotic boundary at $z \longrightarrow 0$, we can look at EQN. [4.4.3] and EQN. [4.4.2] and ascertain the validity of the holographic approach in the study of superfluid vortices. The identification of the free energy of the vortices in the holographic theory of superfluidity with the classical Gross Pitaevskii (GP) theory for superfluid states, provides an important verification of the AdS/CFT principle applied to establish an alternative framework for the physics of strongly coupled low temperature systems like neutron star interiors, extended as a plausible explanation the observational time anomalies in pulsars rotations.

ROTATIONAL FRAME OF MOTION

In the classical sense, the corotating framework with a static external field a_θ and consequential increase in superfluid angular velocity as $[v_s]_\theta \longrightarrow [v_s]_\theta - \Omega r^2$ where $\Omega = a_\theta / r^2$, causes the supercurrent density to change as $j_\theta = \rho_s \left([v_s]_\theta - \Omega r^2\right)$. The superfluid/superconductor correspondence is in identifying the external magnetic field $B = \partial_r a_\theta / r$ with the external rotational velocity Ω (in the limit charge, $e \longrightarrow 0$) as $\Omega \leftrightarrow B/2$. Alternatively, the identification can be expressed as: $\underbrace{[L_\perp(\Omega)]_k}_{\text{angular momentum}} = \pi \int_\xi^R \mathrm{d}r r j_\theta \simeq \pi \rho_s (r \longrightarrow \infty) \left(kR^2 - \frac{R^4}{2}\Omega\right) \longleftrightarrow 2\underbrace{[M(B)]_k}_{\text{magnetization}}$ in a direction perpendicular to the (r, θ) plane.

For non-zero B (equivalently $\Omega \neq 0$), the free energy of the vortex line in EQN. [4.4.3] is estimated as – $\mathcal{F}_k(\Omega) = \mathcal{F}_k(0) - \int_0^{2\Omega} [L_\perp]_k(\Omega)\, \mathrm{d}\Omega$, leading to -

$$\mathcal{F}_k(\Omega) \simeq \mathcal{F}_k(0) + \pi \rho_s(x) \left(k^2 \ln\left[\frac{R}{\xi}\right] - k\Omega R^2\right) \qquad [4.4.4]$$

The calculations of Marc Montull et al. [Montull et al. 2009] and Oriol Domènech et al. [Domenech et al. 2010] show the magnetization,$[M(B)]_k$ (equivalently thought of as the angular momentum $[L_\perp(\Omega)]_k/2$) as $\rho_s([\psi_0]_{\text{GS}}) = 0.48\sqrt{\rho}$, as $[M(B)]_k \simeq 0.7\kappa R^2\sqrt{\rho} - 0.2R^4\sqrt{\rho}B$. This, then put an estimate on the free energy difference of a single vortex configuration as –

$$\frac{\mathcal{F}_1(B) - \mathcal{F}_0(B)}{\sqrt{\rho}} \simeq 0.9 \ln\left(\frac{R}{\xi}\right) - 0.4R^2B$$

In their work, both Marc Montull et al. and Oriol Domènech et al., consider the estimate of the superfluid density $\rho_s(r \longrightarrow \infty) = m(n_0 \equiv [\psi_0]_{\text{GS}})$ (boundary state of $z \longrightarrow 0$ in the (r, θ) plane) as being related to the charge density ρ (for $m^2_{\psi_0} = -2$).

In case of superfluids, the two *critical fields*: angular velocity Ω_{c1} above which the vortex configuration is energetically favoured and Ω_{c2} at which the normal phase is favourable can be defined as $\Omega_{c1} \simeq \frac{1}{R^2}\ln\left(\frac{R}{\xi}\right)$ and $\Omega_{c2} = 1/\xi_{\text{GP}}$ (detailed derivation in [Kopnin 2002]), where ξ_{GP} is the coherence length of the Gross Pitaevskii theory defined as $\xi_{\text{GP}}(T) = \psi_0/\nabla^2\psi_0$. With the computation of the free energy for vortices in the presence of an external rotation (effectively, $\Omega \leftrightarrow B/2$) as done above, the value of $\Omega_{c1} \sim 7k/R^2 \sim 14/R^2$ ($m^2_{\psi_0} = -2$ and $k = 1$), indicating that as $R \longrightarrow \infty \Rightarrow \Omega_{c1} \longrightarrow 0$; i.e., for a large enough sample, homogeneous ground state superfluid solutions are destroyed by any $\Omega \neq 0$. Also, with Ω increasing up to Ω_{c2}, vortices appear in the superfluid, but surpassing Ω_{c2} the normal phase of the fluid returns and condensate goes to zero. Estimating this value, based on the rotation Ω corresponding to zero size superfluid regions in the vortex assembly, Marc Montull et al. [Montull et al. 2009] gave the value for $m_{\psi_0} = -2$ as $\Omega \simeq (5/2)\rho$.

It should be mentioned that the analysis in both these papers above utilized the holographic superconductors perspective where the charge density, $\rho \equiv \partial_z A_t(z \longrightarrow \infty, r)$ in the dual boundary CFT is held fixed: this is equivalent to holding the chemical potential $\mu \equiv A_t(z \longrightarrow \infty, r)$ fixed at the boundary in an analogous superfluid description.

In concluding the discussion on holographic duals to superfluids, it should be noted that strictly speaking, the boundary 2+1 dimensional finite temperature CFT cannot exhibit spontaneous symmetry breaking due to the Mermin-Wagner-Hohenberg theorem that attributes thermal fluctuations as the destroyer of long range angular modes responsible for the condensed phase [Mermin and Wagner 1966; Hohenberg 1967], however in the holographic model this problem is avoided by considering a large N limit field theory. In large N theories, the effect of thermal fluctuation on spontaneous symmetry breaking is exponentially suppressed as vortex loop[19] energy and action of the configuration describing vortex nucleations are proportional to N. This implies that within the finite volume and time scales of the problem, the system-state with a non-zero superfluid velocity can be considered to be in thermal equilibrium.

[19]The thermodynamic phase transition (with critical temperature T_c) of superfluids can be looked at from an alternative disorder field theory of Hagen Kleinert [Kleinert 1990] where the statistical mechanics of the grand canonical ensemble of vortex lines in superfluids determine the superfluid phase transformation. Essentially, the **vortex-loops**, with adjacent *rotons* coupling across their surfaces to form a large vortex-loop surface (containing normal fluid matter within) and the corresponding high configuration-entropy together maintain the vortex-line array structure seen in rotating superfluids up to the critical temperature. Beyond that, the vortex loop proliferate in size and fill the ambient fluid completely, causing a superfluid to normal phase transition with increased angular velocity.

I hold that the mark of a genuine idea is that its possibility can be proved, either a priori by conceiving its cause or reason, or a posteriori when experience teaches us that it is a fact in nature.

Leibniz, 1670

5

Conclusions and Extensions

The phenomenon of pulsar glitches has long been believed to hold important keys to unlocking the hidden physics governing Neutron stars dynamics. The radial-line density dependent distribution of matter in the interior crust of these mysterious objects indicates a complex mixture of strongly-degenerate neutron-pair condensates that inter penetrate a solid crystalline lattice structure. A thermally motivated quantum phase transitions of these macroscopic condensates into superfluid-flows then sets the mandate to understand the anomalous observational behaviour of rotating pulsar systems.

An initial insight into understanding the superfluid dynamics lies with the classical Gross Pitaevskii (GP) model where the inherent U(1) symmetry of the lagrangian is destroyed by *spontaneous symmetry breaking* upon phase transition into the superfluid regime. A detailed analysis reveals that in the classical picture the excitation states of the solitonic solutions of GP lagrangian present quantized vortex-line arrays with vortex cores. The model confirms the presence of the characteristic

logarithmic-divergent free energy configuration of a vortex line with its dependence on the coherence length and sample radial size of cylindrical symmetry.

With this machinery, the origin of pulsar *glitches* in terms of it being the natural macroscopic outcome of the angular momentum exchange between the crust-core regions of neutron star interior can be understood to be mediated by the quantized vortex line dynamics embedded in the internal superfluid layers. The vortex pinning and creep mechanisms, backed by the many sustaining nuclear arguments of binding and pinning energies, advance a considerable support of them being treated as a working model to explain glitches in pulsars and the post glitch recovery physics. However, at the time of writing this, there remains no complete and comprehensive explanation to advance as a coherent model of pulsar glitches within the vortex-structure framework.

In fact, any complex Ginzburg Landau theory (GP being a special case without dissipation) standardly employed in the study of a superfluid system is a phenomenological mean field type equation that describes the ground state of a N body quantum system of *weakly* interacting particles at zero temperature. A finite temperature correction to the energy gap function $\Delta(T)$ and the employment of a critical temperature T_c above which superfluidity is destroyed, enables the standard description of the correlated particle system (condensate wave function) in terms of order parameter (for spontaneously broken symmetry) or quasiparticles (long mode excitations) to superfluid flow generating quantized vortices (or alternately, Bogoliubov quasiparticle excitation states).[20]

Fundamentally though, the application of Bogoliubov perturbation approach is restricted to (**i**) the BCS regime where the weakly-interacting Fermi gas has ground state superfluidity due to loosely-bound Cooper pair condensate [`BCS limit of a` $p_{\mathcal{F}} < 0$ `and` $|ap_{\mathcal{F}}| \ll 1$] and (**ii**) the BEC regime where the Fermions form bound molecules and the system is effectively a weakly interacting Bose gas, with a standard BEC type superfluid ground state [`BEC limit of` $0 < ap_{\mathcal{F}} \ll 1$]; with a as the s-wave scattering length and $p_{\mathcal{F}}$ as the Fermi momentum. In the *strongly* interacting picture with the BCS-BEC cross over in the range $|ap_{\mathcal{F}}| \gtrsim 1$,

[20] A comprehensive and exhaustive review of weakly interacting Bose gas can be found in [Andersen 2004].

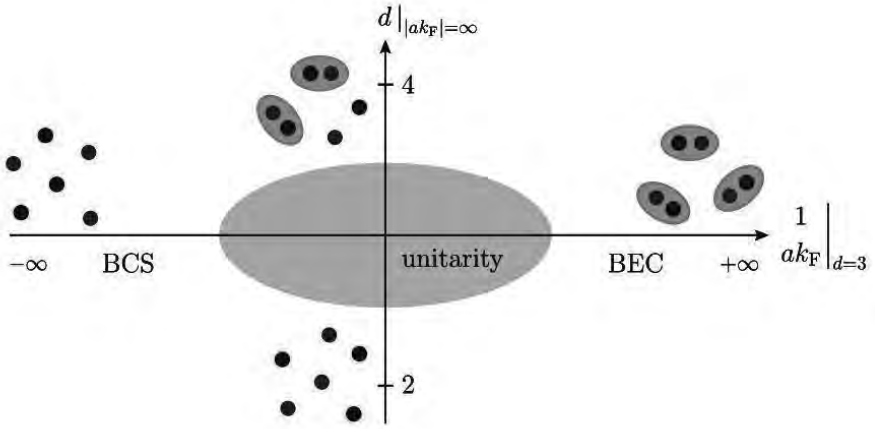

Figure 5.0.1: Phase diagram of BCS-BEC crossover in the plane of inverse scattering length $(ap_{\mathcal{F}})^{-1}$ and spatial dimension d, with the four weak interaction limits at the extremes of the domain of the plane $\left(-\infty < \frac{1}{ap_{\mathcal{F}}} < \infty\right) \times [2, 4]$ and the central-shaded region being strongly interactive.[21]

perturbative interpretation of the system with parameter $|ap_{\mathcal{F}}|$ fails, especially in the *unitary limit* of infinite scattering length, $|ap_{\mathcal{F}}| \longrightarrow \infty$. This unitary limit is comparable with dilute nuclear matter found in neutron star interior ($^1S_0$ paring at density $n_{\text{bound}} \sim 0.004$ fm^{-3} and $p_{\mathcal{F}} \sim 0.5$ fm^{-1}) with neutron-neutron scattering length $a_{nn} \sim -18.5 \pm 0.3$ fm and effective range of inter particle force $r_{nn} \sim 2.75 \pm 0.1$ fm [referenced from Chamel and Haensel 2008, , page 72], satisfying the dilute condition $r_{nn} \ll (n_{\text{bound}})^{-1/3}$. A heuristic picture of the BCS-BEC cross over, with the central region of strong interaction is shown in FIG. 5.0.1.

In neutron stars, the interior density profile indicates a complex mixture of exotic nuclei (including the strong coupling regimes of μ ~400 MeV crystalline quark matter in neutron cores) and raises quantitative uncertainties in nuclear calculation of superfluid-lattice interactions. Their strong coupling regions could involve colour superconductivity at critical temperatures below 10 - 50 MeV, directly influencing glitch physics through vortex interaction [Alford et al. 2001]. For strongly coupled systems at finite temperature, the construction of the thermal partition function from the eigenvalues of many-body Schrödinger equations (with possibly 10^6 particles to model trapped atomic superfluids) requires tremendous computa-

[21]Picture sourced from [Zwerger 2011]

tional ability and is rather difficult [Proukakis and Jackson 2008]. In light of this; intuitively speaking, the holographic approach of a weakly curved higher dimensional gravity theory dual to this strongly coupled QFT seems like an efficient tool of study. [22]

The recent formulation of *holographic superfluidity*, extended formally by Sean Hartnoll, Christopher Herzog and Garry Horowitz [Hartnoll et al. 2008], utilizes the AdS/CFT conjecture of string theory to model a condensed matter superfluid system. In essence, the presence of scalar hairs at low temperatures outside the AdS_{3+1} black hole (BH) horizon forms the thermally-dependent superfluid condensate in the dual gauge theory at the asymptotic conformal boundary CFT_{2+1}; the extra bulk dimension contributing to holographic renormalizable group flows associated with scale invariant Abelian Higgs CFT. Remarkably, this gauge/gravity approach to superfluid systems admits inhomogeneous solution states of topological stability i.e., vortices in the bulk theory that map to similar boundary field theory global solitons; with the vortices having the typical logarithmic-divergent free energy profile. This then forms a good first measure to test the basic validity of the gravitational dual approach to superfluidity and vortex formation.

A universality of AdS/condensed matter extension in studying any finite temperature field theory is in finding the ratio of shear viscosity η to the entropy s given as $\eta/s \sim \hbar/(4\pi k_{\text{Boltzmann}})$ up to leading order in the 't Hooft coupling [Kovtun et al. 2003] — a much celebrated result/test of the AdS/CFT conjecture in light of the RHIC/LHC experimental opportunities (*cf.* [Son and Starinets 2007] for a good developmental review of AdS/CFT universality cover). Essentially, any finite temperature QFT (residing on the boundary) should reflect a hydrodynamic prescription in the long-wavelength limit, being described by the BH horizon geometry and the perturbative quasi normal modes (QNM) (considered through the *membrane paradigm* fluid interpretation of [Kovtun et al. 2003]) of the bulk grav-

[22] There are alternative approaches to study strongly coupled systems like e.g., non perturbative Lattice QCD, finite temperature QCD with different effective field theories, Density Functional theories for unitary Fermi gas (EDF) etc. These approaches have different domains of validity; each with their own specific limitations and difficult problems. A good textbook introduction and review to the basic methodology of thermal field theories — with emphasis towards superconductivity and superdense matter — can be found in [Greiner and Müller 1994; Cooper and Feldman 2011; Shuryak 2004].

itational theory. This has been shown to be just so in [Iqbal and Liu 2009] where they successfully calculated the boundary theory transport coefficients based on the geometric properties at the BH event horizon. A great place to comprehensively review the basic QNM theory with its application in AdS/CFT can be found in [Konoplya and Zhidenko 2011]. Apart from that, a whole vibrant body of literature is currently produced in looking at holographic superconductors/superfluids from various perspectives, e.g., holographic analogy to fluid/superfluid phase diagram [Brihaye and Hartmann 2011], colour superconductivity from holography [Basu et al. 2011], p-wave holographic superconductors [Gubser and Pufu 2008; Roberts and Hartnoll 2008] and back-reactive Gauss-Bonnet holographic superconductors [Barclay et al. 2010].

With the nascent modelling of holographic vortices and calculations of expectation values of condensate profile/currents (in the AdS/CFT framework), as seen in the works of Tameem Albash *&* Clifford Johnson [Albash and Johnson 2009], Marc Montull et al. [Montull et al. 2009], Ville Keränen et al. [Keränen et al. 2010b] and Oriol Domènech et al. [Domenech et al. 2010], many interesting properties/similarities relating to the classical picture of the Ginzburg Landau theory of (BCS) superconductors have emerged. Being analogous in a superfluid context, these marked similarities help conjure support for a holographic superfluid-vortex study, particularly so, as a theorisation of pulsar glitches.

Within the domain of superconductor research, there has been indications that the holographic realizations of Abrikosov lattices in superconductors are thermodynamically favourable [Maeda et al. 2010; Murray and Tešanović 2011] and the dynamics of vortex flow in such cases have been studied [Maeda and Okamura 2011]. In term of superfluid interiors of neutron stars, this presents the possibility of looking at a multiple-vortex lattice structures in the dual picture. With [Iqbal and Liu 2011], the hydrodynamic magnus force experienced by superfluid vortices have been derived from a holographic superfluid Abrikosov string perspective (a 3+1 dimensional flux tube analogue of Nielson-Olesen vortices in the bulk, *cf.* [Vilenkin and Shellard 2000]). This marks an important development in holographic vortex-dynamic modelling in line with the theoretical work on quantized superfluid vortex dynamics found in conventional literature [Barenghi et al. 2001; Tsubota et al. 2010].

5 Conclusions and Extensions

A systematic holographic model of a neutron star with degenerate composite operators in the CFT mapped to a degenerate Fermi gas in the gravitational bulk can be found in [Boer et al. 2010], where backreaction to gravity was considered to estimate the Chandrasekhar limit. This, along with the more modern developments in understanding strongly interacting quantum fluids like QCD plasma and unitary Fermi gases using the tools of AdS/CFT (extensively reviewed in [Adams et al. 2012]), will help in proceeding towards modelling the glitch physics of pulsars in accordance with some of the more conventional models (*cf.* §. 3). An understanding of the density dependent characteristic pinning dynamics of superfluid (superconducting) vortices in the crustal regions can help consolidate a working holographic picture, which can then be tested against the extensive observational data available. Incidentally within the sphere of pulsar modelling using topological currents in dense stars, there are already indications of other observational effects like pulsar kicks being described by models based on AdS/CFT conjecture (a great review is in [Charbonneau 2011]), thereby further strengthening the validity of the holographic approach.

With increasing interest in the area of AdS/condensed matter from various research groups around the world, there has come to be an active and dynamic enclave within the applied mathematics/theoretical physics community. Moreover, the decreasing divide between theoretical and observational physicists with RHIC and LHC experiments (and within the astrophysics/cosmology community) has created an even more enriched and vibrant environment to facilitate collective research. Holographic theories with their extended realm of applications to condensed matter physics find stringent and rigorous scrutiny with the advances in conventional approaches to finite temperature QCD physics. An immediate outcome of this exchange is an ever-increasing mathematical tool kit, an extensive empirical database and a multi-disciplinary perspective: all of which, hitherto had not been universally accessible to all researchers in this field. This makes the nascent frontier of *cosmological laboratory physics* with its open questions and speculations, an invigorating and riveting space to systematically explore the workings of matter in our universe.

Bibliography

Abney, M. and R. I. Epstein (1996). "Ekman Pumping in Compact Astrophysical Bodies". In: *J.Fluid Mech.* 312, pp. 327–340.

Abrikosov, A. A. (1957). "On the Magnetic properties of superconductors of the second group". In: *Sov. Phys. JETP* 5, pp. 1174–1182.

Adams, A. et al. (2012). "Strongly Correlated Quantum Fluids: Ultracold Quantum Gases, Quantum Chromodynamic Plasmas, and Holographic Duality". In: URL: `http://www.arxiv.org/abs/1205.5180`.

Albash, T. (2010). "Phenomenological AdS/CFT Applications to Condensed Matter". PhD thesis. University of South California. URL: `http://digitallibrary.usc.edu/assetserver/controller/item/etd-Albash-3640.pdf`.

Albash, T. and C. V. Johnson (2009). "Vortex and Droplet Engineering in Holographic Superconductors". In: *Phys. Rev. D* 80, p. 126009.

Alford, Mark G., Jeffrey A. Bowers, and Krishna Rajagopal (2001). "Crystalline color superconductivity". In: *Phys.Rev.* D63, p. 074016.

Allen, J. F. and A. D. Misener (1938). "Flow of Liquid Helium II". In: *Nature* 141, p. 75.

Alpar, M. A. (1977). "Pinning and Threading of Quantized Vortices in the Pulsar Crust Superfluid". In: *Astrophysical Journal* 213, pp. 527–530.

Alpar, M. A. and D. Pines (1993). "Pulsar Glitches and Neutron Star Superfluidity: A 1992 Perspective". In: *Isolated Pulsars*. Ed. by K. A. van Ripper, R. I. Epstein, and C. Ho. Vol. 1. Cambridge, UK: Cambridge University Press, p. 17.

Alpar, M. A., D. Pines, J. Shaham, and P. W. Anderson (1981). "Giant Glitches and Pinned Vorticity in the Vela and Other Pulsars". In: *ApJ Letters* 249, p. L29.

Alpar, M. A., D. Pines, P. W. Anderson, and J. Shaham (1982). "The rheology of neutron stars: Vortex line pinning in the crust superfluid". In: *J. Phil. Mag.* 45.A, p. 227.

Alpar, M. A., S. A. Langer, and J. A. Sauls (1984a). "Rapid postglitch spin-up of the superfluid core in pulsars". In: *Astrophysical Journal* 282, pp. 533–541.

Alpar, M. A., D. Pines, P. W. Anderson, and J. Shaham (1984b). "Vortex Creep and the Internal Temperature of Neutron Stars: (I) - General theory". In: *ApJ* 276.A, pp. 325–334.

Alpar, M. A., D. Pines, J. Shaham, and P. W. Anderson (1984c). "Vortex Creep and the Internal Temperature of Neutron Stars: (II) - The Vela Pulsar". In: *Astrophysical Journal* 278.B, p. 791.

Alpar, M. A., H. F. Chau, K. S. Cheng, and D. Pines (1993). "Postglitch relaxation of the VELA pulsar after its first eight large glitches - A re-evaluation with the vortex–creep model ". In: *Astrophysical Journal* 409, pp. 345–359.

Alpar, M. A., H. F. Chau, K. S. Cheng, and D. Pines (1996). "Postglitch Relaxation of the Crab Pulsar after its First Four Major Glitches: The Combined Effects of Crust Cracking, Formation of Vortex Depletion Region and Vortex Creep". In: *Astrophysical Journal* 459, p. 706.

Ammon, M., J. Erdmenger, M. Kaminski, and P. Kerner (2009). "Flavor Superconductivity from Gauge/Gravity Duality". In: *JHEP* 0910, p. 067.

Andersen, Jens O. (2004). "Theory of the weakly interacting Bose gas". In: *Rev. Mod. Phys.* 76 (2), pp. 599–639.

Anderson, P. W. and N. Itoh (1975). "Pulsar Glitches and Restlessness as a hard superfluidity phenomenon". In: *Nature* 256, pp. 25–27.

Andersson, N., G. L. Comer, and R. Prix (2002). "The superfluid two–stream instability". In: *Mon. Not. Roy. Astron. Soc.* 354, pp. 101–110.

Andersson, N., K. Glampedakis, W. C. G. Ho, and C. M. Espinoza (2012a). *Pulsar glitches: The crust is not enough*. Preprint. URL: `http://arxiv.org/abs/1207.0633v1`.

Andersson, N., K. Glampedakis, and M. Hogg (2012b). "Superfluid instability of r-modes in 'differentially rotating' neutron stars". In: URL: `http://arxiv.org/abs/1208.1852`.

Andronikashvilli, E. L. (1946). "Direct Observation of two kinds of motion for Helium II". In: *Zh. Eksp. Theor. Fiz* 16, p. 780.

Annett, J. F. (2004). *Superconductivity, Superfluids and Condensates*. Oxford Master Series in Condensed Matter Physics.

Balasubramanian, Koushik and John McGreevy (2008). "Gravity duals for non-relativistic CFTs". In: *Physical Review Letters* 101 (6), p. 12.

Balasubramanian, Vijay, Per Kraus, and Albion Lawrence (1999). "Bulk versus boundary dynamics in antide Sitter spacetime". In: *Phys. Rev. D* 59 (4), p. 046003.

Barclay, L., R. Gregory, S. Kanno, and P. Sutcliffe (2010). "Gauss-Bonnet Holographic Superconductors". In: *JHEP* 1012, p. 029.

Bardeen, J., L. N. Cooper, and J. R. Schrieffer (1957). "Theory of Superconductivity". In: *Phys. Rev.* 108, pp. 1175–1204.

Barenghi, C. F., R. J. Donnelly, and W. F. Vinen, eds. (2001). *Quantized Vortex Dynamics and Superfluid Turbulence*. Vol. 571. Lecture Notes in Physics. Springer.

Basu, P. et al. (2011). "Towards A Holographic Model of Color Superconductivity". In: *New J.Phys.* 13, p. 055001.

Baym, G. and R. I. Epstein (1988). "Vortex pinning in Neutron Stars". In: *Astrophysical Journal* 320, pp. 680–690.

Baym, G. and D. Pines (1971). "Neutron starquakes and pulsar speedup". In: *Annals of Physics* 66, pp. 816–835.

Baym, G., C. J. Pethick, D. Pines, and M. Ruderman (1969a). "Spin Up in Neutron Stars: The Future of the Vela Pulsar". In: *Nature* 224, p. 872.

Baym, G., C.J. Pethick, and D. Pines (1969b). "Superfluidity in Neutron Star". In: *Nature* 224, p. 673.

Bekenstein, J. D. (1996). "Black hole hair: 25 - years after". In: *Second International A.D. Sakharov Conference on Physics Proceedings*. Moscow, Russia, pp. 216–219.

Beliaev, S. T. (1958). "Energy spectrum of a non-ideal Bose gas". In: *Sov. Phys. JETP* 7, p. 289.

Beliaev, S. T. (1959). "Effect of pairing correlations on nuclear properties". In: *Mat.-Fys. Medd. K. Dan. Vid. Selsk.* 31.11, pp. 1–55.

Beskin, V. S. (1999). "Radiopulsars". In: *Uspekhi Fizicheskikh Nauk* 169.11, pp. 1173–1174.

Bianchi, Massimo, Daniel Z. Freedman, and Kostas Skenderis (2002). "Holographic renormalization". In: *Nucl.Phys.* B631, pp. 159–194.

Blandford, R. D. et al., eds. (1993). *Pulsars as Physics Laboratories*. Oxford, UK: Oxford University Press.

Boer, J. de, K. Papadodimas, and E. Verlinde (2010). "Holographic Neutron Stars". In: *JHEP* 1010, p. 020.

Boer, Jan de, Erik P. Verlinde, and Herman L. Verlinde (2000). "On the holographic renormalization group". In: *JHEP* 0008, p. 003.

Bogoliubov, N. N. (1970). *Lectures on Quantum Statistics*. Vol. 2. New York, USA: Gordon and Breach.

Bohr, A., B. R. Mottelson, and D. Pines (1958). "Possible Analogy between the Excitation Spectra of Nuclei and Those of the Superconducting Metallic State". In: *Phys. Rev.* 110, pp. 936–938.

Boynton, P. E. (1981). "Pulsar". In: *The IAU Proceedings*. Ed. by W. D. Sieber and R. Wielebinski. Vol. 279.

Boynton, P. E., E. J. Groth, R. B. Partridge, and D. T. Wilkinson (1971). "The Crab Nebula". In: *The IAU Proceedings*. Ed. by R. D. Davies and F. G. Smith. Vol. 46, p. 119.

Breitenlohner, P. and D. Z. Freedman (1982). "Positive Energy in anti-De Sitter Backgrounds and Gauged Extended Supergravity". In: *Phys. Lett. B* 115, p. 197.

Brihaye, Yves and Betti Hartmann (2011). "Holographic superfluid/fluid/insulator phase transitions in 2+1 dimensions". In: *Phys.Rev.* D83, p. 126008.

Carter, B., D. Langlois, and D. M. Sedrakian (2000). "Centrifugal buoyancy as a mechanism for neutron star glitches". In: *Astronomy and Astrophysics* 36, pp. 795–802.

Chamel, N. and B. Carter (2006). "Effect of entrainment on stress and pulsar glitches in neutron star crust". In: *Mon. Not. Roy. Astron. Soc.* 368, pp. 796–808.

Chamel, N. and P. Haensel (2008). "Physics of Neutron Star Crusts". In: *Living Reviews in Relativity* 11.10.

Charbonneau, A. J. (2011). "Topological Currents in Dense Matter". PhD thesis. Vancouver, Canada: The University of British Columbia, p. 182. URL: `https://circle.ubc.ca/handle/2429/35918`.

Cheng, K. S., D. Pines, M. A. Alpar, and J. Shaham (1988). "Spontaneous superfluid unpinning and the inhomogeneous distribution of vortex lines in neutron stars". In: *The Astrophysical Journal* 330, p. 835.

Cognard, I. and D.C. Backer (2004). "A Microglitch in the Millisecond Pulsar PSR B1821-24 in M28". In: *The Astrophysical Journal* 612, p. L215.

Cooper, L. N. (1956). "Bound Electron Pairs in a Degenerate Fermi Gas". In: *Phys. Rev.* 104.4, pp. 1189–1190.

Cooper, L. N. and D. E. Feldman, eds. (2011). *BCS: 50 Years*. World Scientific.

Dodson, R., D. Lewis, and P. McCulloch (2002). "High Time Resolution Observations of the January 2000 Glitch in the Vela Pulsar". In: *Astrophysical Journal* 564.II, pp. L85–L87.

Dodson, R., D. Lewis, and P. McCulloch (2007). "Two decades of pulsar timing of Vela". In: *Isolated Neutron Stars: From the Surface to the Interior*. Ed. by S. Zane, R. Turolla, and D. Page. Springer Netherlands, pp. 585–589.

Domenech, O. et al. (2010). "Emergent Gauge Fields in Holographic Superconductors". In: *JHEP* 1008, p. 033.

Downs, G. S. (1981). "JPL pulsar timing observations. (I) - The VELA pulsar ". In: *Astrophysical Journal* 249.II, pp. 687–697.

Eaason, I. (1979). "Long-term changes in pulsar periods and the plasma in neutron star interiors ". In: *Astrophysical Journal* 233, pp. 711–716.

Espinoza, C. M., A. G. Lyne, and M. Kramer (2011). *A study of 315 glitches in the rotation of 102 pulsars*. Preprint. URL: `http://arxiv.org/abs/1102.1743v2`.

Eysden, C. A. van (2011). "Superfluid spin up and pulsar glitch recovery ". PhD thesis. Melbourne, Australia: University of Melbourne. URL: `http://dtl.unimelb.edu.au/researchfile273754.pdf`.

Feynman, R. P. (1955). "Application of quantum mechanics to liquid helium". In: *Progress in Low Temperature Physics* 1, pp. 17–53.

Feynman, R. P. (1972). *Statistical Mechanics*. New York, USA: Addison Wesley.

Franco, L. M., B. Link, and R. I. Epstein (2000). "Quaking Neutron Stars". In: *Astrophysical Journal* 543, pp. 987–994.

Franco, S., A. Garcia-Garcia, and D. Rodriguez-Gomez (2010). "A General class of holographic superconductors". In: *JHEP* 1004, p. 092.

Galloway, D. K., E. H. Morgan, and A. M. Levine (2007). "A Frequency Glitch in an Accreting Pulsar". In: *Astrophysical Journal* 613, pp. 1164–1173.

Gauntlett, Jerome P., Julian Sonner, and Toby Wiseman (2009). "Holographic superconductivity in M-Theory". In: *Phys.Rev.Lett.* 103, p. 151601.

Gavoret, J and P Nozieres (1964). "Structure of the perturbation expansion for the bose liquid at zero temperature". In: *Annals of Physics* 28.3, pp. 349–399.

Gennes, P. G. de (1966). *Superconductivity of Metals and Alloys*. New York, USA: W. A. Benjamin.

Gibbons, G. W. and S. W. Hawking (1977). "Action integrals and partition functions in quantum gravity". In: *Phys. Rev. D* 15 (10), pp. 2752–2756.

Ginzburg, V. L. and D. A. Kirzhnits (1964). "On superfluidity of neutron star". In: *Zh. Eksp. Theor. Fiz* 47.

Glampedakis, K. and N. Andersson (2009). "Hydrodynamical trigger mechanism for pulsar glitches". In: *Phys. Rev. Lett.* 102.14, p. 141101.

Gold, T. (1968). "Rotating Neutron Stars as the Origin of the Pulsating Radio Sources". In: *Nature* 218, p. 731.

Greiner, W. and B. Müller (1994). *Quantum Mechanics: Symmetries*. Vol. 2. Theoretical physics. Springer Verlag.

Griffin, A. (1993). *Excitations in a Bose-Condensed Liquid*. United Kingdon: Cambridge University Press.

Gubser, S. S. (2008). "Breaking an Abelian gauge symmetry near a black hole horizon". In: *Phys.Rev.* D78, p. 065034.

Gubser, S. S., I. R. Klebanov, and A. Polyakov (1998). "Gauge theory correlators from non-critical string theory ". In: *Phys. Rev. B* 428, p. 105.

Gubser, S. S., S. S. Pufu, and F. D. Rocha (2010). "Quantum critical superconductors in string theory and M-theory". In: *Phys.Lett.* B683, pp. 201–204.

Gubser, Steven S. and Silviu S. Pufu (2008). "The Gravity dual of a p-wave superconductor". In: *JHEP* 0811, p. 033.

Haberl, F. et al. (2006). *Evidence for precession of the isolated neutron star RX J0720.4-3125*.

Haensel, P., Paweł Haensel, A. Y. Potekhin, and D. G. Yakovlev (2007). *Neutron stars: Equation of state and structure*. Springer. ISBN: 0387335439.

Hall, H. E. and W. F. Vinen (1956). "The rotation of liquid Helium II". In: *Proc. Royal. Soc. A* 238.1213, pp. 215–234.

Harada, J. (2009). *Roton energy gap and spontaneous symmetry breaking*. Preprint. URL: `http://arxiv.org/abs/0911.1599v1`.

Harrison, B. K., K. Thorne, M. Wakamo, and J. A. Wheeler (1965). *Gravitation Theory and Gravitational Collapse*. Chicago, USA: Chicago University Press.

Hartnoll, S. A. (2009). "Lectures on holographic methods for condensed matter physics ". In: *Classical and Quantum Gravity* 26.22, p. 224002.

Hartnoll, S. A. and C. P. Herzog (2008). "Impure AdS/CFT correspondence ". In: *Phys. Rev. D* 77.10, p. 106009.

Hartnoll, S. A., C. P. Herzog, and G. T. Horowitz (2008). "Building a Holographic Superconductors". In: *Phys. Rev. Lett.* 101, p. 031601.

Hashimoto, M., H. Seki, and M. Yamada (1984). "Shape of Nuclei in the Crust of Neutron Star". In: *Prog. Theor. Phys.* 71, pp. 320–326.

Haskell, B. B., P. M. Pizzochero, and T. Sidery (2012). "Modeling pulsar glitches with realistic pinning forces: a hydro- dynamical approach ". In: *Mon. Not. Roy. Astron. Soc.* 402.II, pp. 658–671.

Hertog, T. (2006). "Towards a novel No-hair Theorem for Black Holes". In: *Phys.Rev.* D74, p. 084008.

Hertog, T. (2009). "Lectures on Holographic Superfluidity and Superconductivity ". In: *Journal of Physics A: Mathematical and Theoretical* 42.34, p. 343001.

Herzog, C. P., P. K. Kovtun, and D. T. Son (2009). "Holographic model of superfluidity". In: *Phys. Rev. D* 79, p. 066002. arXiv:0809.4870 [hep-th].

Heusler, M. (1996). "No hair theorems and black holes with hair". In: *Helv.Phys.Acta* 69, pp. 501–528.

Hewish, A. et al. (1968). "Observation of a Rapidly Pulsating Radio Source". In: *Nature* 217, p. 709.

Hohenberg, P and P Martin (1965). "Microscopic theory of superfluid Helium I". In: *Annals of Physics* 34.2, pp. 291–359.

Hohenberg, P. C. (1967). "Existence of Long-Range Order in One and Two Dimensions". In: *Phys. Rev.* 158 (2), pp. 383–386.

Horowitz, G. T. (2010). "Introduction to Holographic Superconductors". In: URL: `http://arxiv.org/abs/1002.1722v2`.

Horowitz, G. T. (2011). "Surprising Connections Between General Relativity and Condensed Matter". In: *Class.Quant.Grav.* 28, p. 114008.

Iqbal, N. and H. Liu (2009). "Universality of the hydrodynamic limit in AdS/CFT and the membrane paradigm". In: *Phys.Rev.* D79, p. 025023.

Iqbal, N. and H. Liu (2011). "Luttinger's Theorem, Superfluid Vortices, and Holography". In: URL: `http://www.arxiv.org/abs/1112.3671`.

Israel, G. L. et al. (2007). "The Post-Burst Awakening of the Anomalous X-Ray Pulsar in Westerlund 1". In: *The Astrophysical Journal* 664, p. 448.

Jones, P. B. (1990). "Rotation of the neutron-drip superfluid in pulsars - Temperature-dependence of the resistive force". In: *Mon. Not. Roy. Astron. Soc.* 244, pp. 675–679.

Jones, P. B. (1991). "Rotation of the neutron-drip superfluid in pulsars - The interaction and pinning of vortices". In: *Astrophysical Journal* 373, pp. 208–212.

Jones, P. B. (1992). "Rotation of the neutron-drip superfluid in pulsars - The Kelvin phonon contribution to dissipation". In: *Mon. Not. Roy. Astron. Soc.* 257, pp. 501–506.

Jones, P. B. (2002). "Post-glitch relaxation in pulsars ". In: *Mon. Not. Roy. Astron. Soc.* 355.III, pp. 733–740.

Jones, P. B. (2006). "Type I and two-gap superconductivity in neutron star magnetism". In: *Mon. Not. Roy. Astron. Soc.* 371, pp. 1327–1333.

Kapitza, P.L. (1938). "Viscosity of Liquid Helium below the λ-Point". In: *Nature* 141, p. 74.

Kapsi, V. M. and F. P. Gavriil (2003). "A Second Glitch from the Anomalous X-Ray Pulsar 1RXS J170849.0 - 4000910". In: *The Astrophysical Journal* 596, p. L71.

Kapsi, V. M et al. (2007). "A Major Soft Gamma Repeater-like Outburst and Rotation Glitch in the No-longer- so-anomalous X-Ray Pulsar 1E 2259+586". In: *Astrophysical Journal* 588, pp. L93–L96.

Keränen, V. (2011). "Holographic Superfluids and Solitons". PhD thesis. Helsinki, Finland: Helsinki Institute of Physics. URL: `http://hdl.handle.net/10138/27253`.

Keränen, V., E. Keski-Vakkuri, S. Nowling, and K. P. Yogendran (2010a). "Inhomogeneous Structures in Holographic Superfluids: I. Dark Solitons". In: *Phys.Rev.* D81, p. 126011.

Keränen, V., E. Keski-Vakkuri, S. Nowling, and K. P. Yogendran (2010b). "Inhomogeneous Structures in Holographic Superfluids: II. Vortices". In: *Phys.Rev.* D81, p. 126012.

Kiziltan, B., A. Kottas, and S. E. Thorsett (2010). *The Neutron Star Mass Distribution*. Preprint. URL: http://arxiv.org/abs/1011.4291v1.

Klebanov, I. R. and E. Witten (1999). "AdS / CFT correspondence and symmetry breaking". In: *Nucl.Phys.* B556, pp. 89–114.

Kleinert, H. (1990). *Gauge Fields in Condensed Matter: Disorder Fields and Applications to Superfluid Phase Transition and Crystal Melting*. World Scientific.

Kleinert, H. (2008). *Multivalued Fields in Condensed Matter, Electromagnetism, and Gravitation*. World Scientific.

Konoplya, R.A. and A. Zhidenko (2011). "Quasinormal modes of black holes: From astrophysics to string theory". In: *Rev.Mod.Phys.* 83, pp. 793–836.

Kopnin, N. P. (2002). *Introduction to the Theory of Superconductivity and Superfluidity*. Helsinki, Finland. URL: http://ltl.tkk.fi/opetus/supertheory/itss/superlect.pdf.

Kovtun, P., D. T. Son, and A. O. Starinets (2003). "Holography and hydrodynamics: Diffusion on stretched horizons". In: *JHEP* 0310, p. 064.

Larson, M. B. and B. Link (2002). "Simulations of glitches in isolated pulsars". In: *Mon. Not. Roy. Astron. Soc.* 333, p. 613.

Link, B. K. (2003). "Constraining Hadronic Superfluidity with Neutron Star Precession". In: *Phys. Rev. Lett.* 91.

Link, B. K. (2006). "Incompatibility of long-period neutron star precession with creeping neutron vortices". In: *Astronomy and Astrophysics* 458.3, pp. 881–884.

Link, B. K. and C. Cutler (2002). "Vortex unpinning in precessing neutron stars". In: *Mon. Not. Roy. Astron. Soc.* 336, pp. 211–216.

Link, B. K. and R. I. Epstein (1991). "Mechanics and Energetics of Vortex Unpinning in Neutron Stars". In: *ApJ* 373, pp. 592–603.

Link, B. K. and R. I. Epstein (1996). "Thermally Driven Neutron Star Glitches ". In: *ApJ* 457, p. 844.

Link, B. K., R. I. Epstein, and G. Baym (1993). "Superfluid vortex creep and rotational dynamics of neutron stars". In: *Astrophysical Journal* 403, pp. 285–302.

Lombardo, U. and H. J. Schulze (2000). "Superfluidity in Neutron Star Matter". In: *Workshop on Physics of Neutron Star Interiors*. ECT. Trento, Italy.

London, F. (1938). "On the Bose-Einstein Condensation". In: *Phys. Rev.* 54.11, pp. 947–954.

Lyne, A. G. and F. Graham-Smith (2006). *Pulsar Astronomy*. Cambridge, UK: Cambridge University Press.

Lyne, A. G., R. S. Pritchard, and F. Graham-Smith (1993). "Twenty–Three Years of Crab Pulsar Rotational History ". In: *Mon. Not. Roy. Astron. Soc.* 265, pp. 1003–1012.

Maeda, K. and T. Okamura (2011). "Vortex flow for a holographic superconductor". In: *Phys.Rev.* D83, p. 066004.

Maeda, K., M. Natsuume, and T. Okamura (2010). "Vortex lattice for a holographic superconductor". In: *Phys. Rev. D* 81 (2), p. 026002.

Maldacena, J. M. (1998). "The Large N limit of superconformal field theories and supergravity". In: *Adv.Theor.Math.Phys.* 2, pp. 231–252.

Maldacena, Juan (2011). "The gauge/gravity duality". In: URL: http://arxiv.org/abs/1106.6073v1.

Manton, N. and P. Sutcliffe (2004). *Topological Solitons*. Cambridge Monographs on Mathematical Physics. Cambridge, UK: Cambridge University Press.

McDonald, G. B. (2007). "A Review of Pulsar Glitch Mechanisms ". MA thesis. Johannesburg, SA: University of Johannesburg. URL: http://books.google.co.in/books?id=5JhMOAAACAAJ.

McGreevy, John (2010). "Holographic duality with a view toward many-body physics". In: *Adv.High Energy Phys.* 2010, p. 723105.

Melatos, A. and L. Warszawski (2009). "Superfluid vortex unpinning as a coherent noise process, and the scale invariance of pulsar glitches ". In: *The Astrophysical Journal* 700, p. 1524.

Melatos, A., C. Peralta, and J. S. B. Wythe (2008). "Avalanche Dynamics of Radio Pulsar Glitches". In: *The Astrophysical Journal* 672, p. 1103.

Mermin, N. D. and H. Wagner (1966). "Absence of Ferromagnetism or Antiferromagnetism in One- or Two-Dimensional Isotropic Heisenberg Models". In: *Phys. Rev. Lett.* 17 (22), pp. 1133–1136.

Middleditch, J. et al. (2006). "Predicting the Starquakes in PSR J0537-6910". In: *The Astrophysical Journal* 652, p. 1531.

Midgal, A. B. (1959). "Superfluidity and the moments of inertia of nuclei". In: *Nucl. Phys.* 13, p. 655.

Mochizuki, Y. and T. Izuyama (1995). "Self-trapping of superfluid vortices and the origin of pulsar glitches ". In: *The Astrophysical Journal* 440, p. 263.

Montull, M., A. Pomarol, and P. J. Silva (2009). "The Holographic Superconductor Vortex". In: 103, p. 091601.

Murray, J. M. and Z. Tešanović (2011). "Isolated Vortex and Vortex Lattice in a Holographic p-wave Superconductor". In: *Phys. Rev. D* 83, p. 126011.

Nastase, Horatiu (Dec. 2007). "Introduction to AdS-CFT". In: eprint: 0712.0689. URL: http://arxiv.org/abs/0712.0689.

Negele, J. W. and D. Vautherin (1973). "Neutron star matter at sub-nuclear densities". In: *Nucl. Phys.* A 207, pp. 298–320.

Osborne, D.V. (1950). "The Rotation of Liquid Helium II". In: *Proc. Phys. Soc (London)* A63, p. 909.

Papadimitriou, Ioannis and Kostas Skenderis (2007). "AdS/CFT correspondence and Geometry". In: URL: http://arxiv.org/abs/hep-th/0404176v2.

Papantonopoulos, Eleftherios, ed. (2011). *From Gravity to Thermal Gauge Theories: The AdS/CFT Correspondence*. Illustrated. Vol. 828. Springer. 425 pp.

Pathria, R. K. (1996). *Statistical Mechanics*. 2nd. Great Britain: Elsevier.

Peralta, C. A. (2007). "Superfluid spherical Couette flow and rotational irregularities in pulsars ". PhD thesis. Melbourne, Australia: University of Melbourne. URL: http://repository.unimelb.edu.au/10187/1895.

Pethick, C. J., D. G. Ravenhall, and C. P. Lorenz (1995). "The inner boundary of a neutron-star crust". In: *Nucl. Phys.* A 584, p. 675.

Pines, D., M. A. Alpar, J. Shaham, and P. W. Anderson (1980). "Pinned Vorticity in Rotating Superfluids, with Application to Neutron Stars". In: *Prog. Theor. Phys. Suppl.* 69, p. 376.

Pines, D., R. Tamagaki, and S. Tsuruta, eds. (1992). *Structure And Evolution Of Neutron Stars*. Basic Books.

Pires, A. S. T. (2010). "Ads/CFT correspondence in condensed matter". In: URL: http://arxiv.org/abs/1006.5838.

Pitaevskii, L. and S. Stringari (2003). *Bose Einstein Condensation*. Oxford, UK: Clarendon Press.

Pizzochero, P. M. (2011). "Angular Momentum Transfer in Vela-like Pulsar Glitches ". In: *The Astrophysical Journal* 743.II, p. L20.

Polchinski, Joseph (2010). "Introduction to Gauge/Gravity Duality". In: URL: http://arxiv.org/abs/1010.6134.

Proukakis, N. P. and B. Jackson (2008). "Finite Temperature Models of Bose-Einstein Condensation". In: *Journal of Physics B: Atomic, Molecular and Optical Physics* 41, p. 203002.

Radhakrishnan, V. and B. Jackson (1969). "Detection of a change of state in the Pulsar PSR 0833–45 ". In: *Nature* 222, pp. 228–229.

Roberts, Matthew M. and Sean A. Hartnoll (2008). "Pseudogap and time reversal breaking in a holographic superconductor". In: *JHEP* 0808, p. 035.

Rubakov, V. (2002). *Classical Theory of Gauge Fields*. Translated by S. S. Wilson. New Jersey, USA: Princeton University Press.

Ruderman, M. (1969). "Neutron Starquakes and Pulsar Periods". In: *Nature* 223, p. 597.

Ruderman, M. (1972). "Pulsars: Structure and Dynamics". In: *Annu. Rev. Astron. Astrophys.* 10, p. 427.

Ruderman, M. (1976). "Crust–breaking by neutron superfluids and the VELA pulsar glitches ". In: *Astrophysical Journal* 203, pp. 213–222.

Ruderman, M. (1991). "Neutron star crustal plate tectonics. (I) – Magnetic dipole evolution in millisecond pulsars and low-mass X-ray binaries ". In: *Astrophysical Journal* 366, pp. 261–269.

Ruderman, M., T. Zhu, and K. Chen (1998). "Neutron Star Magnetic Field Evolution, Crust Movement, and Glitches". In: *Astrophysical Journal* 492, p. 267.

Ruffini, R. and J. A. Wheeler (1971). "Introducing the Black Hole." In: *Physics Today*, pp. 30–41.

Sachdev, S. (2010). *Condensed matter and AdS/CFT*. Preprint. URL: http://arxiv.org/abs/1002.2947.

Sachdev, Subir (2012). "What can gauge-gravity duality teach us about condensed matter physics?" In: *Annual Review of Condensed Matter Physics* 3 (1), pp. 9–33.

Sedrakian, A. (2005). "Type-I superconductivity and neutron star precession". In: 71.8, p. 083003.

Sedrakian, A. and J. W. Clark (2006). "Nuclear superconductivity in compact stars: BCS theory and beyond". In: URL: http://www.arxiv.org/abs/nucl-th/0607028.

Sedrakian, A. and J. M. Cordes (1999). "Vortex-interface interactions and generation of glitches in pulsars". In: *Mon. Not. Roy. Astron. Soc.* 307.II, pp. 365–375.

Sedrakian, A. and J. M. Cordes (2002). "Inverse Problem of the Theory of Relaxation of the Vela Pulsar's Angular Velocity after Glitches ". In: *Astrophysics* 45, pp. 470–479.

Sensarma, R., M. Randeria, and H. Tin-Lun (2006). "Vortices in Superfluid Fermi Gases through the BEC to BCS Crossover". In: *Physical Review Letters* 96.9.

Shabanova, T. V. (2005). "Observations of three slow glitches in the spin rate of the pulsar B1822-09". In: *Mon. Not. Roy. Astron. Soc.* 356, p. 1435.

Shaham, J. (1977). "Free precession of neutron stars: Role of possible vortex pinning". In: *Astrophysical Journal* 214, pp. 251–260.

Shapiro, S. L. and S.A. Teukolsky (1983). *Black Holes, White Dwarfs, and Neutron Stars: The Physics of Compact Objects*. New York, USA: Wiley.

Shuryak, Edward V (2004). *The QCD Vacuum, Hadrons and Superdense Matter*. II. World Scientific Lecture Notes in Physics. Singapore: World Scientific.

Sidery, T., A. Passamonti, and N. Andersson (2010). "The dynamics of pulsar glitches: contrasting phenomenology with numerical evolutions ". In: *Mon. Not. Roy. Astron. Soc.* 405.II, pp. 1061–1074.

Skenderis, Kostas (2002). "Lecture Notes on Holographic Renormalization". In: *Classical and Quantum Gravity* 19 (22), pp. 5849–5876.

Son, D. T. and A. O. Starinets (2007). "Viscosity, Black Holes, and Quantum Field Theory". In: *Ann.Rev.Nucl.Part.Sci.* 57, pp. 95–118.

Susskind, L. (1994). "Strings, black holes and Lorentz contraction ". In: *Phys. Rev. D* 492, p. 6606.

't Hooft, G. (1993). *Dimensional Reduction in Quantum Gravity*. Preprint. URL: `http://arxiv.org/abs/gr-qc/9310026v2`.

Thorn, C. (1994). *Reformulating String Theory with the* $1/N$ *Expansion*. Preprint. URL: `http://arxiv.org/abs/hep-th/9405069v1`.

Tisza, L. (1938). "Transport Phenomena in Helium II". In: *Nature* 141, p. 913.

Tkachenko, V. K. (1966). "On vortex lattices". In: *Sov. Phys. JETP* 22, pp. 1282–1286.

Troup, G. J. (1967). *Otical Coherence Theory - Recent Developments*. University of California: Methuen's monographs on physical subjects.

Tsubota, M., K. Kasamatsu, and M. Kobayashi (2010). "Quantized vortices in superfluid helium and atomic Bose-Einstein condensates". In: URL: `http://arxiv.org/abs/1004.5458v2`.

Vilenkin, A. and E. P. S. Shellard (2000). *Cosmic Strings and Other Topological Defects*. Cambridge University Press.

Wang, N. et al. (2000). "Glitches in southern pulsars". In: *Mon. Not. Roy. Astron. Soc.* 317, pp. 843–860.

Warszawski, L. and A. Melatos (2008). "A cellular automaton model of pulsar glitches ". In: *Mon. Not. Roy. Astron. Soc.* 390, p. 175.

Watanabe, Gentaro and Toshiki Maruyama (2012). "Nuclear pasta in supernovae and neutron stars". In: *Neutron Star Crust*. Ed. by Carlos Bertulani and Jorge Piekarewicz. United States: Nova Science Publishers. Chap. 2. ISBN: 978-1-62081-960-9.

Witten, E. (1998). "Anti De Sitter Space and Holography". In: *Adv. Theor. Math. Phys.* 2, p. 253.

Witten, Edward (2007). "SL(2,$\mathbb{Z}$) Action On Three-Dimensional Conformal Field Theories With Abelian Symmetry". In: URL: `http://arxiv.org/abs/hep-th/0307041v3`.

Wolf, R. A. (1966). "Some Effects of the Strong Interactions on the Properties of Neutron-Star Matter". In: *Astrophysical Journal* 145, p. 834.

Wong, T., D.C. Backer, and A. G. Lyne (2001). "Observations of a Series of Six Recent Glitches in the Crab Pulsar". In: *Astrophysical Journal* 548, pp. 447–459.

Yamamoto, Y. (2010-2011). "Bose-Einstein Condensation and Matter-Wave Lasers". In: *Quantum Information Lecture Series*.

Yuan, J. P., N. Wang, R. N. Manchester, and Z. Y. Liu (2010). "29 glitches detected at Urumqi Observatory". In: *Mon. Not. Roy. Astron. Soc.* 404.B, p. 289.

Zou, W. Z. et al. (2008). "Observations of six glitches in PSR B1737-30". In: *Mon. Not. Roy. Astron. Soc.* 384, p. 1063.

Zuo, W. et al. (2004). "$^1S_0$ Proton and Neutron Superfluidity in beta-stable Neutron Star Matter". In: *Phys. Lett. B* 595, p. 44.

Zwerger, W. (2011). *The BCS–BEC Crossover and the Unitary Fermi Gas*. Lecture Notes in Physics. Springer.

Zwiebach, Barton (2004). *A First Course in String Theory*. Cambridge: Cambridge Univ. Press.